NTNU
Innovation and Creativity

Direct Driven Permanent Magnet Synchronous Generators with Diode Rectifiers for Use in Offshore Wind Turbines

Tor Inge Reigstad

Master of Science in Energy and Environment
Submission date: June 2007
Supervisor: Tore Marvin Undeland, ELKRAFT

Norwegian University of Science and Technology
Department of Electrical Power Engineering

Problem Description

The thesis is to focus on direct driven permanent magnet synchronous generators (PMSG) with diode rectifiers for use in offshore wind turbines. Reactive compensation of the generator, power losses and control of the generator are to be studied. Configurations for power transmission to onshore point of common connection should also be considered. Costs, power losses, reliability and interface with the PMSG are to be discussed.

The purpose of the laboratory tests and simulations are to learn how a PMSG with diode rectifier behaves. A 55kW PMSG is to be tested in "Vindlabben", with and without reactive compensation. The generator current and generator voltage should be measured and the total harmonic distribution (THD) of the current and the voltage are to be calculated. The results must be compared to simulations on an equal generator in PSCAD/EMTDC. A 2MW PMSG is also to be simulated to compare parallel and series compensation and to find how the generator efficiency varies with the wind speed. The generator is also to be simulated with constant DC-link voltage and varying local wind to find how much the turbine and generator efficiency decreases when a Cluster step-up configuration is used. The DC-link voltage is in this case equal for parts of the wind farm or the whole wind farms. A 3MW ironless PMSG with very low synchronous reactance should finally be simulated to find how this generator behaves with a diode rectifier.

Assignment given: 15. January 2007
Supervisor: Tore Marvin Undeland, ELKRAFT

Abstract

This work is focused on direct-driven permanent magnets synchronous generators (PMSG) with diode rectifiers for use in offshore wind turbines. Reactive compensation of the generator, power losses and control of the generator are studied. Configurations for power transmission to onshore point of common connection are also considered. Costs, power losses, reliability and interface with the PMSG are discussed.

The purpose of the laboratory tests and simulations are to learn how a PMSG with diode rectifier behaves. A 55kW PMSG is tested in "Vindlabben", with and without reactive compensation. The generator current and generator voltage are measured and the total harmonic distribution (THD) of the current and the voltage are calculated. The results are compared to simulations on an equal generator in PSCAD/EMTDC. A 2MW PMSG is also simulated to compare parallel and series compensation and to find how the generator efficiency varies with the wind speed. The generator is also simulated with constant DC-link voltage and varying local wind to find how much the turbine and generator efficiency decreases when a Cluster step-up configuration is used. The DC-link voltage is in this case equal for parts of the wind farm or the whole wind farms. A 3MW ironless PMSG with very low synchronous reactance is simulated to find how this generator behaves with a diode rectifier.

The laboratory tests and PSCAD simulations show that the maximal generator power increases when reactive compensation of the generator is used. The measured and simulated generator voltage and current shapes are found to be approximately equal. Series compensated PMSGs have lower generator current rms and lower current THD than parallel compensated PMSGs when the synchronous reactance is large. Therefore, the generator losses are $2-15\%$ lower and the diode rectifier losses are $0-1\%$ lower, depending on the wind speed. The diode rectifier losses are lower than 1%. The losses can be reduced even more if the diodes are connected in parallel. If a Cluster step-up configuration is used, the turbine efficiency is reduced by $3-4\%$.

The ironless PMSG has a low synchronous reactance and reactive compensation is not needed because the reactive power produced by the generator is low. Parallel connected capacitors have no positive effect and series connected capacitances must be very large and can therefore not be used. The generator current THD is very large when no reactive compensation is used. However, the current THD can be reduced by connecting an inductance to the DC-link.

Cluster step-up, two-step DC/DC system, turbine step-up and series connected wind turbine are the most relevant layouts of the wind farms transmission system discussed in this thesis. The cluster step-up system has low power losses since only one large DC/DC converter is used. Also, the power equipment in the turbine is very reliable. However, the turbine efficiency is reduced since the generator torque and generator speed could not be controlled for one specific turbine. The other transmission systems require DC/DC converters in the turbines and they are therefore probably not as reliable. The total cost is crucial for the chose of the transmission system. Further cost accountings for the different DC systems are needed.

Preface

This report constitutes my Master Thesis spring 2007 and documents the work during the 10.th semester of my education at the Department of electrical power engineering, NTNU.

The laboratory tests and simulation performed during this work shows the advantages and disadvantages of using a direct-driven PMSG with diode rectifier in a wind turbine. It also shows that the power losses of the generator is almost reduced to the minimum if series connected capacitors are used to deliver reactive power to the generator.

I want to thank my supervisors Prof. Tore Undeland and PhD. Thomas Fuglseth for useful help and instructive conversations. I also want to thank Prof. Robert Nielsen for an enthusiastic discussion about permanent magnet generators, PhD. Øystein Krøvel and Steinar Olsen for lending me the PM generator and the converter and helping me in "Vindlabben"and Jon Are Wold Suul for useful help on my PSCAD related questions.

Trondheim, 12.June 2007

Tor Inge Reigstad

Contents

1 Introduction

Floating wind turbines are an exciting area of research with lot of challenges. Some of these challenges are considered in this report. The thesis focuses on configurations for power transmission from the turbine generator to onshore. Most attention is given to the generator diode rectifier and how this rectifier affects the permanent magnet synchronous generator and the generator losses. The reliability of the turbines will be much better if a diode rectifier is used instead of an IGBT rectifier. Different offshore grid configurations are also considered compared, both AC and DC. The aim has been to find a simple, inexpensive, reliably and low losses transmission system which is fitted for the PMSG with diode rectifier.

Essential theory is present in Chapter 2 to 5. Transmission systems for large offshore wind farms will be reviewed in Chapter 2 to get overall view of the system. Different ways of integrating the turbine generators in the transmission system is present. Chapter 3 presents the permanent magnet synchronous generator, how the generator is modelled and how the generator losses are calculated. The PMSG with diode rectifier and reactive compensation of the generator are examined in Chapter 4. At last, the different control system of the generator is present in Chapter 5.

Chapters 6 to 9 present the results of the laboratory work and the simulations in PSCAD/EMTDC. Some results are discussed in this chapter. The modelling of the turbine, PMSG, diode rectifier and controllers in PSCAD is explained in Chapter 6. Turbine, generator and diode rectifier data is also found in this Chapter.

The laboratory work on the 55kW PMSG is present in Chapter 7. The generator is also simulated in PSCAD/EMTDC and the results are compared to the laboratory measurements. The simulations are performed with parallel reactive compensation of the generator, series compensation and no compensation while the generator is tested with parallel compensation and without reactive compensation.

In Chapter 8 simulations of a 2MW turbine is presents. Series reactive compensation is compared to parallel reactive compensation to find what methods which are best fitted for wind turbines. The generator system is also simulated with constant DC-link voltage to find how much the turbine and generator efficiency decrease if a cluster step-up configuration is used.

Simulations of a 3MW ironless PMSG is present in Chapter 9. The ironless generators have a lower synchronous reactance and the simulations are performed to se how this affects the use of diode rectifier.

General discussions are presents in Chapter 10. The chapter also summarize the thesis and draws general conclusions. MatLab-code, some PSCAD-files and some calculations performed in Excel are found on the CD attached to the report. The PSCAS-files and the Excel-files are not user-friendly, but could be a help for people who want to continue my work. The files are sorted by the chapter they are presented in.

2 Grid connection of large offshore wind farms

In this section, different layouts for large offshore grid connections are discussed. Economic and energy efficiency of commercial solutions used today and alternative solutions are considered. In [27] and [28], layouts of various large-scale wind farms, using both HVAC as well as HVDC, are investigated. The criteria in this investigation is the energy production cost, which is defined as the total investment cost divided by the total energy production of the wind farm.

2.1 High voltage DC (HVDC)

HVDC transmission may be the only feasible option for connection of a wind farm if the distance exceeds 100-150 km. HVDC transmission offers many advantages for integration of large offshore wind farms:

- The power follow is fully defined and controlled.
- Faults on one AC network will not directly affect the AC voltage on the other networks because the networks are decoupled by the asynchronous connection.
- There is no technical limit on the transmission distance with a DC cable, as it is for AC cables.
- A pair of DC cable can carry up to 1600 MW.
- The cable power loss is lower than an equivalent AC cable [15]

It is often difficult to find suitable grid connection point. If HVDC is used, the power could be directed to a stronger grid connection point with minimal increase in cost and transmission losses. It might also be necessary to use DC-cables for the onshore transmission, because it could be difficult to get permission to build new over-head lines. [27]

2.1.1 Voltage source converter (VSC)

There are two main HVDC transmission technologies: voltage source converter (VSC) using IGBTs and line-commutated converter HVDC (LCC) using thyristors.

VSC is self-commutating and it does not require an external voltage source for its operation. The reactive power can be controlled by the power converters and it is independent of the active power control. Power can be transported to the wind farm when necessary and the AC voltages on both sides can be controlled. No AC harmonic filters for reactive power control are needed. However, VSC transmission does have higher power loss compared with a LCC HVDC system. Typically, the total losses at full load for the two converters are about 3.5% for VSC and 1.5% for LCC HVDC. [15]

Figure 1 shows the single-line diagram for a VSC transmission system with DFIG generators. A three-level neutral point clamped converter is used instead of a two-level converter, resulting in lower power losses. [15]

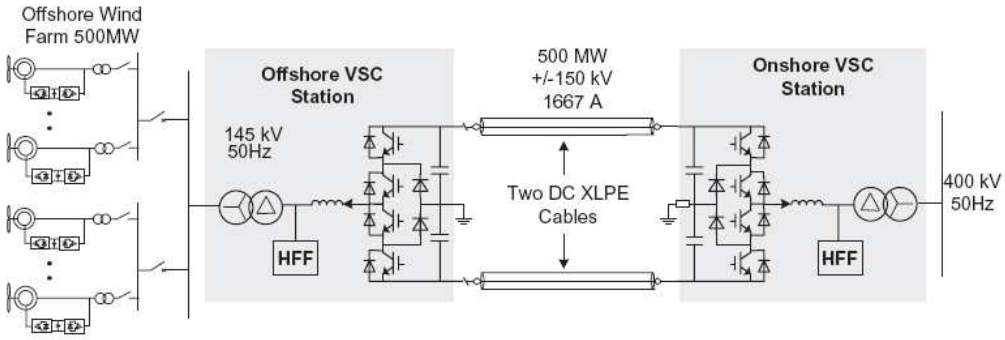

Figure 1: Single-line diagram of wind farm connection using VSC transmission. [15]

The advantages of HVDC VSC solutions are based on its capability to supply and absorb reactive power and to support power system stability. The disadvantage is that ground faults can be problematic. Main components of the transmission system based on VSC devices are; VSC converter station circuit breaker, system side harmonic filter, interface transformer, converter side harmonic filter, VSC unit, VSC DC capacitor, DC harmonic filter, DC reactor, DC cable or overhead transmission line and auxiliary power set. [18]

2.1.2 Line-commutated converter HVDC (LCC HVDC)

Line Commutated Converter (LCC) based transmission systems with thyristors have been successfully installed all over the world. LCC HVDC can be used for higher power levels than VSC. Power levels up to 1600 MW are available pr 2005. However, a LCC HVDC converter station occupies twice the area of a VSC transmission station. It is also necessary to provide a commutation voltage in order for the offshore LCC HVDC converter to work properly. Another draw back of this transmission solution is the required reactive power to the thyristor valves in the converter and the generation of harmonics. Filters and switchgear is therefore needed. Alternatively, a STATCOM could be used. This technology is very large in physical size, and the transistor technology is also more attractive due to the better controllability of the reactive power. [15] [18]

Main components of the transmission system base on LCC devices are; AC and DC filters, converter transformer, converter based on thyristor valves, smoothing reactor, capacitor banks or STATCOM, DC cable and return path, auxiliary power set and protection and control devises. [18]

2.2 Wind farm layouts

In this section different DC wind farm layouts are considered

2.2.1 Series connected wind turbines

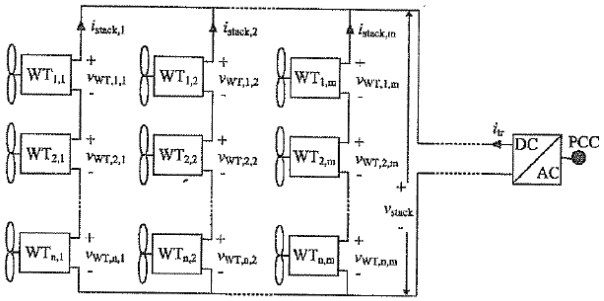

Figure 2: The layout of series-connected wind turbines with a DC output voltage [28]

Figure 2 shows a general layout of a wind farm with series connected wind turbines. There are two major advantages with this solution: no offshore platform is used and high voltage DC is used to bring the energy to shore. The transformers will be smaller and thus possibly cheaper compared to the systems of today, while the cost for the higher isolation at the output of the turbines will be higher. The total cost of the electrical system will probably be lower for the proposed system, according to [28]. For a 160 MW wind farm located at 55 km from a suitable grid connection point, this solution shows a potential of 8% cost reduction. [28]

The benefit of this system is that it, in spite of a relatively large possible size, does not require large DC-transformers and offshore platforms. The drawback with this configuration is that the DC/DC converters in the wind turbines must have the capability to operate towards a very high voltage.

A system with series connected wind turbines and synchronous generators do not need traditional components, such as gear boxes and local wind turbine 50 Hz transformers, which are related to major problems. There are fewer problems related to power electronics. If a diode rectifier is used instead of an IGBT rectifier to rectify the power from the generator, the power electronics will be even more reliable. [28]

2.2.2 Small DC wind farm

Figure 3 shows the electrical system for a small DC wind farm. The electrical system is identical to the system of the small AC wind farm. The only difference is that the transformer in the wind farm grid interface is replaced with a DC transformer and an inverter. Also, a rectifier is needed for each wind turbine, but no offshore platform is needed.

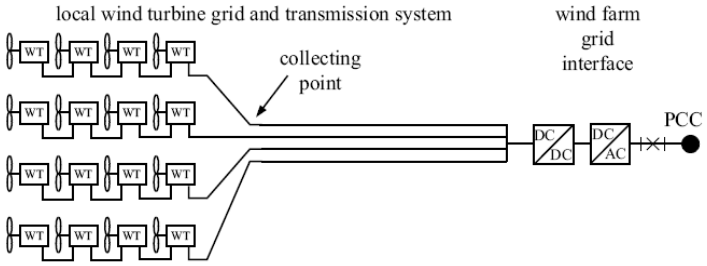

Figure 3: DC electrical system with series connected wind turbines [27]

2.2.3 Two-step DC/DC-converter system

In general, the DC-grid consists of several clusters, which are connected either in parallel or in series. Since the difference between the output power of each turbine and the total power transferred to the shore is huge, several voltage steps are preferred. Otherwise, either the generators must be designed for extremely high voltages or the transmission losses are increased significantly. A DC/DC converter could be used for stepping up the voltage. [6]

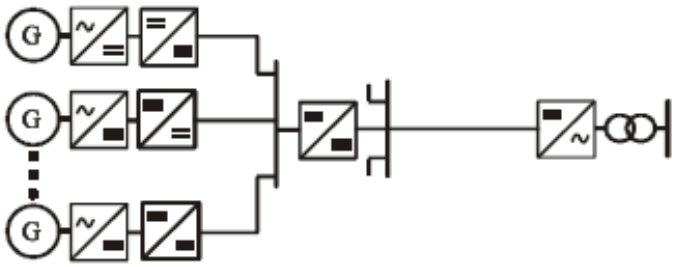

Figure 4: Schematic scheme for a two step-up configuration [6]

The voltage step up can be done in different places. Figure 4 shows the schematic scheme for a two step-up configuration. It uses two DC/DC-converter system, one system is stepping up the voltage after each turbine, up to a medium-voltage level. The power from many turbines is collected and the voltage is stepped up to the transmission level. An advantage of this system is the direct step-up of the voltage after the turbine which leads to reduced cable losses at the distribution level. The DC-link voltage at each turbine could also be controlled individually. However, the additional DC/DC-converter leads to extra losses and investment cost. [6]

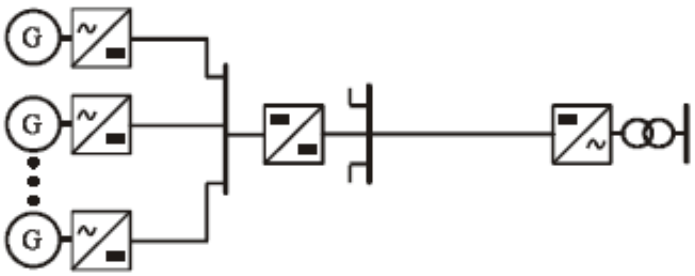

Figure 5: Schematic scheme for a Closter step-up configuration [6]

2.2.4 Cluster step-up

The second system is called a one Cluster step-up system and is shown in Figure 5. The DC-power from the generators is collected on an offshore platform and afterwards a large converter system is stepping up the voltage to the transmission level. The advantage of this system is that the number of converters is minimized and that a large converter has a higher efficiency. Since only two voltage levels are used, the distribution level strongly depends on the generator voltage, which today is limited to 5 kV line-to-line. [6] This system has a disadvantage if a variable speed PMSG with diode rectifier is used because the DC-link voltage could not be regulated individually for each turbine. Therefore the DC-link voltage will be the same for all turbines and the turbine rotation speed will not be ideal. The power will vary some with the turbine rotation speed. If the wind speed is more or less equal for the whole Cluster-area, this will not be a large problem. The DC-link voltage could in this case be regulated in such way that the turbines keep the optimal rotation speed for the average wind speed of all turbines.

2.2.5 Turbine step-up

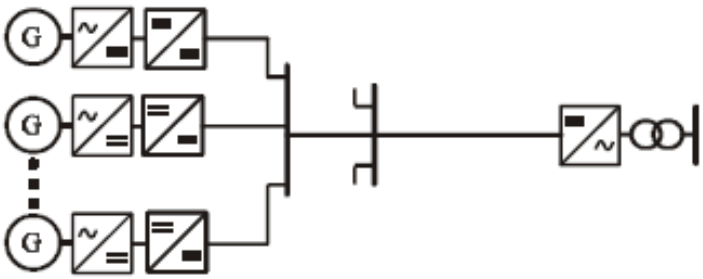

Figure 6: Schematic scheme for a Turbine step-up configuration [6]

The last system, the turbine step-up system shown in Figure 6, has DC/DC converters connected directly to each turbine. Only two voltage levels are used and the distribution level is reduced because of the high voltage. No offshore platforms are required. However, the DC/DC converter has to be designed for a low power level, which could reduce the efficiency of the converter. [6]

2.2.6 Energy losses for the step-up configurations

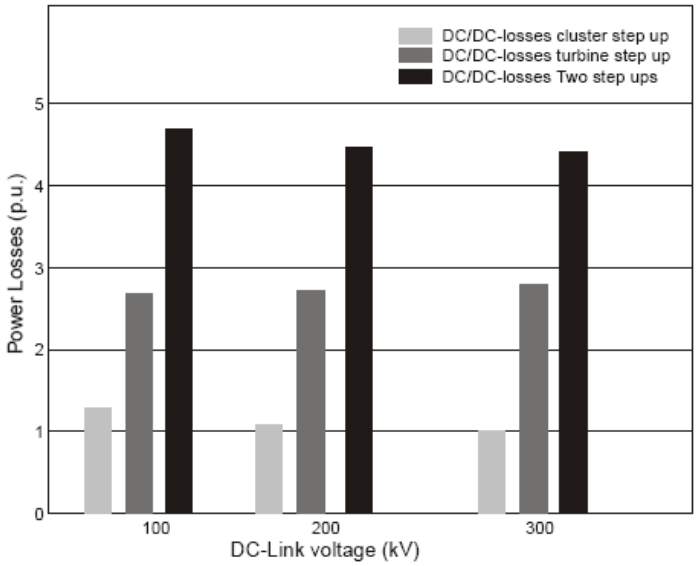

Figure 7: Power losses for different configurations of the DC-grid [6]

Figure 7 shows the losses of these three configurations for different DC-voltage levels. The wind farm size is 500 MW, the losses for the DC/DC converters were calculated analytically in [6] by using values from datasheets for the semiconductors and an additional loss model was used to find the transformer losses. The difference in losses does not vary significantly when the DC-link voltage changes. The figure shows that the Cluster step-up solution has the lowest losses. However, as seen, there are some disadvantages when this configuration is used in a variable speed PMSG application with diode rectifier. The Turbine step-up solution is the next best solution, but the losses are over twice as big as for the Cluster step-up solution. [6]

The main reason why the Cluster step-up solution has the lowest losses is that the distances are quit short within the wind farm. Therefore, it is not necessary to have a large internal DC voltage. Since a large converter has a higher efficiency, the power should be collected before the voltage is raised. The high output voltage of the turbine step-up solution and the low power level result in large losses for this solution. The

two-step-up solution has even more losses due to the use of two DC/DC-converters, one of them with low power level. [6]

2.2.7 System efficiency of two step DC/DC wind farm

System efficiency of a two step DC/DC wind farm layout is investigated in [14]. Three different converters have been compared; the fullbridge converter with phase shift control (FB), the single active bridge converter (SAB) and the series parallel resonant converter (LCC). [14]

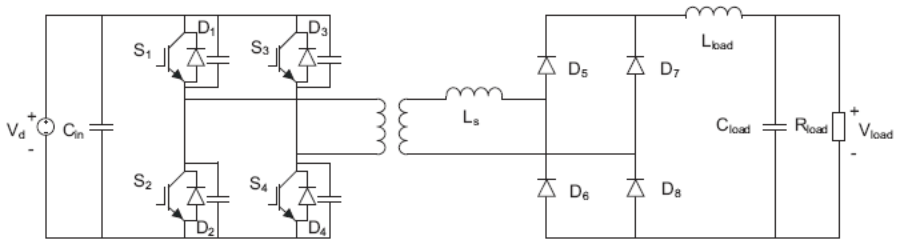

Figure 8: Typology for the fullbridge converter using phase shift control [14]

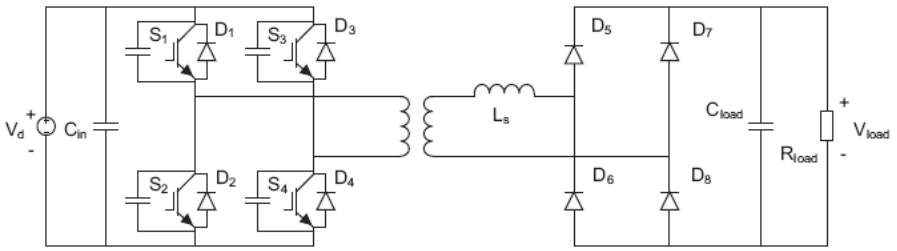

Figure 9: Typology for the single active bridge converter [14]

The typology of the fullbridge converter using phase shift control is shown in Figure 8. This converter has a significantly lowered performance when handling variations in the voltage and power. The output is current-stiff. A single active bridge converter in Figure 9 looks similar to the fullbridge converter. However, the control is different the output filter creates a voltage-stiff output. The series parallel resonant converter, shown in Figure 10, has lower switching losses because it switches at zero current and/or zero voltage. This is why this type of converter often has the lowest power loss. [14]

Two different control strategies are evaluated. In the first strategy (1) the DC/DC converter in the wind turbines handles all voltage variations. The input voltage of the first converter is 2-5 kV while the output voltage is 15 kV. In the second strategy (2) the

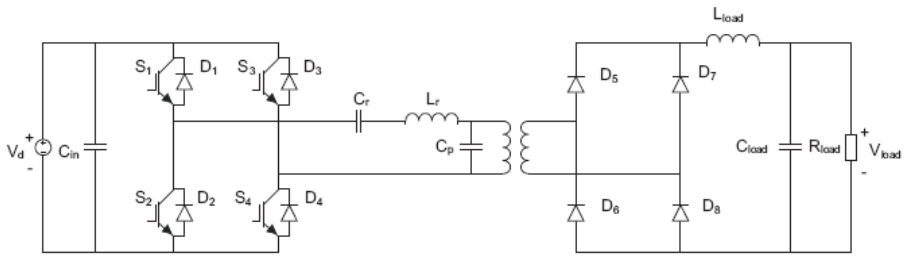

Figure 10: Typology for the series parallel resonant converter [14]

DC/DC converters in the wind turbines only handle the variations between the wind turbines in the same group and the group DC/DC converter handles the variations between the groups. The input voltage of the first converter is 2-5 kV while the output voltage is 6-15 kV. [14]

Control	5.4 m/s	7.2 m/s	10 m/s
1 FB	274 kW, 5.3 %	401 kW, 4.2 %	550 kW, 3.8 %
2 FB	178 kW, 3.5 %	304 kW, 3.2 %	449 kW, 3.1 %
1 SAB	503 kW, 9.8 %	776 kW, 8.2 %	1051 kW, 7.2 %
2 SAB	534 kW, 10.4 %	915 kW, 9.7 %	1331 kW, 9.2 %
1 LCC	123 kW, 2.4 %	214 kW, 2.2 %	318 kW, 2.2 %
2 LCC	143 kW, 2.8 %	256 kW, 2.7 %	385 kW, 2.6 %
Power	5.1 MW	9.5 MW	14.5 MW

Table 1: Average losses for the two control strategies and the three types of converters at different wind speeds [14]

Table 1 shows the average losses for the two different control strategies and for the three different converters. It becomes obvious that the power loss is less with the series parallel resonant converter. The first control strategy with constant output voltage of the first converter has the lowest total converter losses, 2.4%. The loss of the second control strategy is 2.8%. The solution with constant transformation on the second converter is therefore preferable. [14]

2.3 High voltage AC (HVAC)

According to [15], HVAC will be used for most wind farm application with a connection length off less than 50-75 km because this is the simplest and most economic grid connection method. If the connection distance exceeds 50 km, dynamic reactive power compensation may be required when the HVAC solution is used. [15]

2.3.1 Components of the HVAC transmission solution

The voltage level within an offshore wind farm grid is typically in the range of 30-36 kV. Therefore a substation is necessary for a large wind farm, to step up the voltage for the transmission to shore. A HVAC transmission system also needs; HVAC submarine transmission cables, offshore transformers, compensation units like thyristor controlled reactors (TCR) both offshore and onshore and, depending on the grid voltage, onshore transformers. [18]

2.3.2 HVAC transmission losses

%	500 MW		
Cable length	132 KV:3 cables	220 KV:2 cables	400 KV:1 cable
50 km	2,78	1,63	1,14
100 km	4,77	3,07	2,54
150 km	7,53	5,05	4,98
200 km	11,09	7,76	17,59

Table 2: Transmission losses of 500 MW wind farm with 9 m/s average wind speed (in percent) [18]

%	1000 MW		
Cable length	132 KV:5 cables	220 KV:4 cables	400 KV:2 cables
50 km	3,15	1,96	1,14
100 km	5,7	3,67	2,32
150 km	8,75	5,85	4,3
200 km	12,36	7,58	15,14

Table 3: Transmission losses of 1000 MW wind farm with 9 m/s average wind speed (in percent) [18]

Tables 2 and 3 show the transmission losses of wind farms with 9 m/s average wind speed for respectively 500 MW and 1000 MW rated power. The loss is given in percents of the annual wind farm production. As seen, the losses are lowest for the 400 kV solutions in both cases as long as the cable length is below 150-200 km. For larger cable lengths, the voltage level has to be reduced, as shown in Figure 14. This is explained in Chapter 2.4.2. [18]

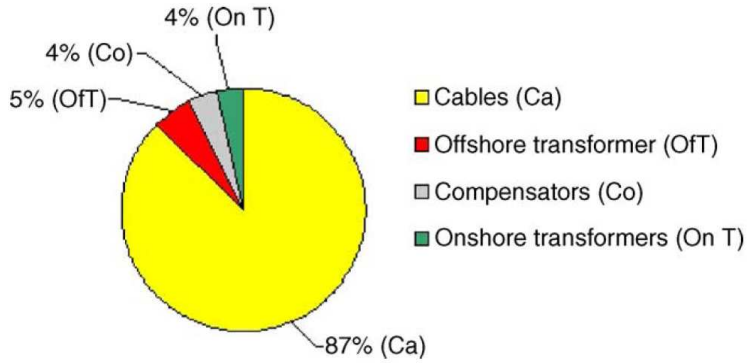

Figure 11: Participation of each transmission component in total transmission losses for 500 MW wind farm, 9 m/s of average wind speed, at 100 km transmission distance, three three-core 132 kV submarine cables [12]

Figure 11 shows the share each transmission component contributes to the total transmission losses for a 500 MW wind farm with a transmission distance of 100 km using a 132 kV cable. As seen from the figure, the cable losses represent the highest share of the total transmission losses. Thus, in order to decrease the total transmission losses, special attention should be given to the cable selection. [18]

2.4 Comparison between HVAC and HVDC

Using conventional HVDC transmission offers many advantages to an AC connection.

- Transmission distance is not a technical limitation since the transmission distance using HVDC is not affected by cable charging current [21] [20]
- Frequency at sending end can be variable and the sending and receiving end frequencies are independent [21] [20]
- Offshore installation is isolated from mainland disturbances [21]
- Power flow is fully defined and controllable [21]
- Proven and reliable equipment [21]

- Low cable power loss, due to no affects of cable charging current. [21]

- High power transmission capability for each cable. A pair of HVDC lines may carry 1.7 times the power of a similar sized AC line. [21]

Many factors influence whether HVAC or HVDC should be used. Kirky suggests in [20] that conventional HVDC will be the optimal solution when the distance offshore is greater than approximately 100 km and the wind farm size is greater than approximately 350 MW. HVDC could also be used when the connection into the AC network is at a weak point or a significant length AC transmission line onshore is needed to reach a suitable AC network connection point. The HVDC control of power may also assist in recovery, limit the effect or even correct the instability after different fault conditions. Therefore HVDC can be used where AC network studies and simulation show unstable behaviour. [20]

The high cost of the associated AC-DC converter infrastructure, offshore platform space and switching losses has generally limited the attractiveness of HVDC to very large installation located a long distance offshore. [1] As wind farms become larger and the distant from shore increases, the justification for using HVDC to transmit the power to the onshore network becomes easier, particularly at power levels of 500 MW or more. For larger wind farms, the cost of the converter stations and platforms per MW will become less. Existing voltage sourced converter (VSC) transmission technology can not offer an economical solution at this power level due to the high cost of the multiple converters and cables that are required. [20]

2.4.1 Energy production cost of different wind farms

Lundberg has analysed the economics of different wind farm layouts in his Phd. Thesis. Figure 12 shows the normalized energy production cost of the different 160 MW wind farms as function of the transmission distance. As seen, the series DC solution is the least expensive for all transmission length larger than 10 km. An increased investment cost of 13% can be allowed for the series DC park before the production cost becomes equal to the large AC park, according to [28].

The work done in [28] also shows that the energy production cost is strongly dependent on the average wind speed. As an example, the energy production cost at an average wind speed of $6.5 m/s$ was twice as high as the cost for an average wind speed of $10 m/s$. It was also found that the energy production cost decreases when the power of the wind farm increases. [27] This is an important reason to build offshore wind parks.

Figure 13 shows the cost of the AC and DC cables per km as a function of the rated power. It can be noted that the DC cables are much cheaper than the AC cables for the same rating.

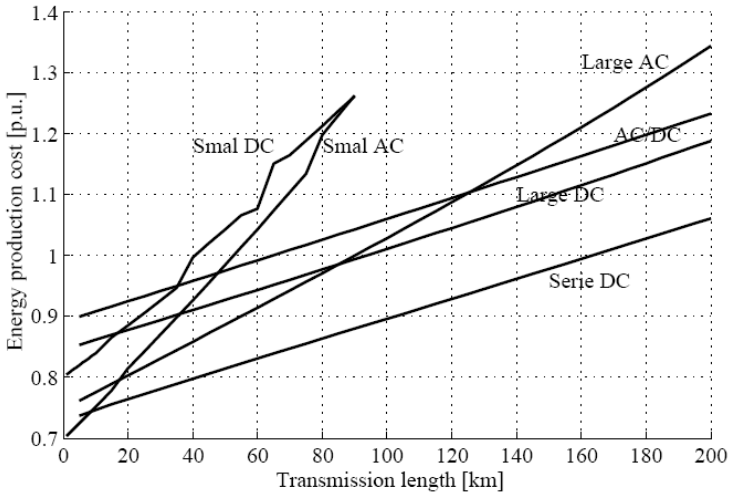

Figure 12: The normalized energy production cost of the different 160 MW wind farms as function of the transmission distance and at an average wind speed of 10 m/s [28]

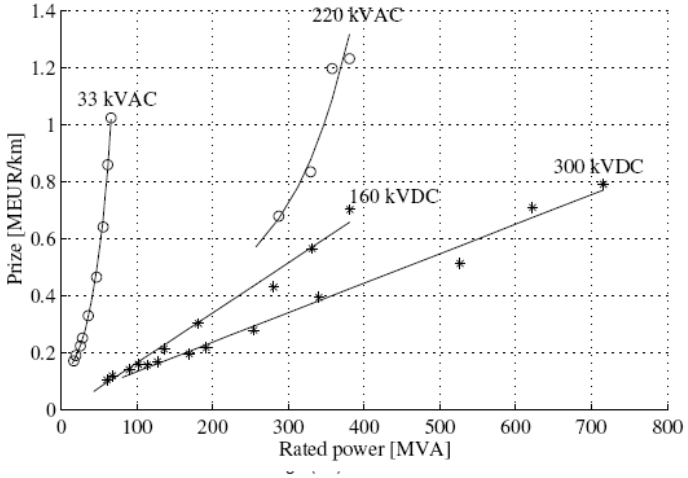

Figure 13: Cost of AC and DC cables per km [27]

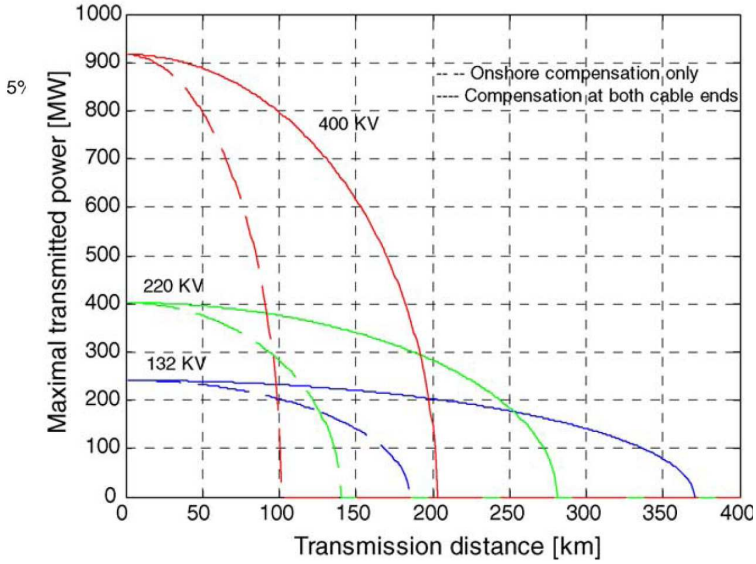

Figure 14: Transmission capacity of different HVAC transmission cables for three voltage levels, 132, 220 and 400 kV. [18]

2.4.2 Loss evaluation of HVAC and HVDC transmission solutions

In [18], losses for HVAC and HVDC transmission solutions for large offshore wind farms are compared. If HVAC cables are used, the transmission distance would be limited. A comparison of the transmission capacity of different cable operated at certain voltage levels (132, 220 and 400 kV) and different compensation solutions (only onshore or at both ends) is presented in Figure 14. The critical distance is achieved when half of the reactive current produced by the cable reaches nominal current at the end of one cable; 370 km, 281 km and 202 km for respectively 132 kV, 220 kV and 400 kV. [18]

	500 MW, 9 m/s			1000 MW, 9 m/s			
Length Cable	500 CS	2 x 250 CS	600 CS	2 x 500 CS	600 CS + 440 CS	500 CS + 600 CS	2 x 600 CS
50 km	1,77	1,81	1,75	1,69	1,60	1,66	1,6547
100 km	1,98	2,14	1,87	1,92	1,77	1,84	1,7819
150 km	2,19	2,48	1,99	2,14	1,95	2,01	1,909
200 km	2,39	2,82	2,11	2,37	2,13	2,19	2,0362

Table 4: Transmission losses for different HVDC LCC converter station layouts with 9 m/s average wind speed (in percent) [18]

Three different HVDC LCC layout are considered for a 500 MW wind farm and four for a 1000 MW wind farm in [18]. Loss model and assumptions are also given here.

The transmission losses are given Table 4. When this table is compared to Tables 2 and 3 it becomes obvious that the transmission losses are much lower for a HVDC LCC solution than a HVAC solution. The total HVDC losses are about one fourth of the HVAC transmission losses for 200 km cable length. [18]

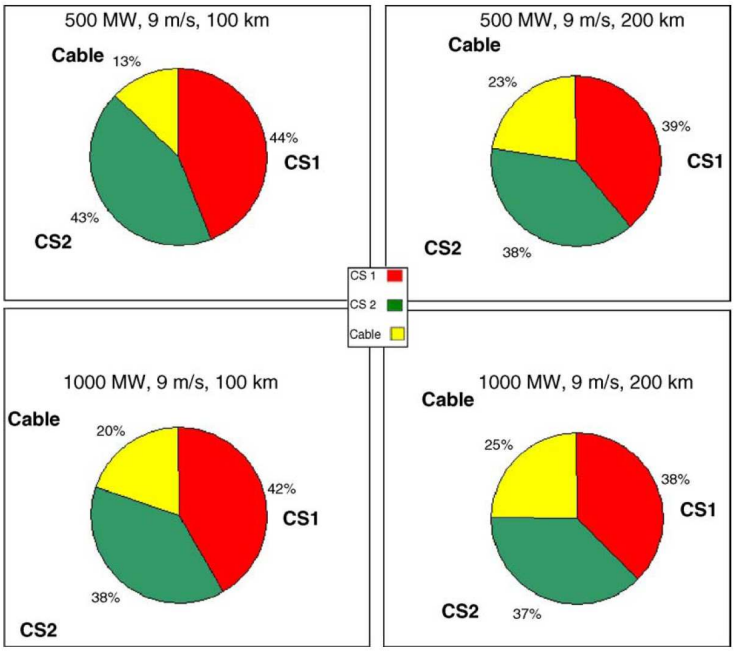

Figure 15: Loss participation for the HVDC LCC system losses. [18]

Loss participation of each component in the system for some configurations is shown in Figure 15. Converter stations are responsible for the highest share of the overall system losses. The participation of the cable increases with cable lengths.

Figure 16 shows the conclusion; HVAC has lowest losses for transmission length less than 55-70 km. The losses in this area depend mostly on the distance to the shore. For larger transmission lengths, the HVDC LCC solution has the lowest losses. As seen from the figure, the losses in this area also vary with the wind farm rated output power. The tendency is that percent loss decrease when the size of the wind farm increase, but the loss percent will also depend on the converter station layout. The HVDC VSC solution has higher losses than the HVDC LCC solution for all power outputs, and are therefore not shown in Figure 16. [18]

In [18], three different HVDC VSC layout are considered for a 500 MW wind farm and two for a 1000 MW wind farm. Loss model and assumptions are given in [18]. The transmission losses are given Table 5. When this table is compared to Table 4 it becomes obvious that the transmission losses are over twice as high for the VSC solution than for the HVDC LCC solution. Figure 17 shows that the converter stations contribute most to the overall system losses and that the share of cable losses increases with length. [18]

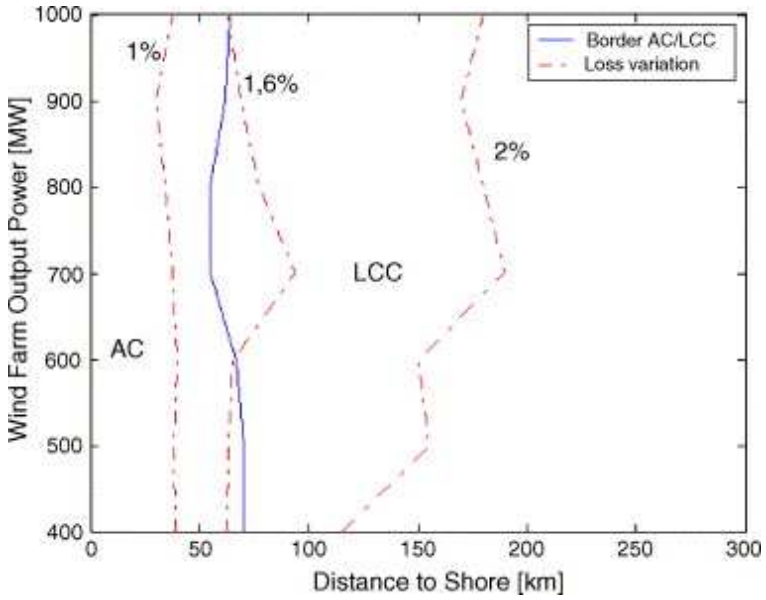

Figure 16: MW-km plane, comparison HVAC-HVDC LCC for different wind farm size and different distances to shore [18]

	500 MW, 9 m/s			1000 MW, 9 m/s	
Length Cable	350 + 220 CS	2 x 350 CS	500 CS	3 x 350 CS	2 x 500 CS
50 km	4,05	4,21	4,43	4,02	4,0893
100 km	4,43	4,58	4,87	4,52	4,5597
150 km	4,82	4,94	5,31	5,02	5,0317
200 km	5,20	5,30	5,75	5,52	5,505

Table 5: Transmission losses for different converter station layouts with 9 m/s average wind speed (in percent) [18]

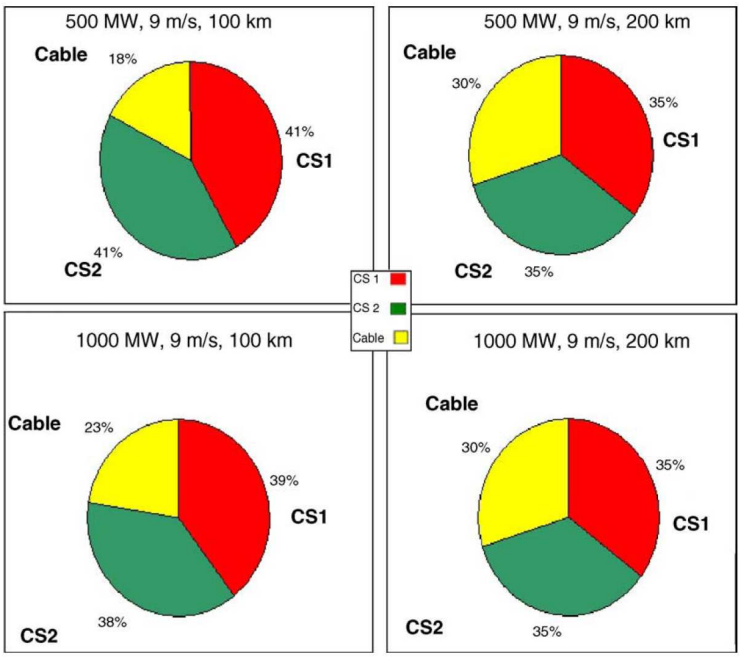

Figure 17: Loss participation for the HVDC VSC system losses. [18]

2.5 Design criteria for offshore installations

Offshore equipment is exposed to extreme weather, salt and moist air and should be designed for these circumstances and the equipment must be located indoors or in sealed enclosures. Equipment should be as compact as possible, to reduce the overall size and weight and thereby the construction cost. Multistorey structure can be used. It should also have high reliability and should be as simple as possible with long maintenance intervals or preferably no maintenance at all. [20]

Some form of UPS, generator, battery or a combination of these is needed to ensure power supply when there is no wind. Load should therefore be graded into essential and non-essential. AC busbar voltage should also be as low as possible to reduce AC harmonic filter and switchgear size.

3 PMSG and generator losses

3.1 PMSG

A direct driven permanent magnet synchronous generator is lighter and more reliable than the traditional solution with an asynchronous generator and a gear. The gear needs maintains and is very heavy. Both weight and reliability are important for offshore floating wind turbines. A light nacelle means less force on the tower. The tower and the floating structure can therefore be made cheaper. Good reliability is important because it is difficult and expensive to access the turbines.

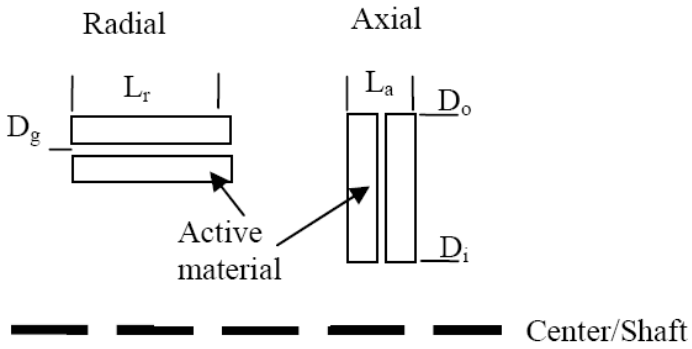

Figure 18: Comparison of the diameter of active material in radial and axial machines [33]

There are generally three types of permanent magnet machines; radial, axial and transversal flux machines. The radial flux machine (RFPM) is the classic type and the most common. The rotor can have buried or surface mounted magnets and the both the stator windings and tooth shape are quit similar to other AC-machines. The active materials, such as copper, magnets, iron and sheet metal is the material converting the mechanical energy to electrical. These are place along the air gap. In wind turbines the generator diameter is large and thereby the layer with active material is pretty thin. Since the radius is large, the torque will also be large. [33]

Axial flux machines (AFPM) is magnetized in the axial direction, as shown in Figure 18. Given the same outer diameter and the same force per area in the air gap, the AFPM has a lower torque per volume of active material due to the fact that much of the force is working in a smaller radius and thus producing less torque. However, the volume of the machine can be reduced because the power density (W/m^3) is higher. The AFPM usually has a large diameter and a short length. The generator has a disc shaped design and these discs can be connected in series. As for RFPM the rotor in an AFPM can be made with surface mounted or buried magnets. [33]

The third machine is the most complex and least equal to classic machine design, the transversal flux machine (TFPM). It can be single sided or double sided respectively

with one or two wound rings of copper with iron cores to lead the magnetic flux around the copper. The permanent magnets can be either buried or surface mounted. The machine has very high force and power density, and is therefore ideal for high torque, low speed applications, such as wind turbines. To achieve this high power density, the synchronous reactance becomes very high, which makes the converter expensive. The TFPM itself can also be expensive due to the complex design and many parts. [33]

3.2 Modelling of a PMSG

The permanent magnet synchronous generator is modelled in a d-q-o reference frame fixed to the rotor. Equation (1) and (2) are found in [9]. Equation (1) shows the stator voltage equations and Equation (2) shows the flux linkage equations. The damping windings are replaced with two equivalent windings D in direct and Q in quadrature axis. Figure 19 shows the schematic model. The electromagnetic torque is given by Equation (3). The simulink model is found in [9].

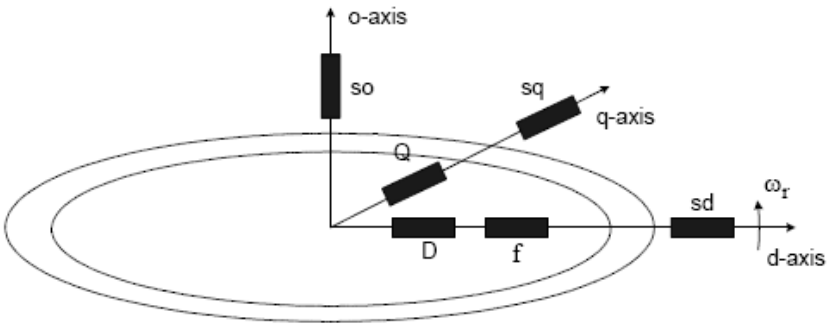

Figure 19: Schematic of the transformed model for PM synchronous machine in the d-q-0 reference frame [9]

$$
\begin{aligned}
u_d^s &= R_s i_d^s + \frac{d\psi_d^s}{dt} - \omega_r \psi_q^s \\
u_q^s &= R_s i_q^s + \frac{d\psi_q^s}{dt} + \omega_r \psi_w^s \\
u_0^s &= R_s i_0^s + \frac{d\psi_0^s}{dt} \\
u_D &= R_s i_D + \frac{d\psi_D}{dt} \\
u_Q &= R_s i_Q + \frac{d\psi_Q}{dt}
\end{aligned}
\tag{1}
$$

$$
\begin{aligned}
\psi_d^s &= L_d i_d^s + M_f I_f + M_D i_D \\
\psi_q^s &= L_q i_q^s + M_Q I_Q \\
\psi_0^s &= L_0 i_0 \\
\psi_f &= L_f I_f \\
\psi_D &= L_D i_D + M_{fD} I_f + M_D i_d^s \\
\psi_Q &= L_D i_Q + M_Q i_q^s
\end{aligned}
\tag{2}
$$

$$
T_e = \frac{3}{2} P \left(\psi_d^s i_q^s - \psi_q^s i_d^s \right) \tag{3}
$$

The model takes into account the iron losses as well as the parameters´ variation with the operating temperature. The temperature depends on the rotor speed [9]

3.3 Harmonics and losses in the generator

The total harmonic distortion (THD) describes the content of harmonics in a voltage or current waveform. A low THD means the first harmonic is dominating and the content of higher harmonics is low. This is normally preferred since only the first harmonic is contributing to power production, while higher harmonics causes losses. The THD in the current is define in Equation (4). I_{s1} is the first harmonic of the current and I_{sh} is the h^{th} harmonic of the current. [22]

$$
THD\neg_i = \sqrt{\sum_{h \neq 1} \left(I_{sh} I_{s1} \right)^2} \tag{4}
$$

Harmonic currents in the stator cause losses in the generator. Basically the total power losses generated in the permanent machine can be divided into two groups; copper losses and core losses. The copper losses (P_{cu}) are produced in the stator winding and depend on the RMS current. This is shown in Equation (5). I_{a_i} is the RMS value of the i^{th} harmonic component of the current I_a and R_a is the stator equivalent resistance. When the current level increases, the temperature increases and so the stator resistance R_a. This effect is not included in the calculations. [26]

$$
P_{CU} = 3 R_a \sqrt{\sum_{i=1}^{\infty} I_{a_i}^2} \tag{5}
$$

Equations (4) and (5) show that the copper power losses are proportional to $1 + THD$. If a diode rectifier is used to rectify the voltage from a permanent magnet synchronous generator, the THD of the current may be about 0.30, resulting in 30% larger copper power loss than the case with no current harmonics. The harmonics causes high frequency flux changing, causing hysteresis (P_h) and eddy current power

losses (P_e). The total core losses are given by Equation (6). Equations (7) and (8) show the hysteresis and eddy current power losses when the harmonics of the voltage are known. [26]

$$P_{core} = P_e + P_h \cong \left(k_e f^2 B_{max}^2 + k_h f B_{max}^2\right) \times Weight \tag{6}$$

$$\frac{P_e}{P_{e1}} \approx \sum_{i=1}^{\infty} \left(\frac{V_i}{V_1}\right)^2 \tag{7}$$

$$\frac{P_h}{P_{h1}} \approx \sum_{i=1}^{\infty} \left(\frac{V_i}{V_1}\right)^2 \frac{1}{i} \tag{8}$$

k_e and k_h are constants, B_{max} is peak flux density, f is the rated frequency, weight represents the core and copper weight, P_{h1}, P_{e1} and V_1 are the hysteresis losses, eddy current losses and the line to line output voltage respectively at the nominal condition resistive load without harmonics. These equations show that the core losses increase when the voltage harmonics increase. [26]

4 PMSG with diode rectifier

In this chapter, a solution with a PMSG with diode rectifier is considered. When a diode rectifier is used, special attention on the reactive power from the rectifier, power support to the generator and on the low order harmonics created by the diode rectifier is needed. The low orders harmonic can create ripple in both the torque produced by the generator and in the power after the rectifier. The number of phases in the generator can reduce the impact of the harmonics. Filters can also be placed between the generator and the rectifier. A DC/DC converter is used to control the DC-link voltage, and thereby the torque of the PM generator with diode rectifier. The DC-link voltage is controlled by controlling the current going into the DC/DC converter. [28]

4.1 PMSG with active rectifier

A solution with a diode bridge rectifier is much simpler and more reliable than a solution with IGBTs. However, the stator flux can not be controlled. [16] suggest that the generator volume is almost doubled compared to using an active rectifier.

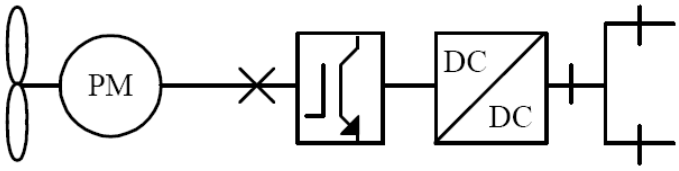

Figure 20: Principal scheme of the 2MW DC wind turbine with full variable speed and IGBT rectifier [28]

Figure 20 shows a principal scheme of a permanent magnet generator with IGBT rectifier and a DC/DC converter. The benefit with the IGBT rectifier is that the torque of the generator, the generator currents, stator flux and active and reactive power to the generator can easily be controlled. Since the generator current can be controlled for maximum torque output, the generator size, weight and cost can be minimized. It is also easy to obtain a smooth torque, a desirable flux level in the generator and a good quality of the DC-link voltage. [16] [28]

Any type of generator can be used since the reactive power can be controlled. Another advantage of the IGBT rectifier is that it keeps the input voltage to the DC/DC converter constant. The DC/DC converter can therefore be optimized because it operates as a constant ratio DC transformer in normal operations. However, these active rectifiers are both expensive and subject to failure. Reliability is important for offshore applications since maintenance and repair is extremely expensive and the access to the turbines is difficult in bad weather conditions. [16] [28]

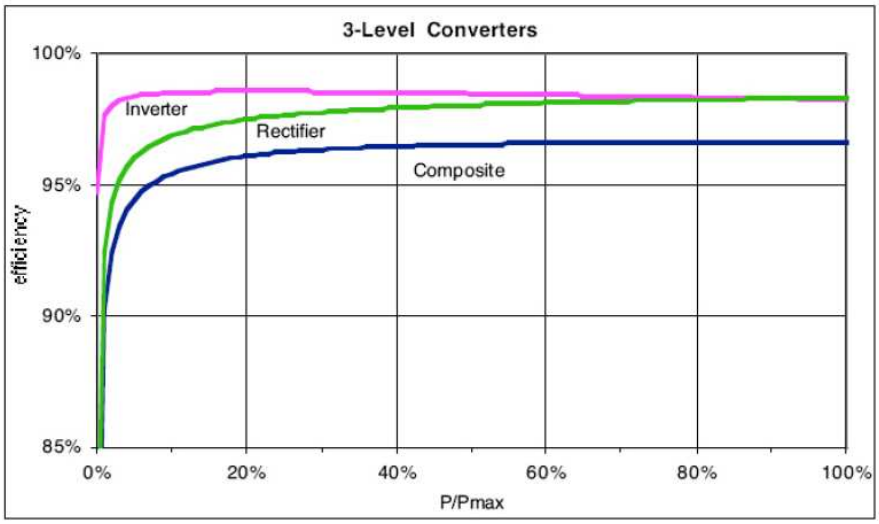

Figure 21: 3-level IGBT converter efficiency. [17]

Figure 21 shows the IGBT rectifier efficiency for a 50kW converter for wind power applications. The losses is about 2% for rated power, and the efficiency of the converter decreases when the power level decrease.

4.2 Three-phase, full bridge diode rectifier

A three-phase, full-bridge diode rectifier is shown in Figure 22. The inductors L_s is in this case the synchronous reactance of the permanent magnet synchronous generator. The DC-link voltage is found from Equation (9). V_{LL} is the line-to-line induced voltage in the generator, I_d is the phase current and ΔV_d is the voltage drop on the DC-link caused by the synchronous reactance. As seen from this equation, the DC-link voltage will decrease when the current in the machine increase, or the current will increase when the DC-link voltage decrease. Thereby, the DC-link voltage can be used to control the machine current and the machine power.

$$V_d = V_{do} - \Delta V_d = 1.35 V_{LL} - \frac{3}{\pi} \omega L_s I_d \tag{9}$$

4.3 PMSG with diode rectifier and series compensation

The generator could be equipped with phase compensating capacitors, in series with the stator windings, as shown in Figure 24. If a diode rectifier is used to rectify the power from a permanent magnet generator, the load power angle is always zero, and can not be controlled. Figure 23 shows the phasor diagram for a series compensated generator. The load voltage U_{load} is in phase with the generator current I. To have a

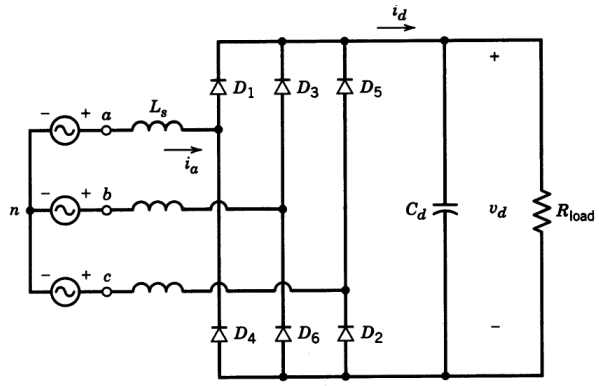

Figure 22: Three-phase, full-brigde rectifier [22]

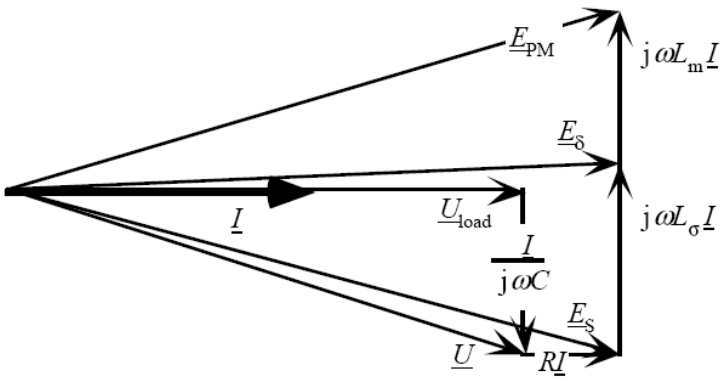

Figure 23: The phasor diagram for the series-compensated generator, drawn for one specific compensation. [3]

maximum power output from the generator, the current I has to be in phase with the induced voltage E_{PM}. The size of the capacitor has to be chosen so that this fits for the highest rotation speeds and the maximal power.

Series compensation has the advantage that the reactive power produced by the compensation follows the variations in the generators reactive power consumption, as the generator currents changes. However, the compensation level change when the generator speed change since the inductance reactance decrease when the generator speed decrease, and the capacitor reactance increase when the generator speed decrease. This is shown in Equation (10). [3]

$$\begin{aligned} U_{load} &= E_{PM} - \left(j\omega \left(L_m + L_\sigma \right) I + RI + \frac{I}{j\omega C} \right) \\ &= E_{PM} - \left(j\omega LI + RI + \frac{I}{j\omega C} \right) \end{aligned} \tag{10}$$

E_{PM} is the induced voltage in the generator, U_{load} is the generator output voltage, I is the generator current, R is the stator resistance, L_m is the magnetising inductance, L_σ is the leakage inductance, L is the total inductance and ω is the electrical frequency.

The total impedance of the generator synchronous reactance and the serie connected capacitance is given by Equation (11). As seen, the capacitance needs to be quite high to make the total impedance zero. If the capacitance is to low, the generator will be overcompensated.

$$X_{total} = \omega L - \frac{1}{\omega C} = \omega \left(L - \frac{1}{\omega^2 C} \right) \tag{11}$$

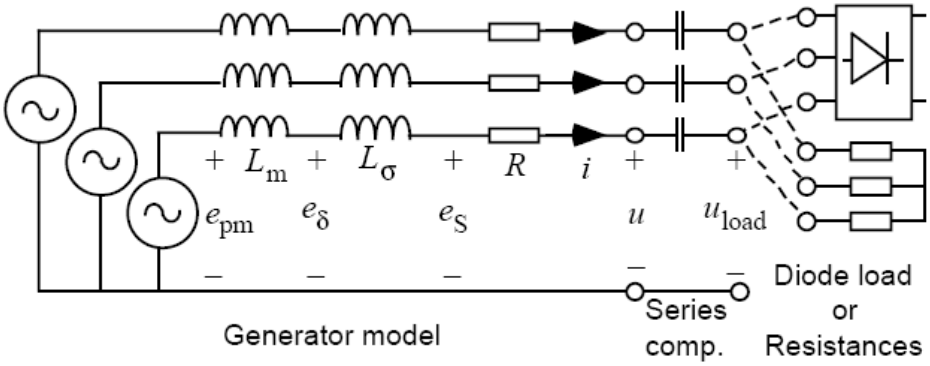

Figure 24: The series compensated generator with diode rectifier [3]

The emf e_{PM}, shown in Figur 24, is the no-load voltage, produced by the permanent magnets and depends on the generator speed. e_δ is the voltage induced by the air gap

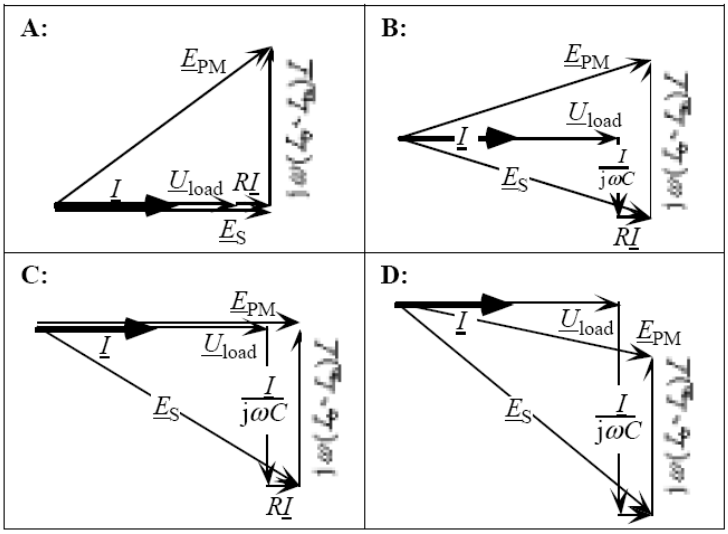

Figure 25: Phasor diagram for different compensation: A) no 0% B) half 50% C) full 100% D) overcompensated 133% [3]

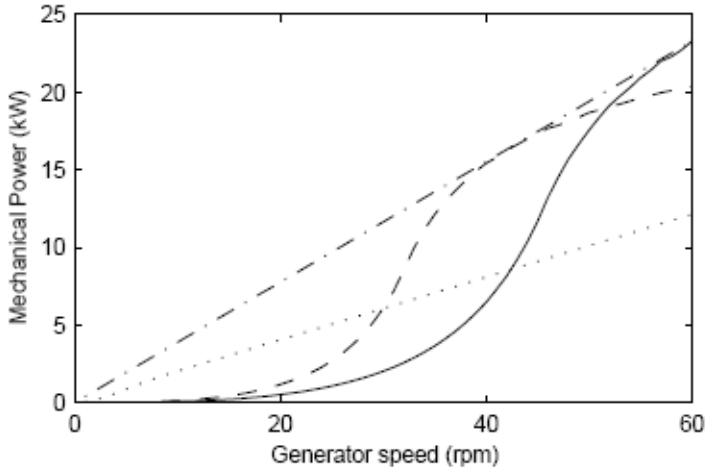

Figure 26: The maximal mechanical power as a function of speed. No compensation (dotted), 50% compensated (dashed), 100% compensated (solid) and maximum power output (dash-dotted) [3]

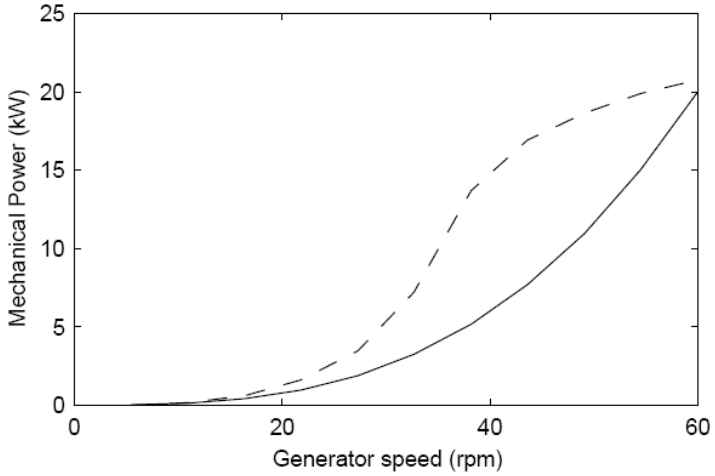

Figure 27: The maximal mechanical power with 50% compensation at rated speed (dashed) and power production by a wind turbine (solid) [3]

flux density. The total emf in the stator winding is e_s, which is proportional to the flux linkage of the stator.

The compensation level is defined as the relative size of the generators total inductance, $\omega\left(L_\sigma + L_m\right)$. This is the same as the percentage of the generators reactive power consumption which is produced by the series compensation. Figure 25 shows phasor diagram for different compensation levels. As seen from the figure, the angle between the induced voltage E_{PM} and the current I decreases when the generator speed increases. [3]

However, the compensation level change when the generator speed change, as explained earlier. The generator reactance decreases and the capacitor reactance increase when the generator speed decreases. Consequently, the level of compensation increases and the generator will be overcompensated at low speed. Over compensation will reduce the maximum power production for low speed in the same way as under compensation for high generator speeds. As mention, to have a maximum power output from the generator, the current I has to be in phase with E_{PM}. This is equal to 100% compensation. If the generator is overcompensated (over 100% compensation), the current I is before the induced voltage E_{PM}, causing the maximum power to decrease. [3]

In Figure 26, the maximum mechanical power of the generator, as a function of generator speed, is plotted for different compensation levels. Full compensation at rated speed leads to the highest power at rated speed, shown as solid. However, as the speed decreases, the maximal generator power is quickly reduced because of the generator being more and more overcompensated. If the turbine is half compensated at rated speed, shown as dashed, the maximal power decreases slower when the

generator slows down. If no reactive compensation is used, the maximal power for the highest generator speed is reduced to about half of the maximum power with reactive compensation. [3]

Figure 27 shows the maximum mechanical power of a generator with 50% compensation at rated power and the power produced by the wind turbine. As seen from the figure, the power produced is lower than the maximum mechanical power for all generator speeds. [3]

The maximum power output from the generator is achieved when the current I is in phase with E_{PM}. However, it is more likely that a generator with high inductance will be controlled to keep the absolute value of E_S equal to the absolute value of E_{PM}. The flux leakage of the stator is proportional to E_S so a smaller compensation level allows a smaller generator design. In this case, the stator flux linkage equals the no-load value. [3] 50% compensation is therefore used in the simulations.

To minimize the losses in the generator, the current and the magnetic flux should be minimized. They are both causing losses, which is usually the main limiting factor in large electrical machines. The core losses are much lower than the copper losses in a low speed generator and are therefore neglected in this model. The induced voltage e_{PM} is assumed to be sinusoidal because the harmonics content is only a few percents of the total voltage. This means that the current harmonics cannot contribute to the produced power. [3]

The size of the capacitors can be changed to change the compensation level when the rotating speed increases or decreases. This will make the power output from the turbine as high as possible for all rotating speeds. The variations must be done in steps, and as few steps as possible because each step increase the system costs. One possibility is to have a 100% compensation level for rated speed. When the speed decreases to a certain level, the size of the total capacitor increases so that the compensation level becomes 100% for this generator speed. [3]

There are two ways of connecting the capacitors: in parallel or in series. A switch is needed to disconnect one of the capacitors. If a parallel connection is used, the second capacitor has to be connected to increase the capacitance, since the total capacitance is the sum of the two capacitors, as shown in Equation (12). C_1 has to be dimensioned for maximal current and voltage at rated speed. C_2 can be dimensioned for a lower current.

$$C_{tot} = C_1 + C_2 \tag{12}$$

If the capacitors are connected in series, the second capacitor has to be disconnected to increase the capacitance, since the total capacitance is given in Equation (13). C_1 can therefore be dimensioned for some lower voltage than for the alternative with parallel connection. The current rating will be the same.

$$C_{tot} = \frac{C_1 \cdot C_2}{C_1 + C_2} \tag{13}$$

The generator currents depend on whether the diode rectifier is connected to a

voltage stiff or to a current stiff DC-link. If a current stiff DC-link is used, the current going into the generator will be nearly square, resulting in harmonics and lower maximum power output. It is only the fundamental current component which produces active power while the limited rated current is the rms-value of the current, including the harmonics. Therefore the harmonics should be reduced to increase the maximal power output and reduce the losses.

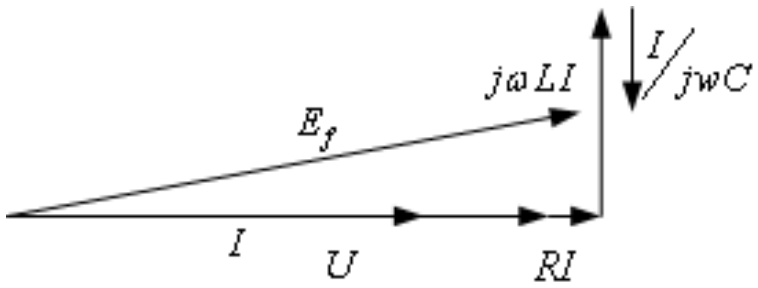

Figure 28: Phase diagram for series connected capacitors

Figure 28 shows the phase diagram for a PMSG with series connected capacitors. It is assumed that all currents and voltages are sinusoidal; no harmonics appears. As seen from the figure, the angle between the induced voltage and the generator current can be reduced by selecting a suitable value of the capacitor. If the capacitance is to low, the induced voltage will have a negative angle compared to the generator current, and the system will be overcompensated.

Equations (14) to (18) are used to calculate the generator current as a function of the output voltage. In Equations (14) and (15) the real and imaginary part of the induced voltage E_f is found from the phase diagram. This is used to find the absolute value of E_f in (16). A second order expression for the generator current I is found in Equation (17) and the generator current is expressed in Equation (18).

$$E_{f,re} = U + RI \tag{14}$$

$$E_{f,im} = XI \tag{15}$$

$$E_f^2 = E_{f,re}^2 + E_{f,im}^2 \tag{16}$$

$$(R + \omega L)\, I^2 + 2RUI + U^2 - E^2 = 0 \tag{17}$$

$$I = \frac{-2UR + \sqrt{(2UR)^2\, 4\,(R + \omega_e L)\,(U^2 - E_P M^2)}}{2\,(R + \omega_e L)} \tag{18}$$

Some simple tests using these equations are performed in MatLab. The machine data for the 55kW PMSG in "Vindlabben "is used. These are shown in Table 6. The result is shown in Figures 29, 31 and 30. All voltages and currents are assumed to be sinusoidal. When a diode rectifier is used, this will not be the case. The DC-link voltage is also assumed to be proportional to the voltage on the input of the diode rectifier.

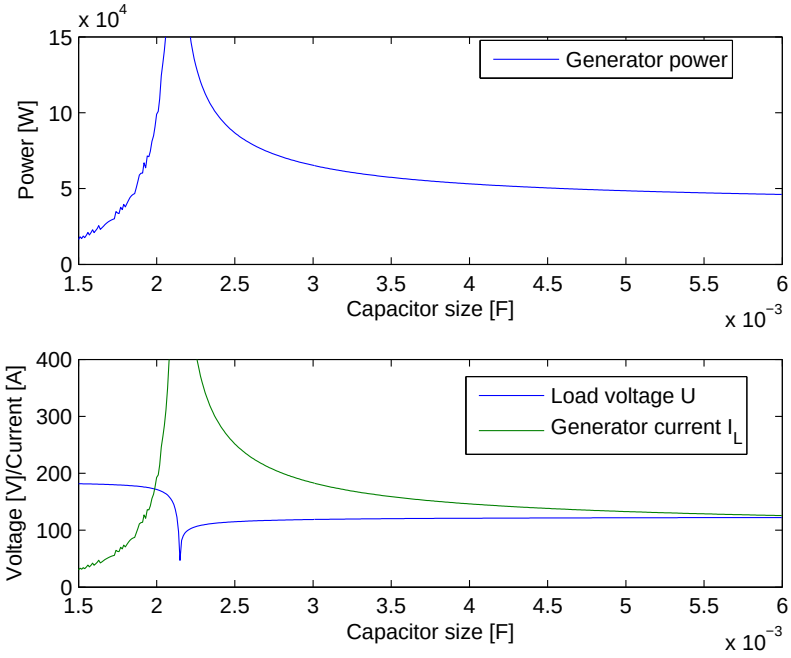

Figure 29: Maximum power [W] with respectively load voltage [V] and generator current [A] as a function of capacitor size

Figure 29 shows the maximum power output with respectively load voltage and generator current for increasing capacitor size. If the capacitor is less than 2300μF, the generator is overcompensated at a generator frequency at 50Hz. If the capacitor is larger, the generator is undercompensated, as wanted. For a capacitor size of about 2300μF, the sum of the generator synchronous reactance and the reactance of the capacitor is about zero. This will allows a very large current to flow through the generator, because only the resistance of the generator windings limits the current. The generator power is also high, due to the high current. The generator current can be reduced by increasing the load voltage.

Figure 30 shows the maximum power output with respectively load voltage and generator current as a function of generator frequency. As seen the generator power is very low for low frequencies, however, the turbine power is also low because of the low wind speed. The total reactance is almost zero when the generator frequency is 33Hz.

Figure 31 shows the power output and the generator current at 50Hz generator frequency as a function of the load voltage. As seen from the figure, the current

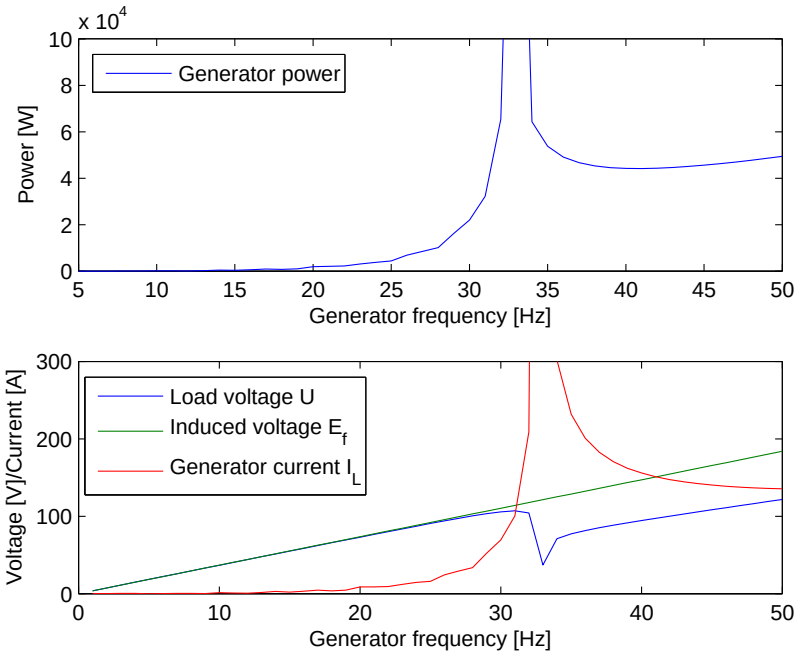

Figure 30: Maximum power [W] with respectively load voltage [V] and generator current [A] as a function of generator frequency

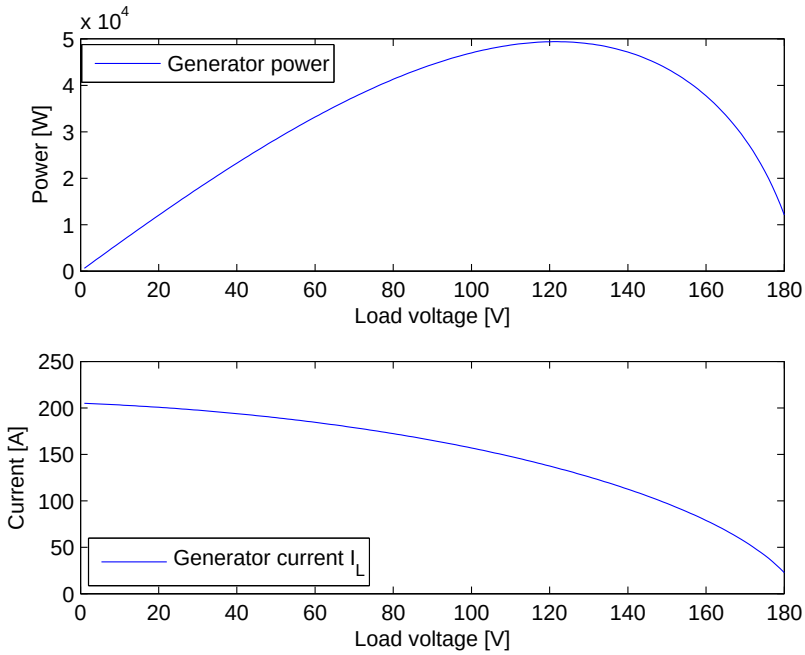

Figure 31: Maximum power [W] with respectively generator current [A] as a function of load voltage

is actually decreasing when the generator power increases. The maximum power is reached for a relatively low load voltage.

4.4 PMSG with diode rectifier and parallel compensation

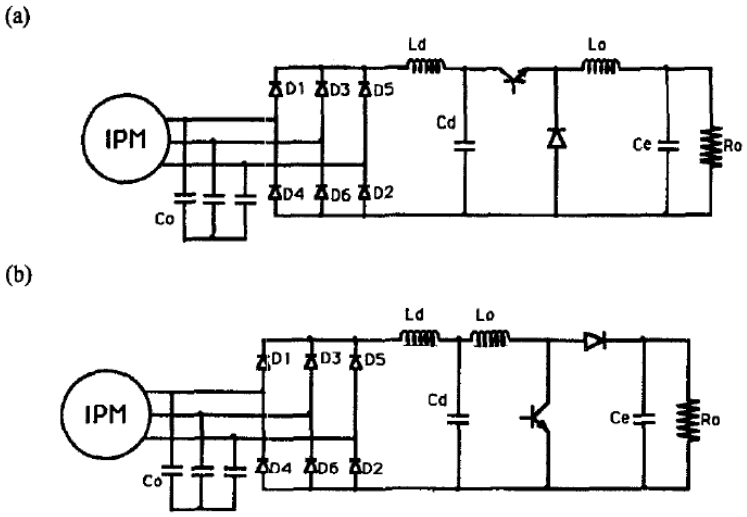

Figure 32: Schematic diagram of PM generator system. (a) With DC-DC buck converter, (b) With DC-DC boost converter [24]

The reactive power absorb by the permanent magnet synchronous generator could also be compensated with conductors in parallel with the generator. Figure 32 shows a schematic diagram for a PM generator with parallel compensated stator windings, diode rectifier and DC-DC converter. The power limit imposed by the series reactance leads to poor utilisation and leaves little torque margin to cope with transient torque due to wind gusts. Therefore, some form of compensation is needed, particularly at high speed. [32]

Use of parallel capacitors raises the power capacity, but causes increased loss. With a parallel capacitor, the peak power capability into a resistive load is increased by the factor given by Equation (19). This means that any desired power can be delivered with appropriate choice of capacitors. [32]

$$\frac{1}{1-\omega^2 L/C} \tag{19}$$

The reactive power produced by the generator in one phase is given by Equation (20). The reactive power consumed by the capacitance per phase is given by Equation (21). As seen from the equations, both the reactive power produced by the generator and the reactive power consumed by the capacitor increase linearly to the generator frequency.

$$Q_{gen} = X_{gen} I_{gen}^2 = \omega L_{gen} I^2 \tag{20}$$

$$Q_{cap} = \frac{U_{cap,phase}^2}{X_{cap}} = \omega C_{phase} U_{cap,phase}^2 \tag{21}$$

As the wind speed increase, both the generator current I_{gen} and the capacitor voltage $U_{cap,phase}$ will increase. The induced voltage E_f is proportional to the rotation speed and the electrical frequency. This means that the capacitor has little effect at low frequencies and speeds, but increasingly draws additional current as the frequency increases. [8]

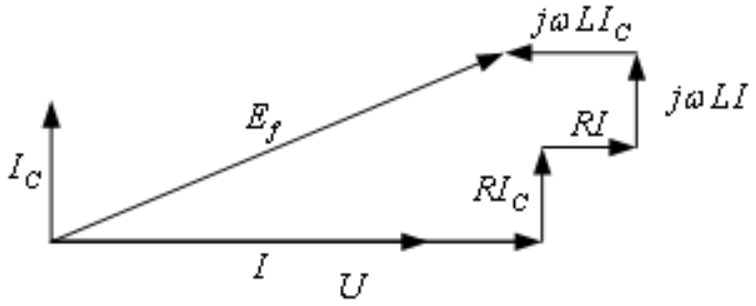

Figure 33: Phase diagram for parallel connected capacitators

$$E_{f,re} = U + RI - XI_C \tag{22}$$

$$E_{f,im} = RI_C + XI \tag{23}$$

$$E_f^2 = E_{f,re}^2 + E_{f,im}^2 \tag{24}$$

$$\left(R^2 + (\omega L)^2\right) I^2 + 2RUI + U^2 E_f^2 + \omega^4 L^2 C^2 U^2 2\omega^2 LCU^2 = 0 \tag{25}$$

$$I = \frac{-2RU + \sqrt{(2RU)^2 - 4\left(R^2 + (\omega L)^2\right)\left(U^2 E_f^2 + \omega^4 L^2 C^2 U^2 2\omega^2 LCU^2\right)}}{2\left(R^2 + (\omega L)^2\right)} \tag{26}$$

Figure 33 and Equations (22) to (26) show how the current is found when the generator voltage and the induced voltage is know. It is assumed that all voltage and currents are sinusoidal. In Equations (22) and (23) the real and imaginary part of the induced voltage E_f are found from the phase diagram, Figure 33. The absolute value of

E_f is found in (24) and this is used to find a second order expression for the generator current I, Equation (25). Now the current can be found as shown in Equation (26).

Some simple calculations using the equations for parallel compensated PMSG are also performed in MatLab. The assumptions and machine data are the same as for the MatLab calculations of the series compensated system. The result is shown in Figures 34, 35 and 36.

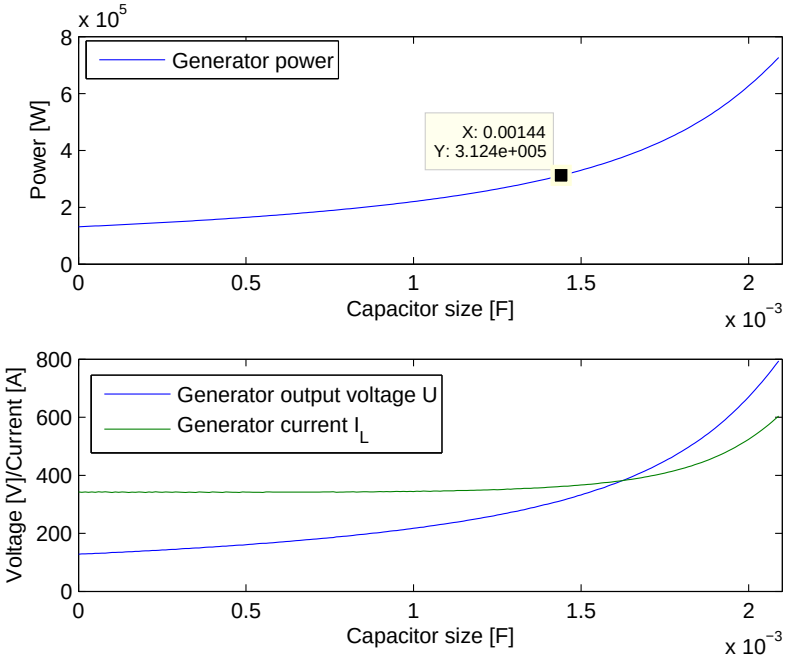

Figure 34: Maximum power [W] with respectively load voltage [V] and generator current [A] as a function of capacitor size

Figure 34 shows the maximum power output with respectively load voltage and generator current for increasing capacitor size. As seen, the generator voltage and turbine power increase when the generator power increase, while the generator current is more or less constant until the capacitor size is about $1500\mu F$. The capacitor size used in the laboratory is therefore chosen to be $1440\mu F$.

Figure 35 shoes the generator power as a function of the generator voltage when the turbine is operating at nominal speed. The generator current is decreasing when the voltage increases, and the generator power will have a maximum when the generator voltage is 316V.

The maximum generator power is plotted as a function of generator frequency in Figure 36. As seen, both the generator current and generator voltage is increasing linear to the generator frequency.

A permanent magnet synchronous generator with a diode rectifier and parallel connected capacitors is suggested in [32]. Some simulations on the equivalent circuit

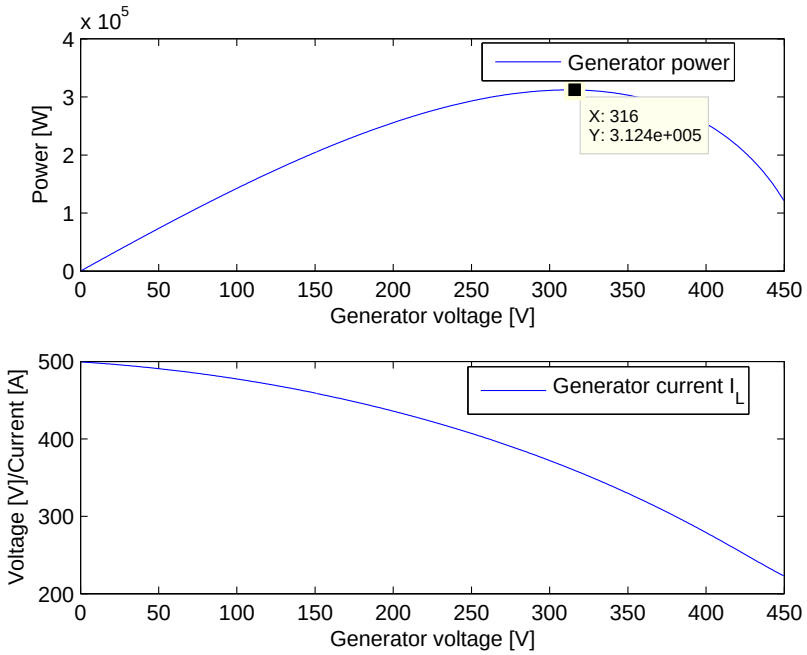

Figure 35: Maximum power [W] with respectively generator current [A] as a function of load voltage

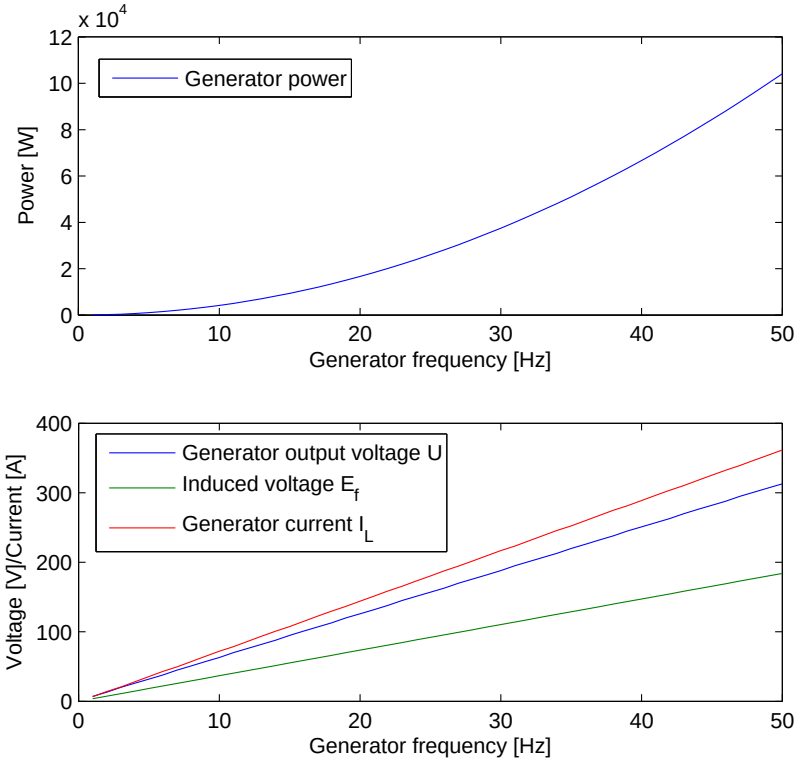

Figure 36: Maximum power [W] with respectively load voltage [V] and generator current [A] as a function of generator frequency

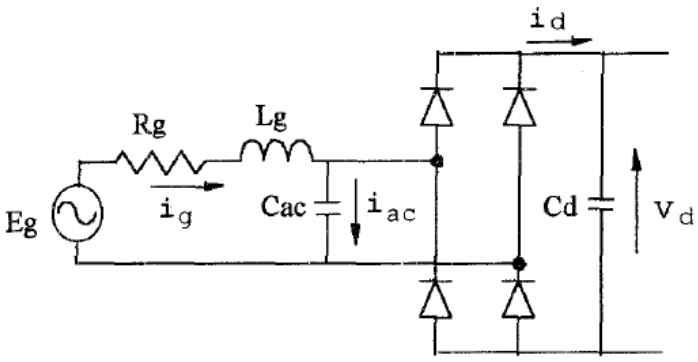

Figure 37: Equivalent circuit including capacitor [32]

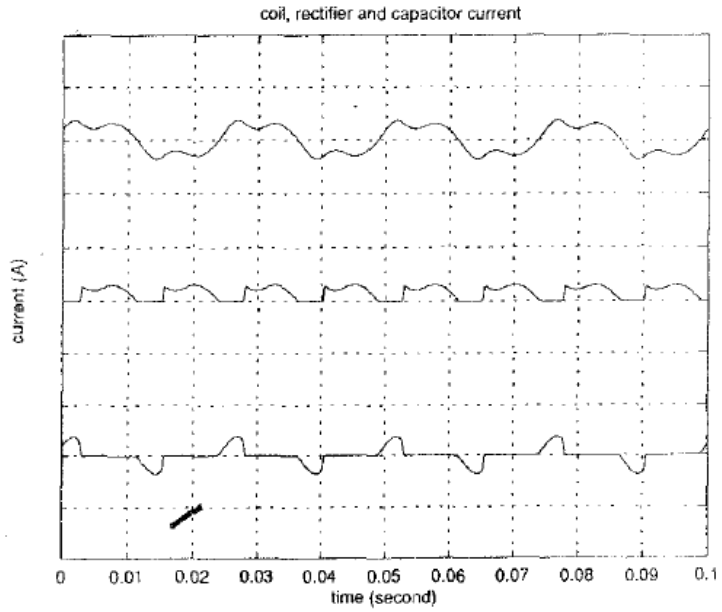

Figure 38: Simulated currents with capacitor [32]

shown in Figure 37 are performed. The results are shown in Figure 38; The upper graph shows the generator current, the middle shows the current going into the diode rectifier and the lowest shows the capacitor current. When the capacitor voltage exceeds the DC-link voltage, the diode begins to conduct. At this point the capacitor voltage is clamped to the DC-link voltage and the capacitor current becomes zero. The coil current continues to flow and diverts into the DC-link. The subsequent behaviour of the current is determined by the LR circuit and the DC and AC voltages with finite initial current. [32]

Figure 39 shows power as a function of DC voltage for different sizes of capacitors; $0\mu F$, $100\mu F$, $200\mu F$ and $400\mu F$. The lines show the simulated power and the points show the measured power. As the size of the capacitor increases, the maximum power output also increases. As seen from the figure, the power will increase when the DC-link voltage increase until a certain point where the power reaches it´s maximum. When the DC-link voltage is further increased, the current will decrease quicker than the voltage increases, and the power output will decrease. [32] The generator is then operating on the right side of the power curve where the generator power is decreasing with increasing generator voltage.

The AC capacitors partly compensate the effect of the generator inductance, resulting in higher voltage and power. However, the compensation must not be taken too far because of the danger that resonance might leads to damaging high voltage. The worst case is if a loss of grid connection leads to acceleration of the generator. The

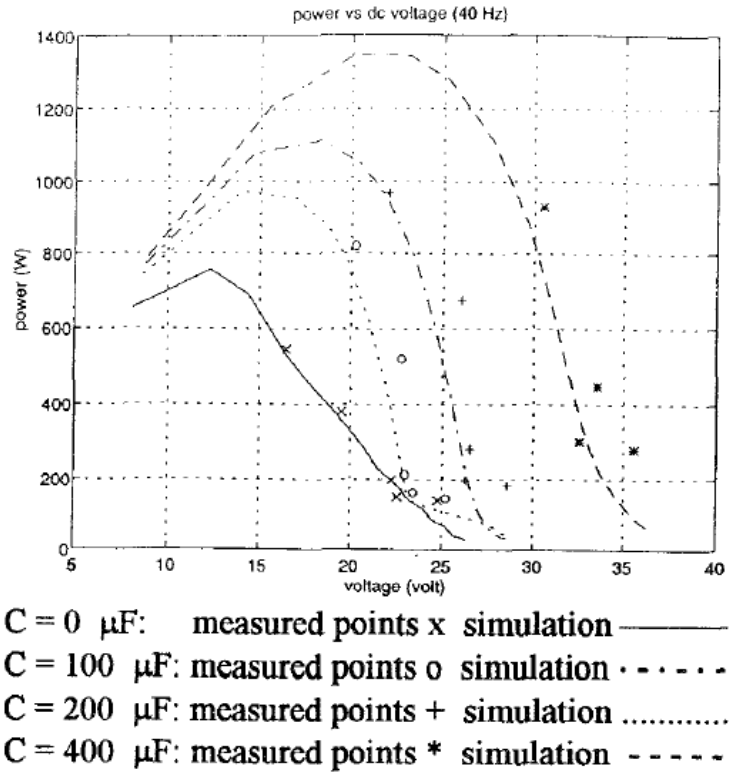

Figure 39: Power versus DC voltage for different capacitor sizes [32]

pitch control will use some time to stop the turbine. Meanwhile, the frequency of the generator will increase towards resonance between the generator impedance and the capacitors. The resulting high capacitor current passing through the coil might lead to demagnetisation of rotor modules if the capacitor or rectifier does not fail first. [32] This problem will probably not appear in a large wind turbines due to the large moment of inertia. The acceleration of the turbine will therefore be small before the pitch-controller starts to reduce the speed of the turbine.

Spooner and Chen suggest in [32] that each coil in the permanent magnet synchronous generator may be connected individually to a single-phase rectifier bridge. This will make the complex interconnections of a three-phase winding unnecessary and the DC-link voltage will have very little ripple because of the large number of phases. Thereby, a DC-link filter may not be needed. [32]

4.5 Passive filters for reducing current harmonics

Passive filters can be used for reducing current harmonics. However, the passive filters have some drawbacks. The filtering characteristics are strongly affected by the source impedance. Due to the resonant nature of passive filters there may be unwanted resonant interactions with the supply system. This affect can be avoided if the filters are off-tuned or damping is added. The filter also causes additional losses. Active filters also have also some drawbacks. It is difficult to construct a large-rated current source with a rapid current response. They have also high initial cost and running costs. [30]

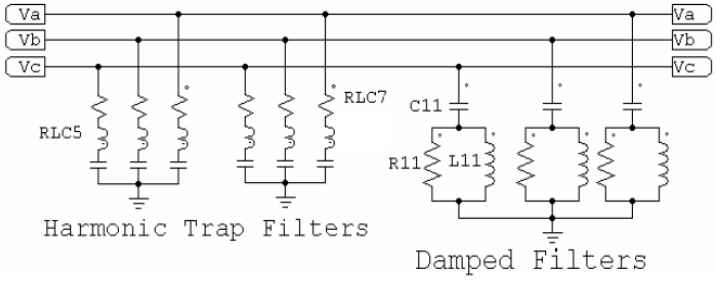

Figure 40: Shunt configuration of harmonic trap filters [30]

A classical harmonic trap filter, as show in Figure 40 can be used for harmonic elimination. The main disadvantage with this filter is that is has to be tuned for an electrical frequency. The wind turbine rotation speed is changing with the wind speed, and thereby also the frequency of the voltages and currents from the generator. The trap filter can be tuned for one wind speed, but it will not work properly for other wind speeds and rotation speeds. It is also need for one filter per harmonic which should be filtered. The size of the inductor L, the capacitor C_n and the resistor R is decided by Equations (27) to (29). [30]

$$nf_{e,1} = \frac{1}{2\pi\sqrt{LC_n}} \tag{27}$$

$$Q = \frac{X_0}{R} \tag{28}$$

$$X_0 = \sqrt{\frac{L}{C_n}} \tag{29}$$

$nf_{e,1}$ is the tuned frequency in n^{th} order of the fundamental and the Q factor is determined by R, L and C_n. The value varies from 30 to 60. Figure 40 also shows damped filters. They provide low impedance for a wide spectrum of harmonics without the need of subdivision of parallel branches. The behaviour of the damped filter is given by two parameters given in Equations (30) and (31). Typical m values vary from 0.5 to 2. [30]

$$F_0 = \frac{1}{2\pi CR} \tag{30}$$

$$m = \frac{L}{R^2 C} \tag{31}$$

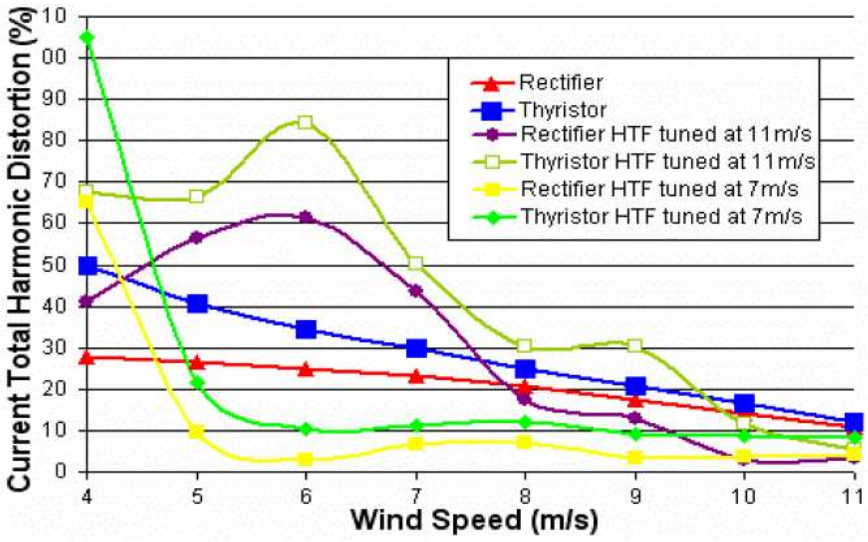

Figure 41: Summary of line current THD content [30]

Figure 41 and 42 shows the total harmonic distortion for diode and thyristor rectifier with harmonic trap filters tuned at different wind speeds. It shows that the solution with a diode rectifier and harmonic trap filter tuned at a wind speed of $7m/s$ gives

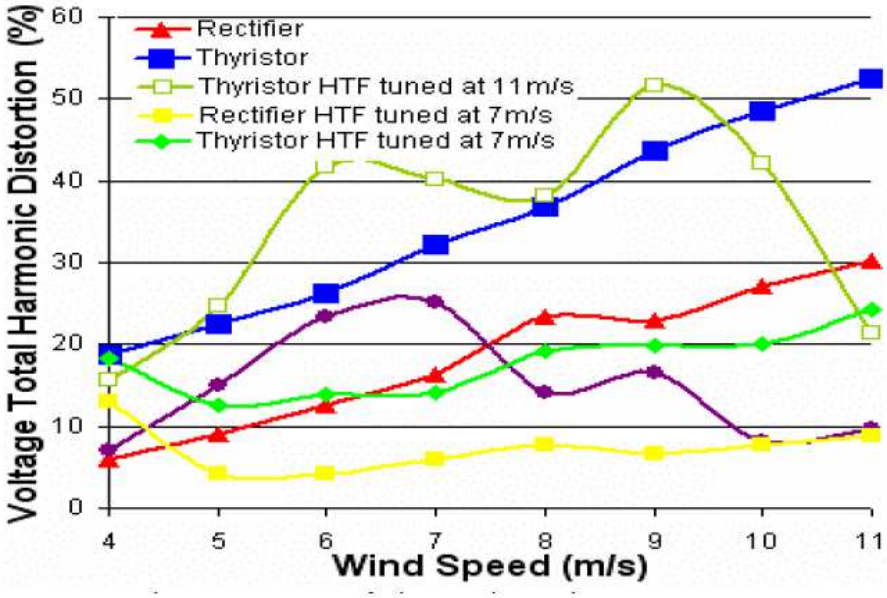

Figure 42: Summary of line to line voltage THD content [30]

the least current THD and voltage THD. The figure also shows, not surprisingly, that the THD generated from a thyristor rectifier is larger then from a diode rectifier. The disadvantage with the harmonic trap filters is that a lot of energy is lost in the filter. The generator losses are about 10% lower with harmonic trap filters. However the total losses are some higher, according to [30].

4.6 Active shunt filter for reducing current harmonics

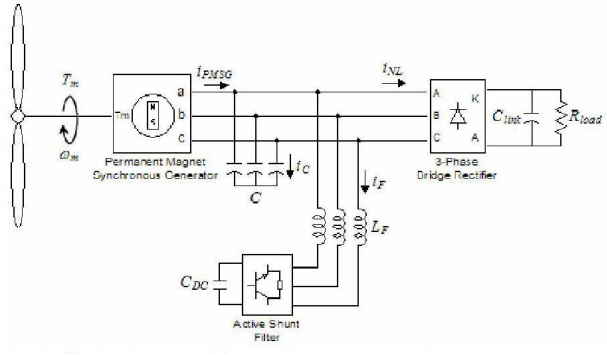

Figure 43: Basic diagram of WECS with active shunt system [25]

An active shunt filter (ASF) for harmonic mitigation in wind turbines generators is present in [25]. Figure 43 shows the basic diagram of the system. The ASF controls the filter current to actively shape the generator current into the sinusoid. With this active filter the THD of the generator current is reduced from 10.68% to 2.60%. The harmonic content of the PMSG output voltage is also reduced, from 29.15% to 20.77%.

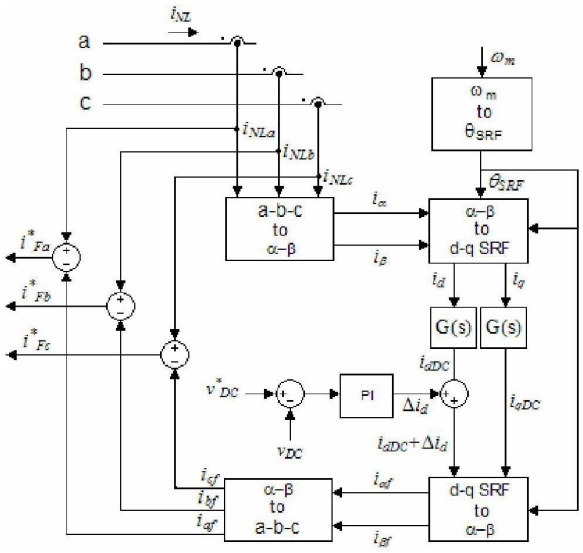

Figure 44: Block diagram of the ASF harmonic currents calculation and v_{DC} voltage control [25]

The control system of the ASF is described in [25]. The block diagram of the ASF harmonic current calculation is shown in Figure 44. The current is transformed from

three-phase to the $\alpha - \beta$ frame and then to the d-q frame and i_d and i_q are filtered with a low pass filter.

The DC bus nominal voltage V_{DC} must be greater than or equal to the line-to-line voltage peak to actively control the current going into the filter. In order to maintain the DC bus voltage, an amount of active current must be delivered to the ASF. Therefore a PI-regulator is used to control i_d. The d-q current is then transformed to the $\alpha - \beta$ frame and then to three-phase current. This is compared to the actual generator current and used as a reference to the active filter current.

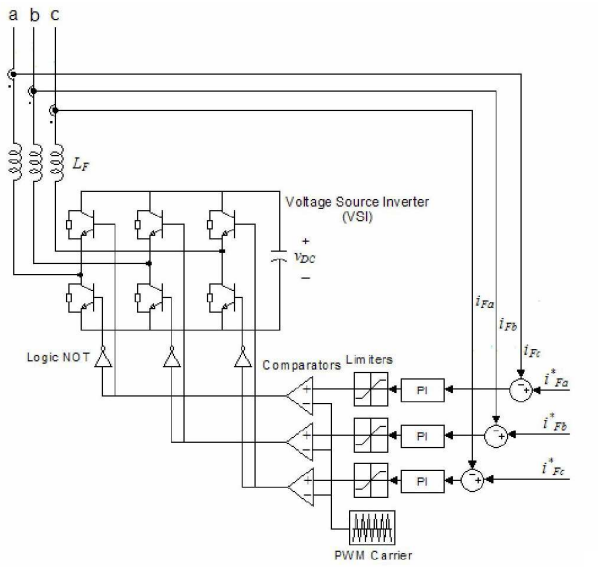

Figure 45: PWM carrier control for ASF current [25]

Figure 45 shows how the voltage source inverter is controlled. The filter reference current is compared to the actual filter current for each of the three phases and the switching of the IGBTs is controlled by a PI-regulator and a PWM carrier strategy.

The filter inductance L_F and the capacitor size C_{DC} must be chosen properly. A practical choice of L_F guarantees that the active filter can generate a current with a slope equal to the maximum slope of the load current. The ability to track the desired source current improves if the filter inductance is smaller. However, a smaller filter inductance requires a higher switching frequency to keep the ripple in the line current acceptably small. The capacitor size is decided based on the filter current I_F and the maximum accepted voltage ripple Δv_{DCmax}. Power losses in the ASF consist of losses in the passive parts such as the inductors and the capacitor and losses in the active parts, the IGBTs. The simulations performed in [25] shows that the total electrical efficiency is 88.05% for the system without AFT and 84.74% with AFT. The ASF losses are 3%. The rectifier and PMSG copper losses also increase when the AFT is used.

5 Control systems

The swaying of an offshore floating wind turbine has to be controlled to reduce the mechanical forces on the tower and to prevent the tower to tip. Therefore the thrust force exerted on the blades has to be controlled. Besides the wind speed, the pitch angle and the turbine rotating speed affects this force. Since the moment of inertia of the rotor is quite large, the time constant of the rotation speed is also large. The rotation speed do also affects the power coefficient c_p of the turbine. A small difference between the actual rotation speed and the optimal rotation speed results in a relative large decrease in power production.

The pitch angle can be controlled much faster than the rotation speed. It is therefore much more suitable for controlling the swaying of the wind turbine. However, the power coefficient c_p is also decreasing when the pitch angle differ from its ideal value.

The pitch angle should therefore be used to control the swaying of the wind turbine and to reduce the turbine power when the turbine power exceeds the rated power. The generator torque should be used to control the speed of the rotor. Some regulation strategies for speed control are present in the following chapters.

5.1 Speed and torque control

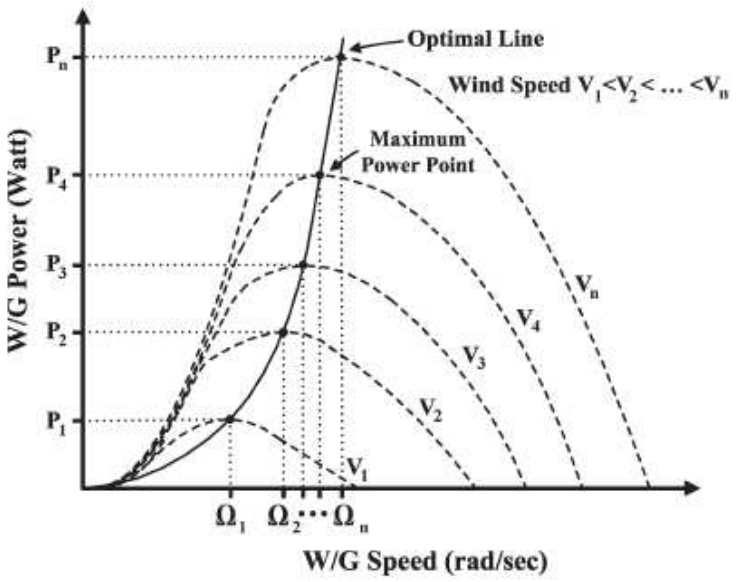

Figure 46: Wind generator power curves at various wind speeds. [7]

The turbine rotation speed is important to obtain a maximum power production. Figure 46 shows the turbine power curves for various wind speeds. The optimal power production line is also drawn. This is the rotation speed which gives the maximum

output power for different wind speeds. The value of the tip-speed ratio λ is constant for all maximum power points, while the turbine rotation speed is related to the wind speed as given in Equation (32).[7]

$$\Omega_n = \lambda_{opt} \frac{V_n}{R} \tag{32}$$

Two types of tracking algorithms (MPPT) exist; Methods based on the knowledge on the $C_p(\lambda)$ characteristic and methods allowing to seek the optimal operation without knowing the turbine characteristic.

5.1.1 MPPT with knowledge of the turbine characteristic

Three different tracking algorithms for systems with known turbine characteristic will be mention here; speed control, torque control and a diode bridge with DC-DC chopper structure. If speed control is used, the power curve is used to find the optimal speed reference versus power.

Tip-speed ratio control or speed control regulates the rotational speed of the generator to maintain an optimal tip-speed ratio, λ. The power curve is used to find the optimal speed reference versus power. Both the wind speed and the rotational speed need to be measured to calculate the tip-speed ratio. This will increase the system cost and present difficulties in practical implementation. The optimal tip-speed ratio must also be known. This can vary from one wind turbine to another. A PWM controlled IGBT converter is used to control the turbine speed. [10] [4]

When torque control is used, the power curve is used to find the optimal torque reference. Optimal torque control adjusts the generator torque to an optimal one at different wind speed. The optimal tip-speed ratio and generator parameters are needed, and the control precision depends on the precision of these variables. A PWM controlled IGBT rectifier is needed. [10] [4]

The third alternative is a diode AC-DC converter linked to a DC-DC chopper. Seeking the optimal operation can be achieved by controlling the load current by obtain an optimal load characteristic versus the DC voltage. The DC-link voltage is directly related to the generator electromotive forces magnitude. These forces are proportional to the turbine speed. The configuration is simple and inexpensive, with a low cost AC-DC converter and a minimum of sensors. [4]

According to [4], the structure including a diode converter with a DC-DC chopper is a cheaper and simpler solution and the simulation results are quite satisfactory. Even if the tuning of the generator is indirect and highly slower, the high inertia of the turbine operates as a filter, filtering the wind fluctuations. The relationship between the output current and the DC-link voltage at the output of the diode rectifier can be determined by simulation and by experiment. This curve will include the system losses for any operation points. [4]

Figure 47 shows the overall control scheme of the wind turbine with anemometer sensor. The anemometer is used to find the tip-speed ratio and provides the wind

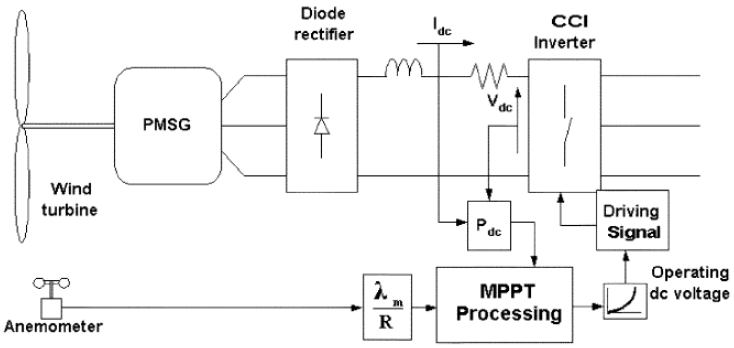

Figure 47: Block diagram of the WECS-controlled system with anemometer [13]

power reference to the MPPT controller. The input operating DC voltage reference can be found by comparing this reference to the turbine power. This signal is fed into the current control loop of the CCI inverter, which control the DC-link voltage. The DC-link voltage controls the current from the generator, and thereby the generator torque and the generator speed. [13]

5.1.2 MPPT without knowledge of the optimal turbine characteristic

If neither the turbine characteristics nor the wind speed are supposed to be known, an MPPT algorithm has to be implemented using operational seeking method based on behavioural rules linked to power and speed variations. [4]

Hill-climb searching control needs no parameters and is extremely robust. However, it works well only when the wind turbine inertia J is very small, because a large inertia results in a slow and ineffective control. When the turbines size is growing, the inertia of the turbines is getting larger and more kinetic energy is stored in the turbines. The inertia affects the response time of the MPPT, which decides the yield of wind energy in transient state. [10]

In [31] a design of a buck-boost converter circuit used to achieve the maximum power control of wind turbine driven PMSG is described. Figure 48 shows the schematic diagram. The PMSG is suitably controlled according to the generator speed and thus the power from a wind turbine settles down on the maximum power point by the proposed MPPT control method, where the wind turbine´s maximum power curve and the information on wind velocity are not required. [31]

5.1.3 Comparison between the control strategies

According to the research present in [4], the hill-climb search control is less powerful than the others control strategies. The control strategies with knowledge about the turbine characteristic are more efficiency than the control strategies without knowledge

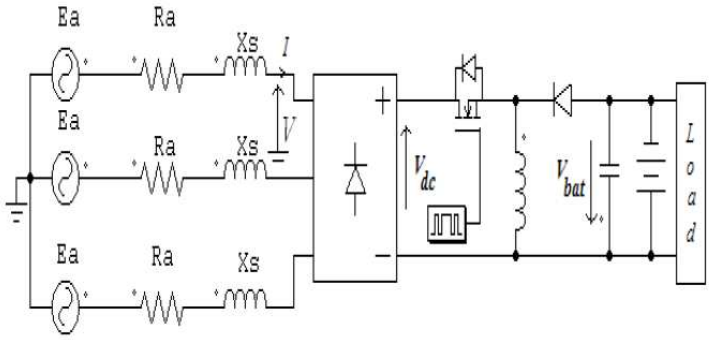

Figure 48: Schematic diagram for diode rectifier and buck-boost converter [31]

about the turbine characteristic. [4] This turbine´s maximum power curve needs to be obtained via simulations or tests for individual wind turbines, which increases the cost of implement. However, this strategy avoids the fluctuation in output power and is easy to execute in practice. [10] Also, for large turbines the cost of obtaining the wind turbine´s maximum power curve is very low compared to the total system cost.

The torque controlled MPPT has a little bit better efficiency than for the speed control and the ripples in power and torque are also less. Also, the speed controller is sensitive for high values of inertia and its dynamic must be sufficiently slow to avoid the system to be unstable, particularly during star-up transients. The torque controller is also more simple and robust.

5.2 Fixed DC-link voltage

In this case, the DC-link voltage of the inverter is fixed at a targeted optimum wind speed, typically optimised knowing the Weibull distribution for wind speed on the site. Since the DC-link voltage is constant in this case, the power output from the generator is not regulated to obtain the best rotation speed and the system efficiency will be lower for wind speed above and below the optimum wind speed. [13]

Rated power	$55kVA$	$2MVA$	$3MVA$
Rated voltage (L-L)	$319V$	$1kV$	$603.5V$
Rated frequency	$50Hz$	$30Hz$	$29.47Hzpu$
Stator winding resistance	$0.070pu$	$0.03pu$	$0.060pu$
Stator leakage reactance	$0.365pu$	$0.4pu$	$0.065pu$
Unsaturated reactance X_d	$0.730pu$	$0.8pu$	$0.1178pu$
Unsaturated reactance X_d	$0.730pu$	$0.8pu$	$0.1178pu$

Table 6: PMSG data for 55kW, 2MW and 3MW turbines used in the simulations

6 Modelling of the wind turbine

The power system is modelled in PSCAD/EMTDC. PSCAD is a time domain simulation tool for studying transient behavior of electrical networks made by the Manitoba HVDC Research Centre. PSCAD is the interface on personal computers, while EMTDC is a powerfull program performing the simulations. [5]

6.1 Permanent magnet synchronous generator

A component model of a permanent magnet synchronous machine found in the PSCAD library is used. In addition to the three stator windings, two additional, short-circuited windings are included to model the effect of electromagnetic damping. These equations is found in Chapter 3.2. The speed of the machine may be controlled directly by inputting a positive value into the W input of the machine, and T_e is the output electrical torque. L_m is the magnetising inductance, also called the air-gap inductance, and represents the influence of the stator currents on the air gap flux density, while L_σ is the leakage inductance of the stator winding. In this simulation it is assumed that the value of these two inductances is equal, as assumed in [3]. The sum of these two inductances is called the synchronous reactance (unsaturated reactance). [2] The permanent magnets are assumed to be placed in the air-gap. Since the permanent magnets and the air have the same permeability, the d- and q-component of the synchronous reactance will be the same size. [19] The generator data for the 55kW, 2MW and 3MW PMSG is shown in Table 6. A simplified schematic figure of the PMSG, diode rectifier and DC-link modelled in PSCAD is shown in Figure 49.

6.2 Diode rectifier

Six diodes are used to build the three-phase diode rectifier. The nominal data is found in Table 7. The data from the IGBT´s diodes, FS450R12KE3, is used. This is the same diodes used in the laboratory experiment, and the data is found in [23].

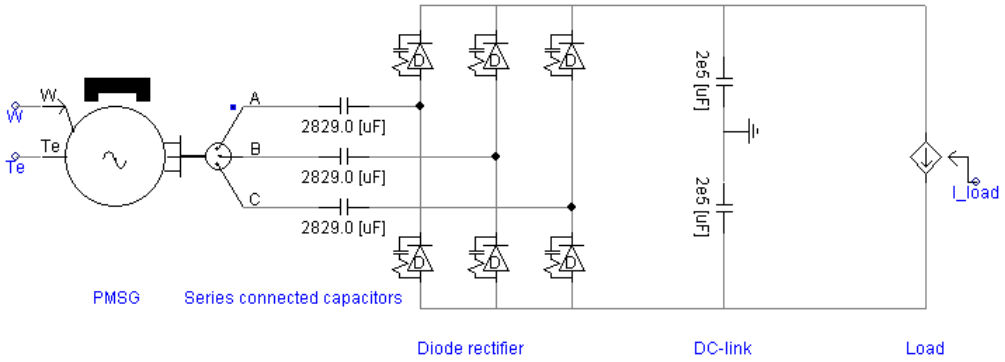

Figure 49: Simplified schematic figure of the PMSG, diode rectifier and DC-link modelled in PSCAD

Diode on resistance	0.00144Ω
Diode off resistance	$1e6\Omega$
Forward voltage drop	$1V$
Forward breakeover voltage	$1e5V$
Reverse withstand voltage	$1e5V$
Snubber resistance	5000
Snubber capacitance	$0.05\mu F$

Table 7: Diode data used in the simulations

6.3 The inertia of the wind turbine

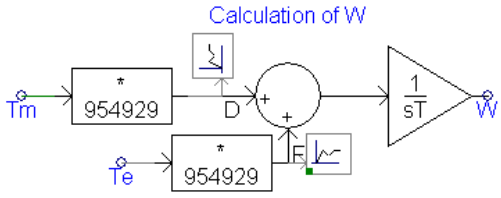

Figure 50: Calculation of the rotation speed Ω in PSCAD

The moment of inertia, J, for the rotating parts of a 2 MW wind turbine with PMSG is assumed to be $5.9 \cdot 10^6 kgm^2$. In this case the generator frequency is 30 Hz and the nominal turbine rotating speed is 20 rpm. The values for the 3MW turbine is $10 \cdot 10^6 kgm^2$, 30 Hz and 17 rpm. To calculate the rotation speed Ω, the pu values of the generator torque and the turbine torque have to be referred to the generator axis. The reference generator and turbine torque is found in Equation (33). The rotating speed Ω can be calculated as shown in Equation (34). Equation (35) shows how it is calculated in the frequency domain. Figure 50 shows how the equation is implemented in PSCAD.

$$T_{gen,ref} = T_{turb,ref} = \frac{P_{ref}}{\Omega_{ref}} = \frac{2MW}{2\pi \frac{20rpm}{60s/min}} = 954930Nm \tag{33}$$

$$\frac{d\Omega}{dt} = \frac{1}{J}\left(T_{turb} - T_{gen}\right) \tag{34}$$

$$\Omega = \frac{1}{s}\frac{1}{J}\left(T_{turb} - T_{gen}\right) \tag{35}$$

6.4 Control system

6.4.1 Pitch controller

A component model of a pitch angle regulator of a wind turbine found in the PSCAD library is used. The inputs to the model are the mechanical speed of the machine W_m and the power output of the machine P_g. The output is the pitch angle of the turbine.

6.4.2 Speed controller

The DC-link voltage reference is calculated from the rotating speed and the rotating speed reference. A PI regulator is used to find a suitable DC-link voltage. This is shown in Figure 51.

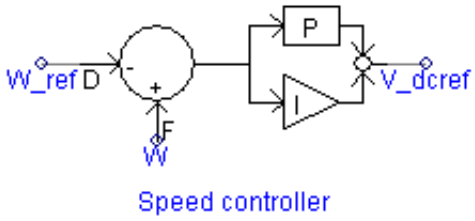

Figure 51: Speed controller

To find suitable regulator parameters, a simplified state space model (Figure 52) and a transfer function (Equation 36) is found. The rotation speed Ω is assumed to be constant. A linear relation between the DC-link power and the DC-link voltage is found by looking at simulation results. The linearization is shown in Equation (37).

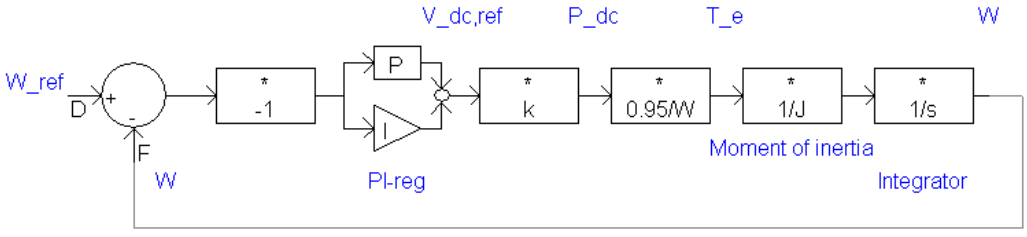

Figure 52: Simplified state space model

$$h_u = \frac{\omega(s)}{V_{dc,ref}(s)} = k\frac{0.95}{\omega}\frac{1}{J}\frac{1}{s} = \frac{0.1276}{s} \tag{36}$$

$$k = \frac{dP_{dc}}{dV_{dc}} = 1.66 \tag{37}$$

In [11], regulator parameters for different transfer functions and regulators are suggested. The suggested parameters is found in Equation (38) and (39). ω_c is the preferred bandwidth of the regulator. The fluctuations of the rotor speed reference shows that a bandwidth of 0.5 is suitable.

$$K_p = \frac{1}{K}\omega_c = 3.9 \tag{38}$$

$$T_i = \frac{5}{\omega_c} = 10 \tag{39}$$

These values give a rather large variation in DC-link voltage and generator voltage. K_p is therefore lowered to 0.3 which makes the regulator output much smoother.

6.4.3 Calculation of optimal turbine rotation speed

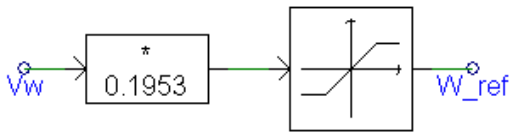

Figure 53: Calculation of optimal turbine rotation speed in PSCAD

The tip-speed ration is used to find the optimal turbine rotation speed, as shown in Equation (32) and Chapter 5.1.1. The optimal tip-speed ratio is 7.812 for the 2MW turbine. The wind speed is used to calculate the optimal turbine rotation speed. The PSCAD implementation is shown in Figure 53.

6.4.4 Load current controller

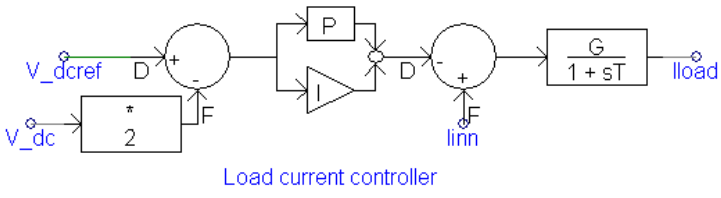

Figure 54: Load current controller

The load current controller is used to control the current going out of the DC-link. This current is used to control the DC-link voltage. If the load current is larger than the current going into the DC-link, the DC-link voltage will decrease. The load current is controlled with a quick PI-regulator and the regulator parameters are found from testing. The current going into the DC-link is forward biased and the output is filtered. Since the diode capacitance is relative large, the load current can be filtered without causing voltage ripple on the DC-link. Figure 54 shows the regulator implemented in PSCAD.

In a real turbine, the load current will be controlled by the DC/DC converter in the turbine. A single active bridge converter, consisting of one IGBT inverter, a coupling transformer and a passive diode rectifier are most likely to be used. The load current is then controlled by the duty cycle of the IGBTs.

7 Simulations and laboratory tests of a 55 kW radial PMSG

A 55 KW PMSG with diode rectifier is tested in "Vindlabben". The purpose of this work has been to find the harmonic distribution in the generator current and voltage and learn how the harmonic distribution is affected of reactive compensation.

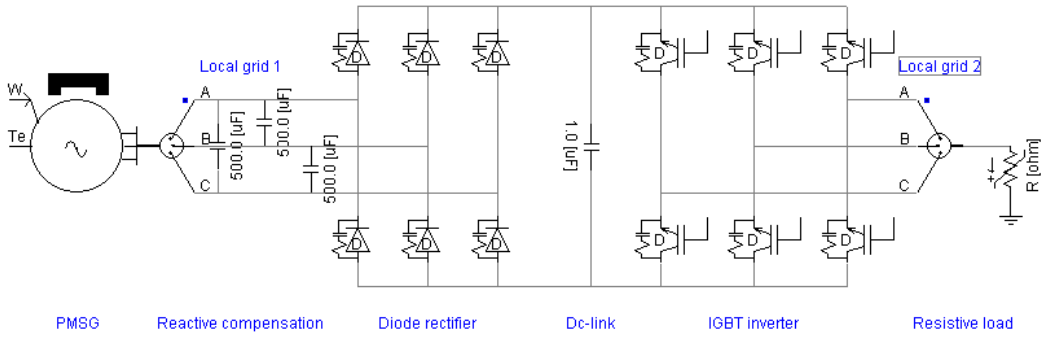

Figure 55: Schematic diagram of the PM generator system

Figure 55 shows the schematic diagram of the PM generator system. A picture of the generator is shown in Figure 56. The generator is connected through the local grid 1 to a diode rectifier. This rectifier is actually an IGBT three-phase converter with diodes in parallel with the IGBTs. No gate voltage is applied on the IGBTs, so the diodes will carry all the current.

$$C_{phase,\Delta} = 3C_{capacitance} \tag{40}$$

AC-capacitors could be connected in parallel with the generator in the local grid 1. The capacitors are $480\mu F$ and connected in delta. Equation (40) shows that the phase equivalent is three times as big when the capacitors are connected in delta. The per phase equivalent capacitance is therefore $1440\mu F$.

The size of the capacitors is chosen so that the reactive power produced by the capacitors equals the reactive power consumed by the total inductance for rated power and 50Hz generator frequency. This means that the generator current is in phase with the induced voltage E_{PM}. The power output can therefore reach its maximum for the rated current and the generator is fully compensated, as shown in Chapter 4.4. Since both the reactive power produce by the capacitance and the reactive power consumed by the generator inductance are proportional to Ω, the optimal capacitance size will not be much affected by the generator frequency. However, when the generator speed decreases, the induced voltage and the generator voltage also decreases. This means that less reactive power is delivered from the capacitances. However, the generator current is also reduced, so the reactive power produced by the stator windings is lower.

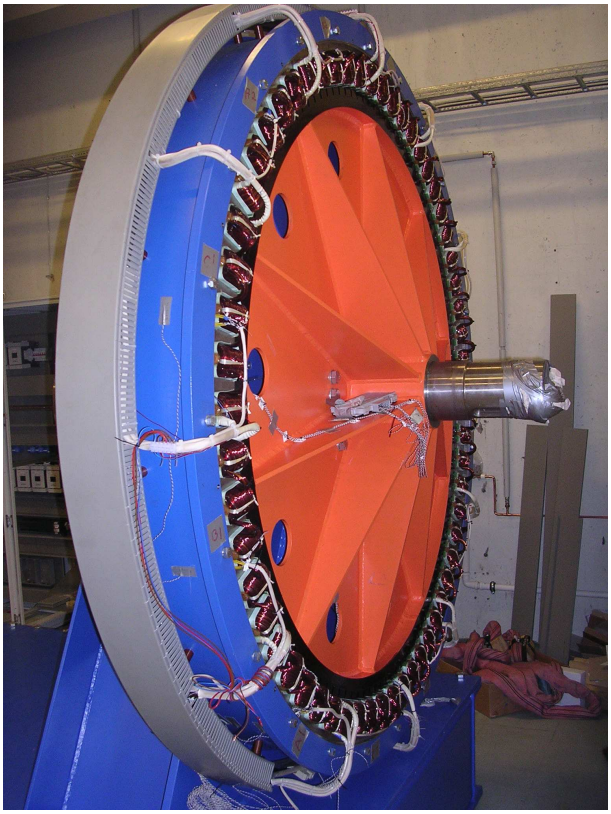

Figure 56: PMSG in vindlabben

	50Hz		27.5Hz	
Reactive compensation	yes	no	yes	no
V_{gen}	21.6%	26.4%	19.7%	21.8%
I_{gen}	24.6%	16.7%	16.9%	17.4%
I_{dio}	28.7%		20.1%	
I_{cap}	73.9%		108.7%	

Table 8: Measured total harmonic distribution (THD)

	50Hz		27.5Hz	
Reactive compensation	yes	no	yes	no
V_{gen}	12%	30%	21%	32%
I_{gen}	12%	20%	15%	12%

Table 9: Simulated total harmonic distribution (THD)

The DC side of the converter is connected to a DC-link capacitor and an IGBT inverter, similar to the rectifier. The inverter is connected to a water-cooled resistive load through local grid 2. The main purposes of the inverter are to regulate the DC-link voltage and to generate an AC voltage so the water-cooled resistances could be used. The resistance is not designed for DC voltage, so they can not be connected directly to the DC-link. A V/f control is used to generate this AC voltage.

Generator current, generator voltage and diode current are measured for two different frequencies, both with and without reactive compensation. The total harmonic distribution is shown in Table 8. These values are calculated in MatLab. The simulated THD values are found in Table 9. Measurements for 15.5Hz generator frequency is also performed, but the results are not presented here because it is very similar to the case with a generator frequency at 30Hz.

The most important of these THD values is the THD of the generator current. As seen earlier, a high THD in the generator current causes unnecessary losses in the generator because the harmonics of the generator current does not produce any power, just losses. As seen from Table 8, the THD is higher for the cases with reactive compensation when the generator frequency is 50Hz. For 27.5 Hz the THD is almost the same for the cases with and without reactive compensation.

7.1 Generator frequency at 50 Hz

7.1.1 Measurements with reactive compensation

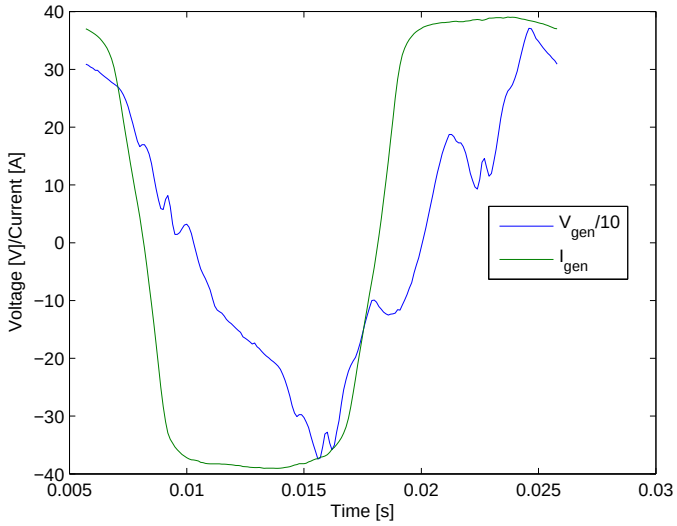

Figure 57: Measured generator voltage and generator current for 50Hz generator frequency and with parallel connected capacitors

Figure 57 shows the measured generator phase voltage and generator current for 50Hz generator frequency and with reactive compensation. The generator is operating at the left side of the power curve, where the power is increasing when the DC-link voltage increases. The generator current is more or less squared, the generator voltage is more or less triangular with some disturbances each time one of the diodes switch. The first harmonic of the generator current is about 20° before the first harmonic of the generator voltage. The generator can therefore deliver more active power since reactive power is delivered to the generator.

There are large fluctuations with high frequencies in the DC-link voltage because the DC-link capacitance is too small. The frequency of the DC-link voltage fluctuations depends on the inverter switching frequency. The disturbances are transmitted to the generator voltage and are found in the measurement of the generator voltage. Figure 57 has a lower sample rate than the other measurements. The voltage disturbances are not shown in this graph since the sampling rate of the measurements is to low. If the sampling rate had been higher, the voltage shape would look more like the other measurements.

Figure 58 shows the measured generator, diode and capacitor current for 50Hz generator frequency and with reactive compensation. The diode current is square wave like for a current stiff diode rectifier. In the following this shape is tried to be explained.

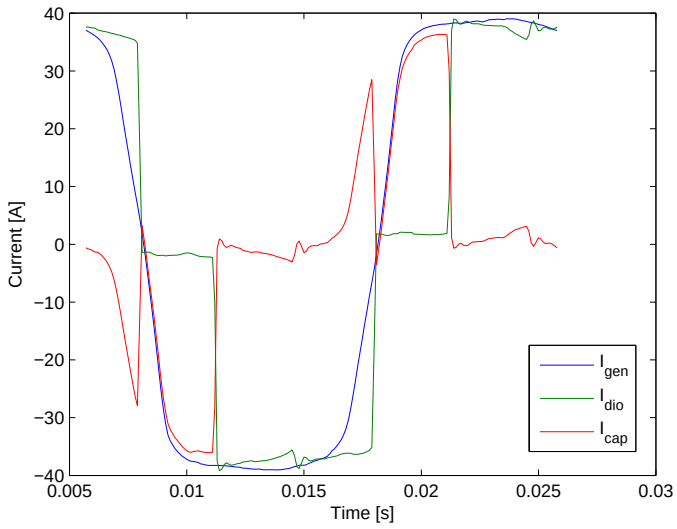

Figure 58: Measured generator, diode and capacitor current for 50Hz generator frequency and with reactive compensation

Only one of the three upper diodes is conducting at the same time. When none of the two diodes connected to a phase conducts, the current from the generator is going into the capacitance causing the generator voltage to increase. When the generator voltage reaches the DC-link voltage, the diode rectifier will start to conduct. At the same time, another diode will stop conducting, causing the DC-link current to be quite constant.

Figure 59 shows the harmonic distribution of the generator current. As shown, the third and fifth harmonics are most dominating. If passive filters are to be used, they are most likely to be tuned for the third harmonic or the third and fifth harmonics. There are also some 7.th, 9.th, 11.th, 13.th and 15.th harmonics.

7.1.2 Simulations with reactive compensation

Figures 60 and 61 show the currents, voltages and THD simulated in PSCAD/EMTDC. In the simulation the DC-link voltage is increased from $0V$ to $1250V$ in $25sec$ while the rotation speed is fixed at rated speed. In this way it is possible to se how the currents, voltages, power, torques, THD and losses is affected by the DC-link voltage and how the DC-link voltage can be used to control the turbine power and the rotational speed. Figure 60 shows the generator voltage and the currents for the same generator voltage as found in the measurements. The shape of the generator voltage is more or less as measured. As seen, there are four voltage steps, depending on which diodes conducts.

The simulated generator current has a flat top; however the measured current is more squared. The diode current is zero for some periods because neither of the two diodes connected to a phase are leading. This is the case when the generator voltage

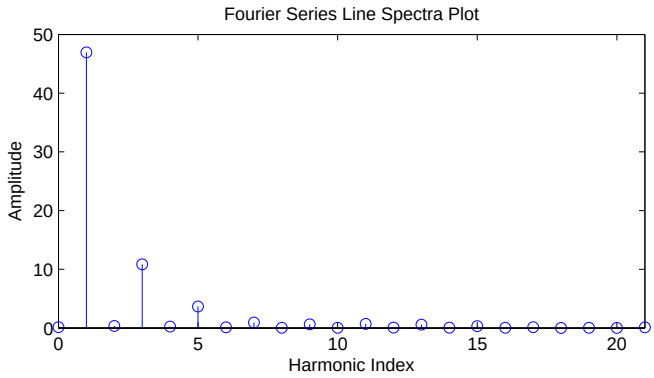

Figure 59: The harmonic distribution of the generator current

increases from zero. All the current from the generator is going into the capacitor. Next the upper diode starts to conduct and the current from the generator is going directly into the DC-link. The generator voltage increases even more, causing current to flow into the capacitance. However, the generator current is more or less unchanged, so the increase in generator voltage causes the diode current to decrease. When the generator current starts to decrease, the generator voltage and the voltage over the capacitor also start to decrease. The capacitor will therefore deliver current to the DC-link and the diode current will be more squared than the generator current.

Generator voltage, currents, power and THD of the generator voltage and current for increasing DC-link voltage is shown in Figure 61. When the DC-link voltage is zero, the generator is short-circuited and the generator current is therefore high, $140A$. Due to the paralleled capacitance, the generator current will remind high when the DC-link voltage increases. The generator power increases until the DC-link voltage reaches $650V$. The generator output power is then $75kW$. The generator current is 155A, much higher than the rated value of the generator, 99A.

The diode rectifier loss depends mainly on the diode current. Since the diode current rms-value actually decreases when the DC-link voltage increases, the losses will be highest for the lowest generator power. When the generator power is $75kW$, the diode rectifier loss is only about 1%.

The generator current THD increases when the DC-link voltage increases. The measured generator current THD is 24% while the simulated THD is 12%. The generator voltage THD is also less in the simulation, 12% instead of 21%. Some of this difference could be explained with the fact that simulations are more ideal than real experiments. The actual machine and capacitor data can also differ from the given

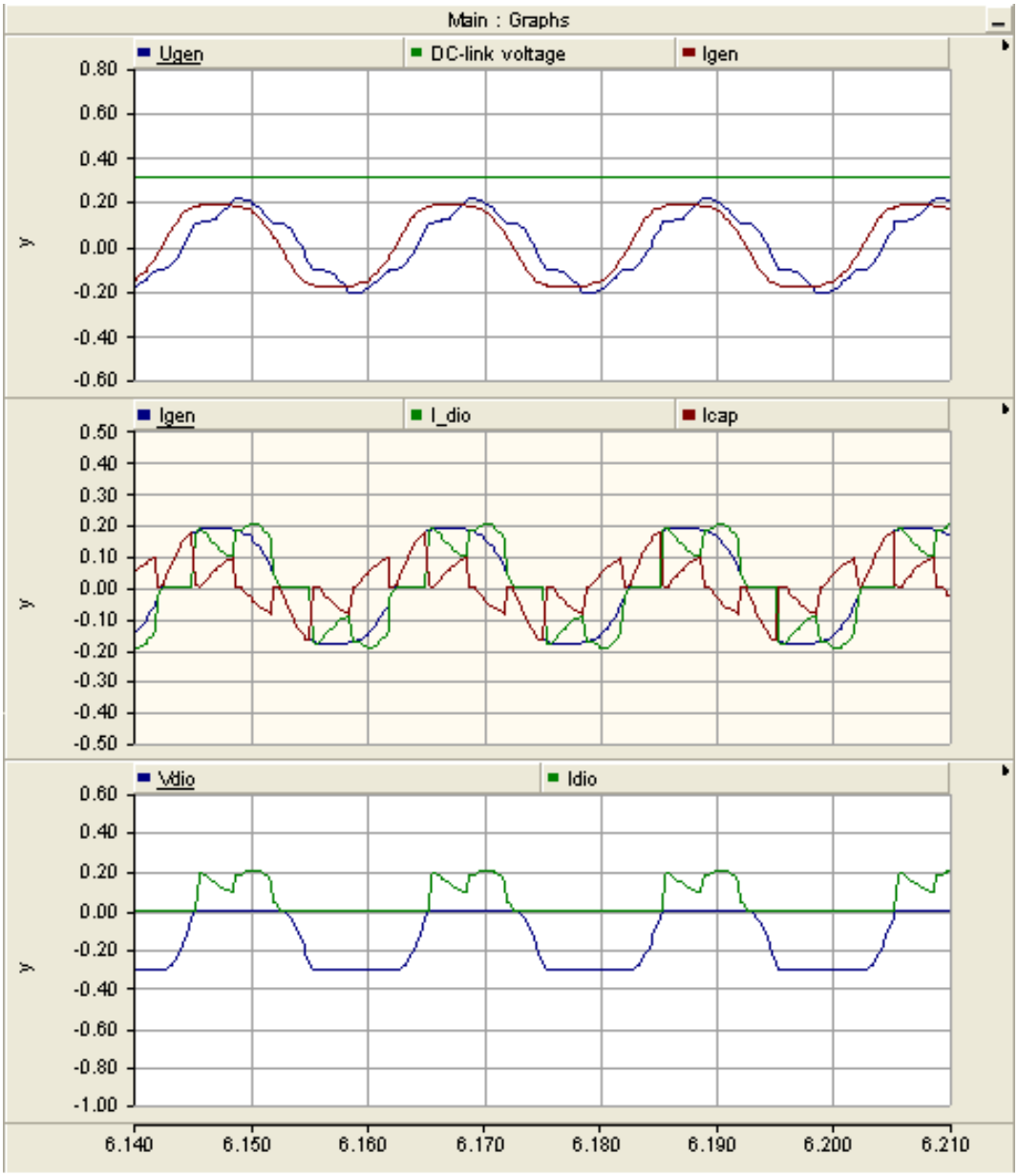

Figure 60: Simulated generator phase voltage [kV], generator current [kA], diode current [kA] and capacitor phase current [kA] for 50Hz generator frequency and with reactive compensation

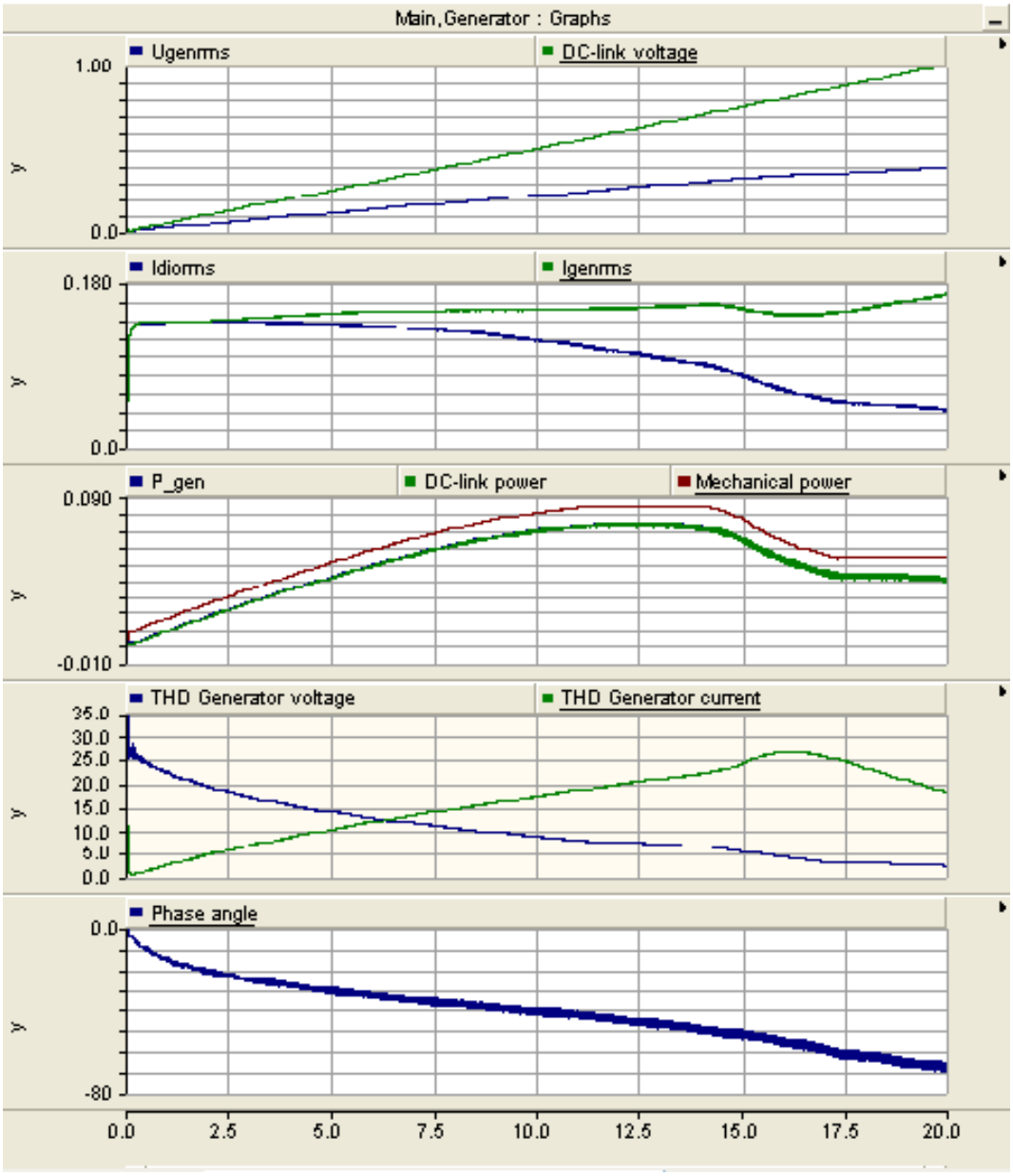

Figure 61: Simulated generator phase rms voltage [kV], diode current rms [kA], generator current [kA], generator power [MW], DC-link power [MW], generator voltage THD and generator current THD for increasing DC-link voltage, 50Hz generator frequency and with reactive compensation

values. All the simulated THD values are shown in Table 9.

The shape of the generator power curve as a function of the DC-link voltage, as shown in Figures 61 and 70, is interesting. The power reaches a top for a certain DC-link voltage. If the DC-link voltage is further increased, the power starts to decrease. This is caused by the reduced diode current. Since the diode current is reduced, the power losses in the diode converter are also decreased. However, due to the increasing generator THD and power angle, the generator current is not decreasing. If the size of the capacitors is reduced, the generator current rms could also be reduced, causing lower generator losses.

When the DC-link voltage is increased above a certain level, none of the diodes are conducting for some of the time. This causes very strange generator currents and high current harmonics. It will also be very difficult to regulate the generator power and torque when the turbine operates in this area. A higher rotation speed will result in a lower turbine efficiency. The DC-link voltage must therefore be controlled very quickly to keep the rotation speed optimal.

7.1.3 Measurements without reactive compensation

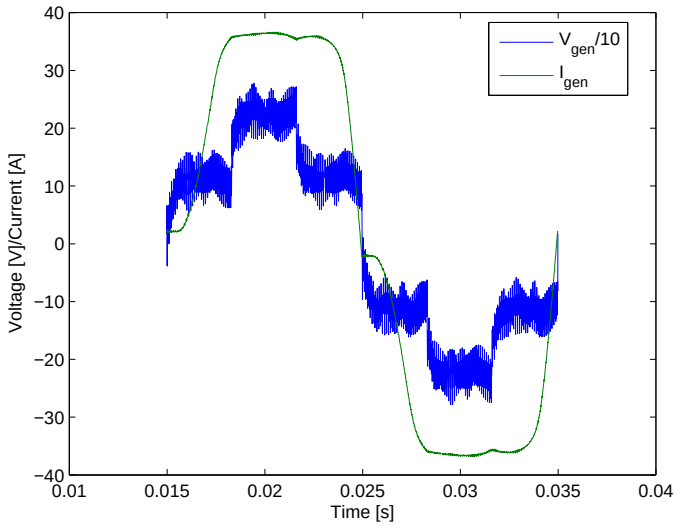

Figure 62: Measured generator voltage and generator current for 50Hz generator frequency and with no reactive compensation

Figure 62 shows the measured phase generator voltage and generator current for 50Hz generator frequency with no reactive compensation. The first harmonic of the generator current is more or less in phase with the first harmonic of the generator voltage. The maximum power output from the generator can therefore not be reached.

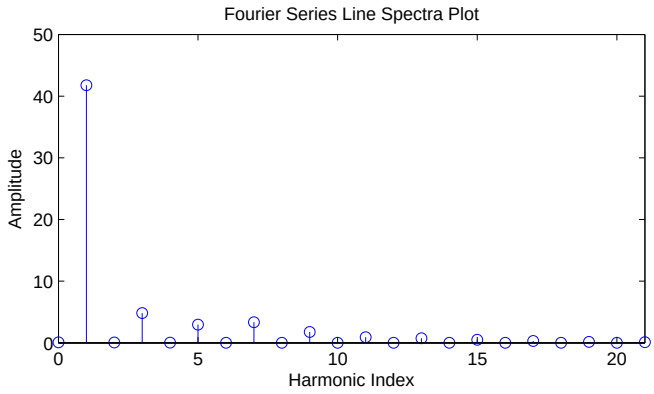

Figure 63: The harmonic distribution of the generator current

Figure 63 shows the harmonic distribution of the generator current. The 3.th, 5.th and 7.th harmonics are dominating and need special attention.

7.1.4 Simulations without reactive compensation

Figures 64 and 65 show the result from the simulation without any reactive compensation and generator frequency at $50Hz$. As seen from Figure 64 and Figure 57, the generator voltage is very similar to the measured voltage shape when the noise from the inverter is filtered. The shape of the current differs some from the laboratory measurement. The simulated current is more sinusoidal and one of the two capacitors connected to the phase is always conducting.

Figure 65 shows that the generator current actually decreases when the DC-link voltage increases. The voltage drop over the synchronous reactance becomes less when the DC-link voltage increases. This allows less current to flow. The maximal generator power at $27kW$ is achieved with a DC-link voltage at $240V$. This is only one-third of the maximal power achieved with reactive compensation.

Booth the THD of the generator current and the generator voltage are higher in the simulation than in the laboratory measurements. The current THD is 20%, 3% higher than the laboratory measurements and the voltage THD is 30%, 4% higher than the laboratory measurements.

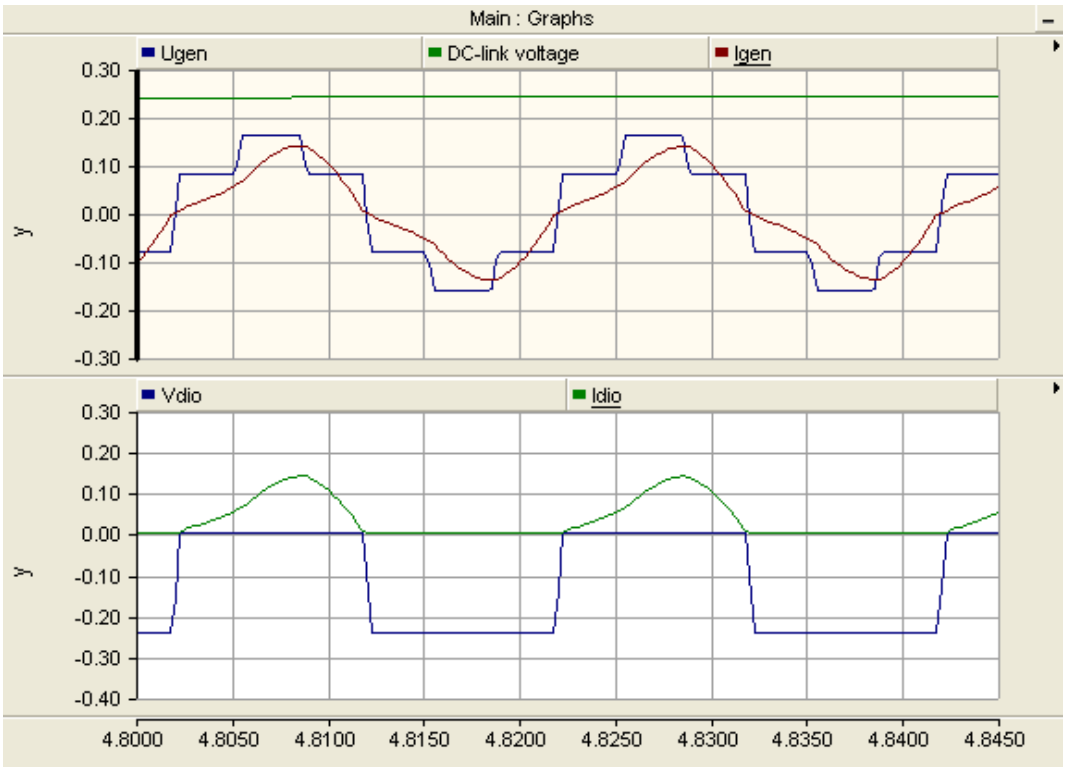

Figure 64: Simulated generator phase voltage [kV], generator current [kA], diode current [kA] and diode voltage [kV] for 50Hz generator frequency and without reactive compensation

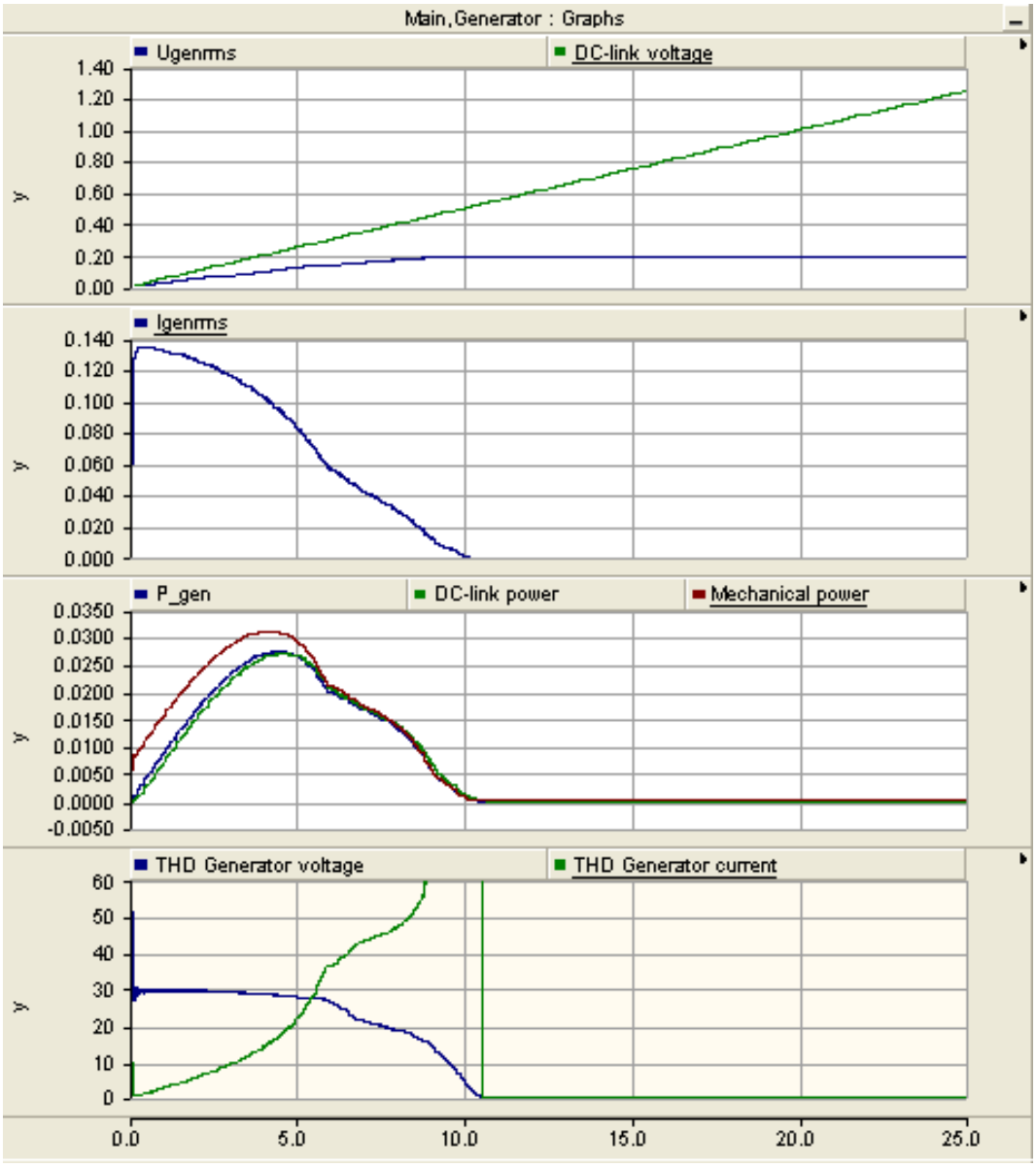

Figure 65: Simulated generator phase rms voltage [kV], diode current rms [kA], generator current [kA], generator power [MW], DC-link power [MW], generator voltage THD and generator current THD for increasing DC-link voltage, 50Hz generator frequency and without reactive compensation

7.2 Generator frequency at 27.5 Hz

In direct driven wind turbines low frequency generator voltage is preferred since this allows a smaller turbine diameter with fewer poles. Normally frequencies around 30Hz are used. Therefore the generator has been tested for lower electrical frequency. When the rotation speed decreases, the induced voltage also decreases. The current limit in the stator is still the same, so a lower rotation speed results in lower power output.

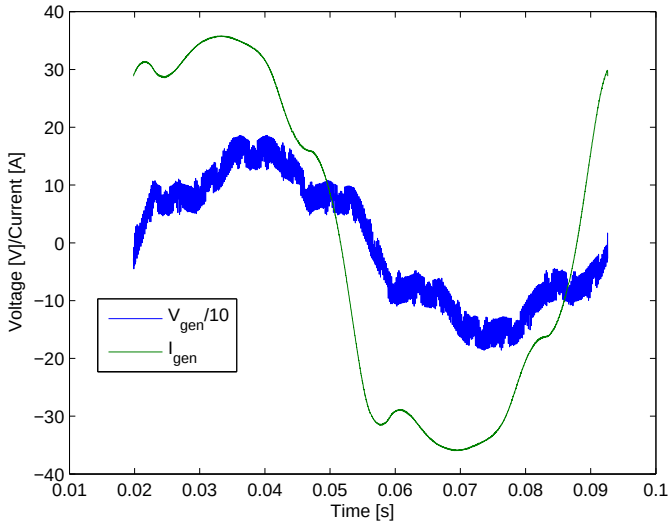

Figure 66: Measured generator voltage and generator current for 27.5Hz generator frequency and with reactive compensation

7.2.1 Measurements with reactive compensation

The measured generator voltage and generator current with reactive compensation for a generator frequency at 27.5Hz are shown in Figure 66. The first harmonic of the generator current is before the first harmonic of the generator voltage and the phase angle is about 20°.

The measured generator, diode and capacitor currents for 27.5Hz generator frequency with reactive compensation are shown in Figure 67. The diode current is square shaped while the generator current is more sinusoidal.

Figure 68 shows the harmonic distribution of the generator current. The 3.th, 5.th and 7.th harmonics are dominating and special attention should be made to these. The other harmonics are very small.

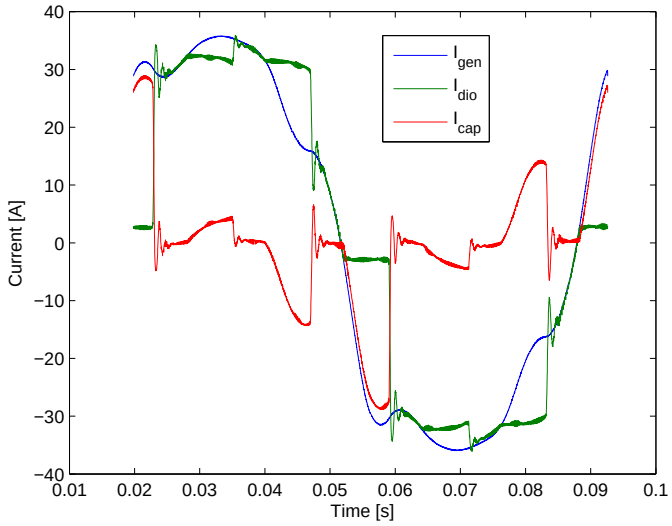

Figure 67: Measured generator, diode and capacitor current for 27.5Hz generator frequency and with reactive compensation

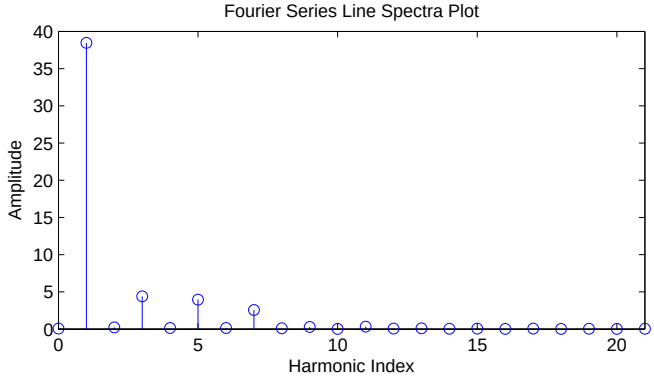

Figure 68: The harmonic distribution of the generator current

Figure 69: Simulated generator phase voltage [kV], generator current [kA], diode current [kA] and capacitor phase current [kA] for 27.5Hz generator frequency and with reactive compensation

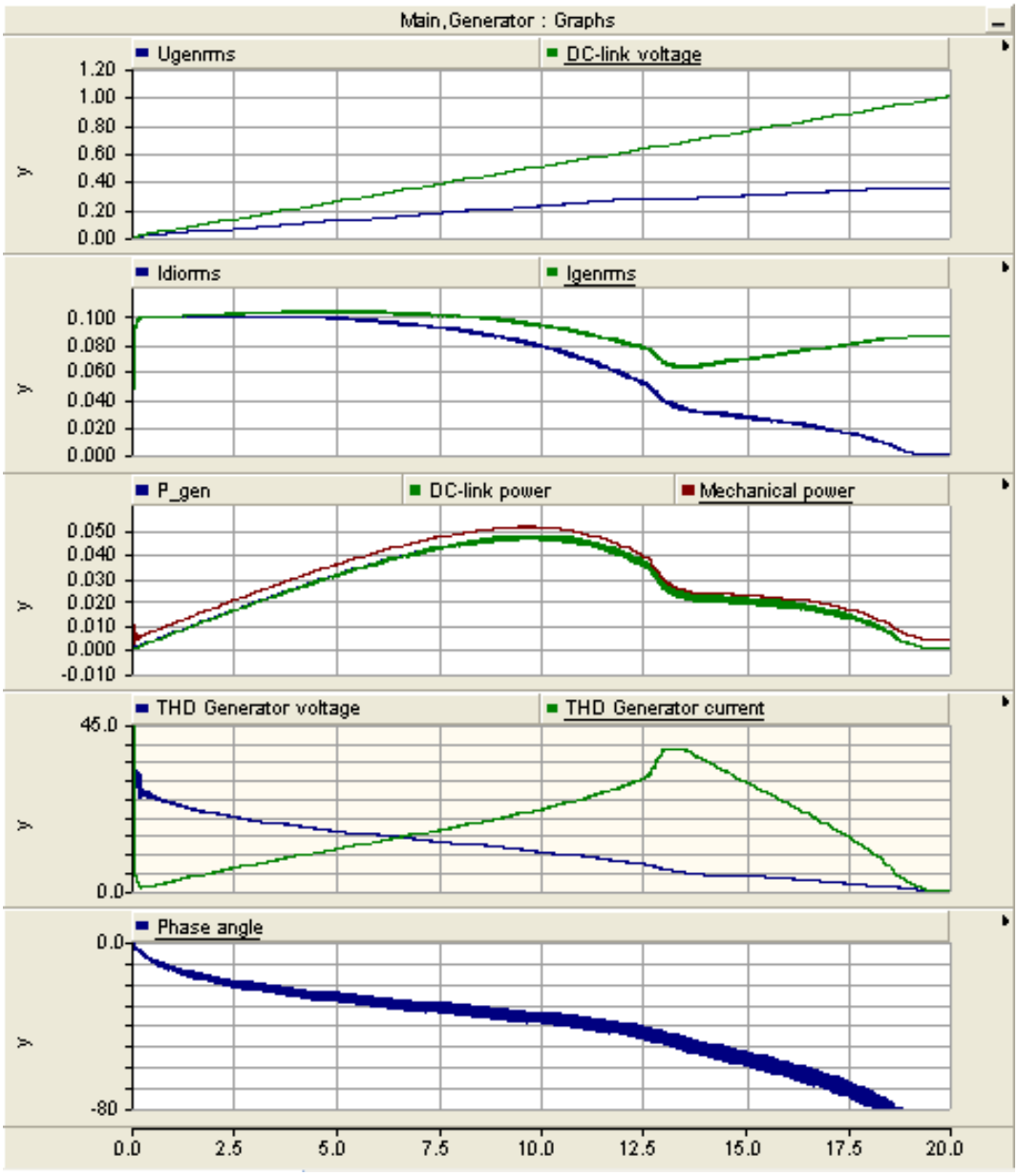

Figure 70: Simulated generator phase rms voltage [kV], diode current rms [kA], generator current [kA], generator power [MW], DC-link power [MW], generator voltage THD and generator current THD for increasing DC-link voltage, 27.5Hz generator frequency and with reactive compensation

7.2.2 Simulations with reactive compensation

Figures 69 and 70 show the result from the simulation with reactive compensation and generator frequency at 27.5Hz. As seen from Figure 69 and 66, the generator voltage is very similar to the measured values when the noise from the inverter is filtered. The generator current shape is also more or less similar to the laboratory measurement. However, the special current shape is more pronounced in the laboratory measurement. The explanation of the shape of the generator current, diode current and capacitor current is the same as explained for 50Hz.

The generator current decreases when the DC-link voltage increases, according to Figure 70. The capacitance value is chosen for the case with generator frequency at 50Hz and the size of the capacitors is therefore not optimal for this case. However, the maximal power is as large as 53kW with a DC-link voltage at 500V. The simulated current and voltage THD´s are very similar to the THD´s found in the laboratory. The simulated values are 15% and 21% for respectively current THD and voltage THD, while the measured values are respectively 17% and 20%.

7.2.3 Measurements without reactive compensation

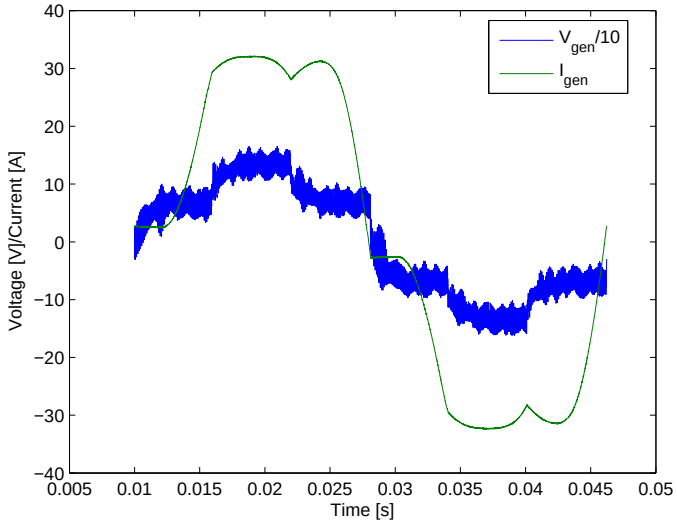

Figure 71: Measured generator voltage and generator current for 27.5Hz generator frequency and with no reactive compensation

Figure 71 shows the measured generator voltage and generator current when the output frequency is 27.5Hz and there is no reactive compensation. The situation is very similar to the one shown in Figure 62. The harmonic distribution is shown in Figure 72. The 5.th and 7.th harmonic are dominating.

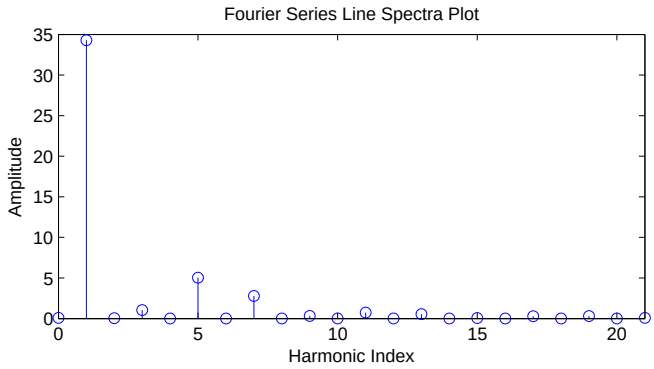

Figure 72: The harmonic distribution of the generator current

7.2.4 Simulations without reactive compensation

Figures 73 and 74 show the result from the simulation without any reactive compensation and generator frequency at 27.5Hz. When Figure 73 is compared to Figure 71, the generator voltage is found to be more or less the same for both the simulation and the laboratory measurement. However, the generator current differs much from the measured value. The simulated current shape is more sinusoidal and one of the two diodes connected to one phase is always conducting.

Figure 74 shows the same as for the situation with reactive compensation; the generator current decreases when the DC-link voltage increases. The maximal generator output power, 23kW, appears with a DC-link voltage at 210V. The generator current THD is 12% in the simulation while the measured value is 17%. However, the simulated generator voltage THD, 29%, is larger than the measured value, 22%.

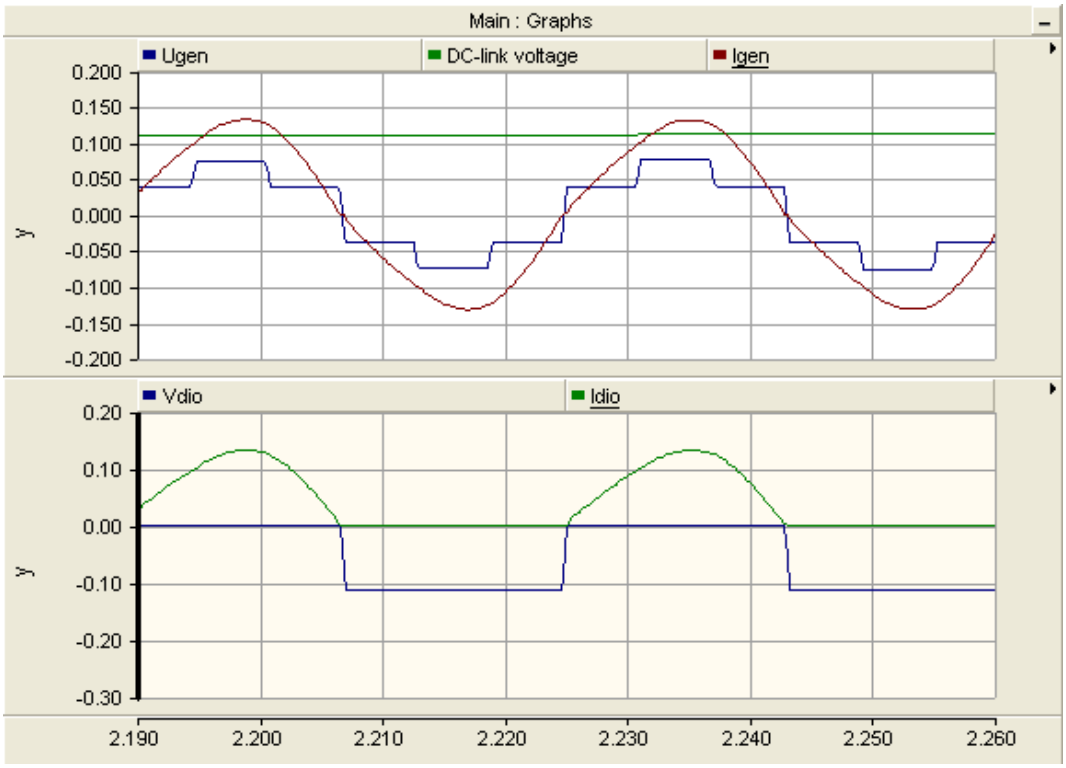

Figure 73: Simulated generator phase voltage [kV], generator current [kA], diode current [kA] and capacitor phase current [kA] for 27.5Hz generator frequency and with no reactive compensation

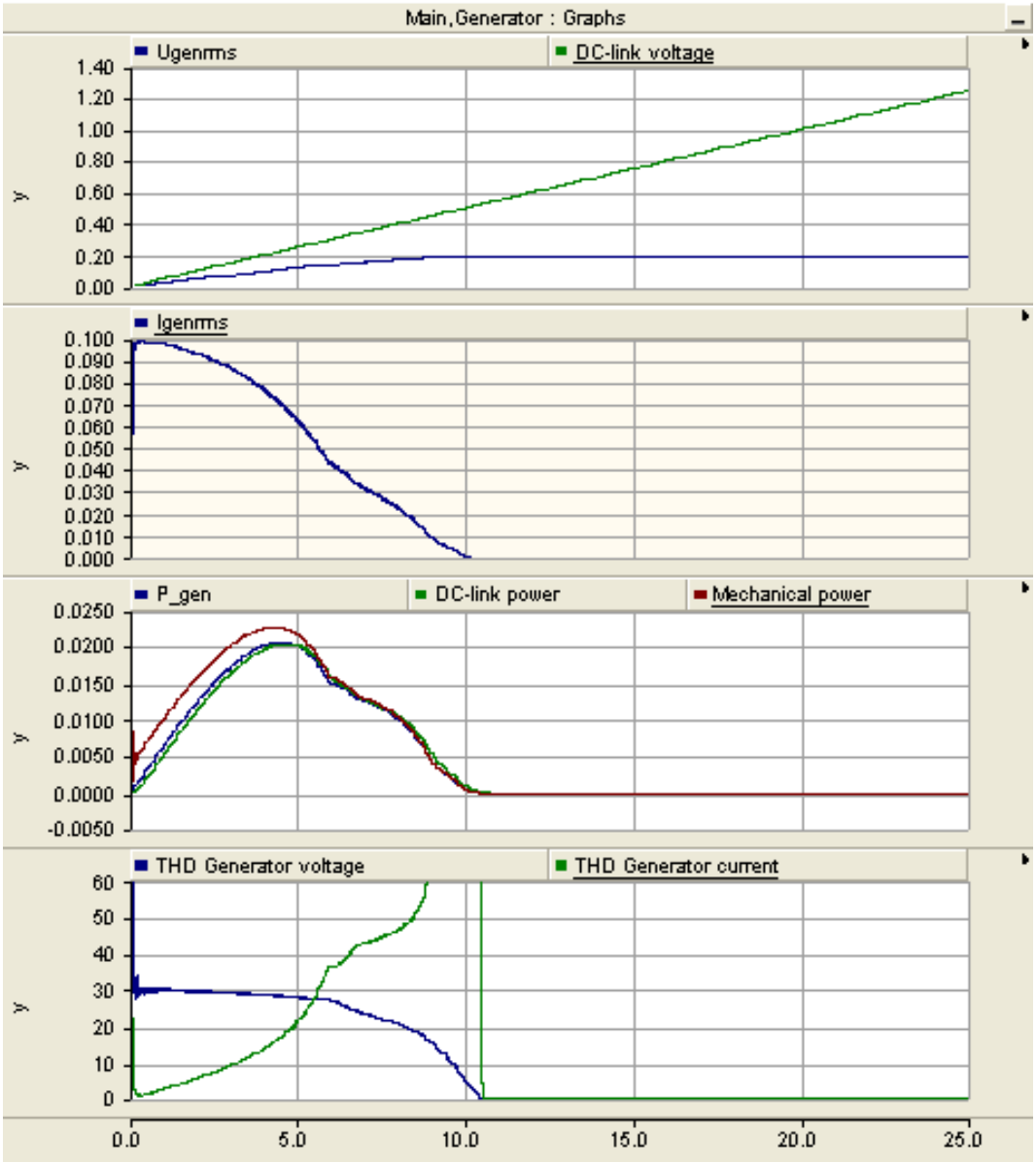

Figure 74: Simulated generator phase rms voltage [kV], diode current rms [kA], generator current [kA], generator power [MW], DC-link power [MW], generator voltage THD and generator current THD for increasing DC-link voltage, 27.5Hz generator frequency and with no reactive compensation

7.3 Series compensated PMGS

Series compensated PMSG with diode rectifier is also simulated in PSCAD. The data from the 55kW generator in "Vindlabben "is used. No tests in the laboratory is accomplished because to little capacitance was obtained. However, the simulation results shows the main problem with series compensation; very high current when the DC-link voltage is low.

Figure 75 shows the currents, voltages and powers when the DC-link voltage increases. A 50% series reactive compensation is used, which means that the capacitor value is $4713\mu F$, twice the size when 100% compensation is used. As seen from the figure, the generator voltage is more or less constant, while the generator current actually decreases when the DC-link voltage increases. The angle between the generator current and the generator voltage is also almost 90°. This means that the generator is delivering very much reactive power, causing high power loss in the generator. The short circuit current of the generator is very large due to the series compensation. Therefore the generator has to be dimension for a large current. High current can also cause demagnetising of the permanent magnets, according to [3].

The total reactance between the induced voltage in the generator and the diode rectifier is the sum of the synchronous reactance and the reactive compensation. The idea of the reactive compensation is to make the total reactance smaller, or zero. However, this causes some trouble when the DC-link voltage, and thereby the generator power is low. In this case, there is a large voltage drop between the induced voltage and the diode rectifier and the total reactance is low. This will cause a large current to flow. When the turbine is rotating at nominal speed and the power is for instant 50% of the rated power, the generator current is very much higher than necessary. This causes very high losses in the generator, and it seems like this solution is not any god. The maximal power is also low. A positive factor with this solution is the low current THD. This is also seen in Figure 76. The generator current shape is very sinusoidal and the generator voltage is not bad either.

To reduce the generator current, the generator could operate with a higher DC-link voltage at the right side of the power curve. This will reduce the power angle. However, the generator current THD will be high.

Figures 77 and 78 show the same information as Figures 75 and 76, but in this case the compensation level is 100%. The same results can be found in this simulation; however the situation is much worse. Both the generator current and voltage are very large when the DC-link voltage and the generator power is low, causing extremely high losses in the generator. The power factor is almost zero and the utilization of the generator is very bad. The generator current is 12 times the rated value and the maximum generator power is only $20kW$. However, the generator voltage and current THD is very low.

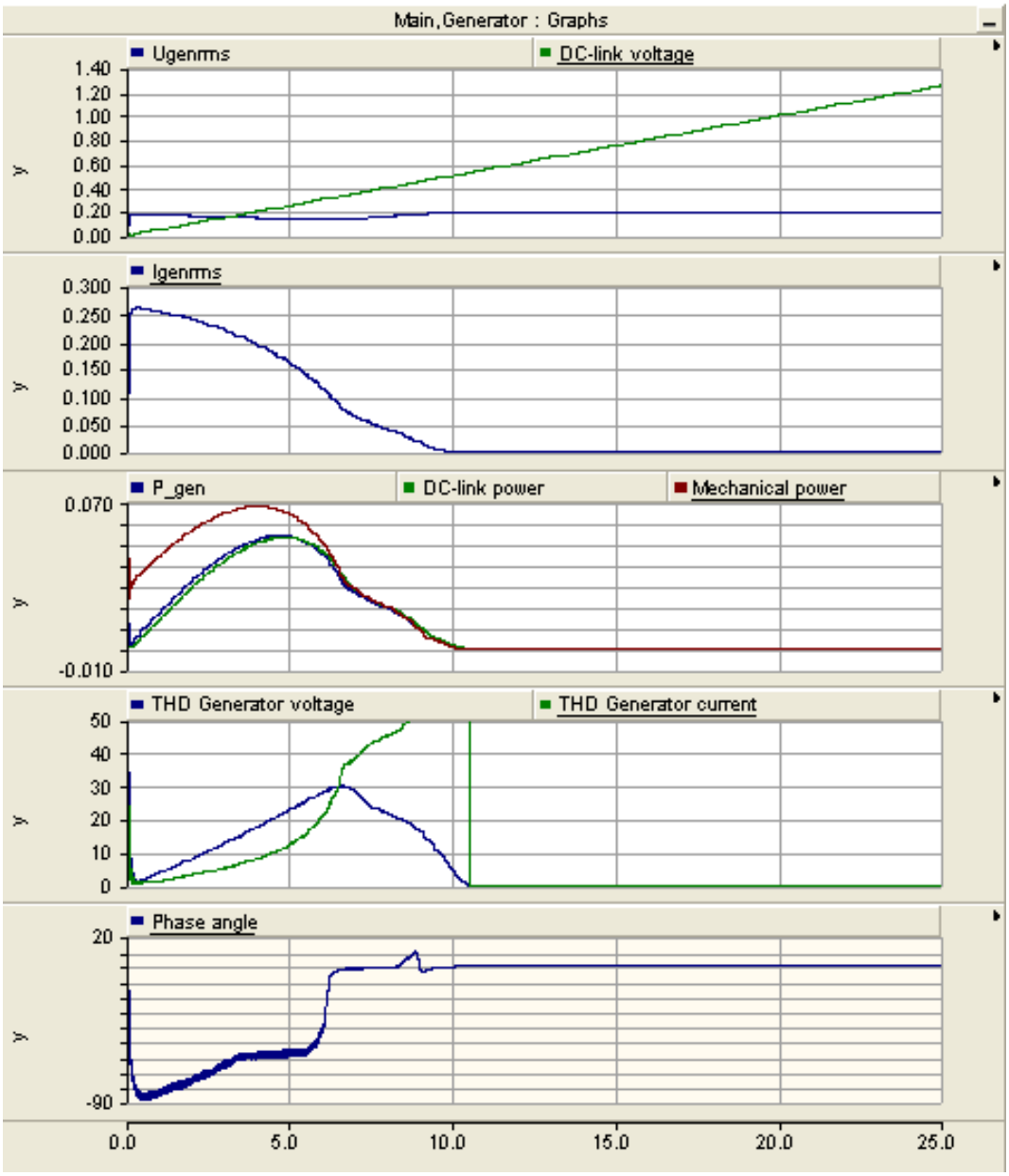

Figure 75: Simulated generator voltage [kV], generator current [kA], generator power [MW], mechanical power [MW], DC-link power [MW], generator voltage THD and generator current THD for increasing DC-link voltage and 50Hz with 50% series reactive compensation

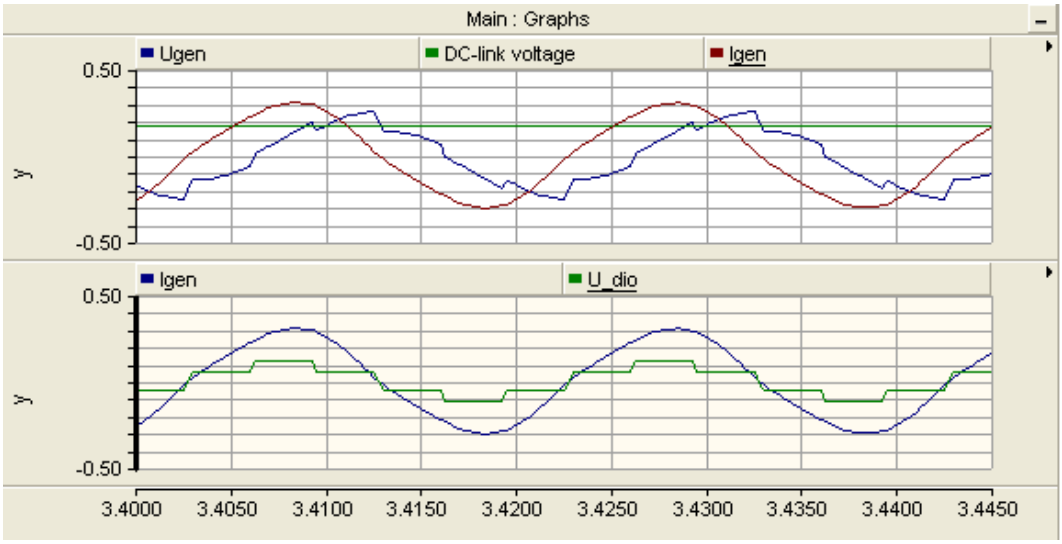

Figure 76: Simulated generator voltage [kV], generator current [kA], diode voltage [kV] and DC-link voltage [kV] for 50Hz with 50% series reactive compensation

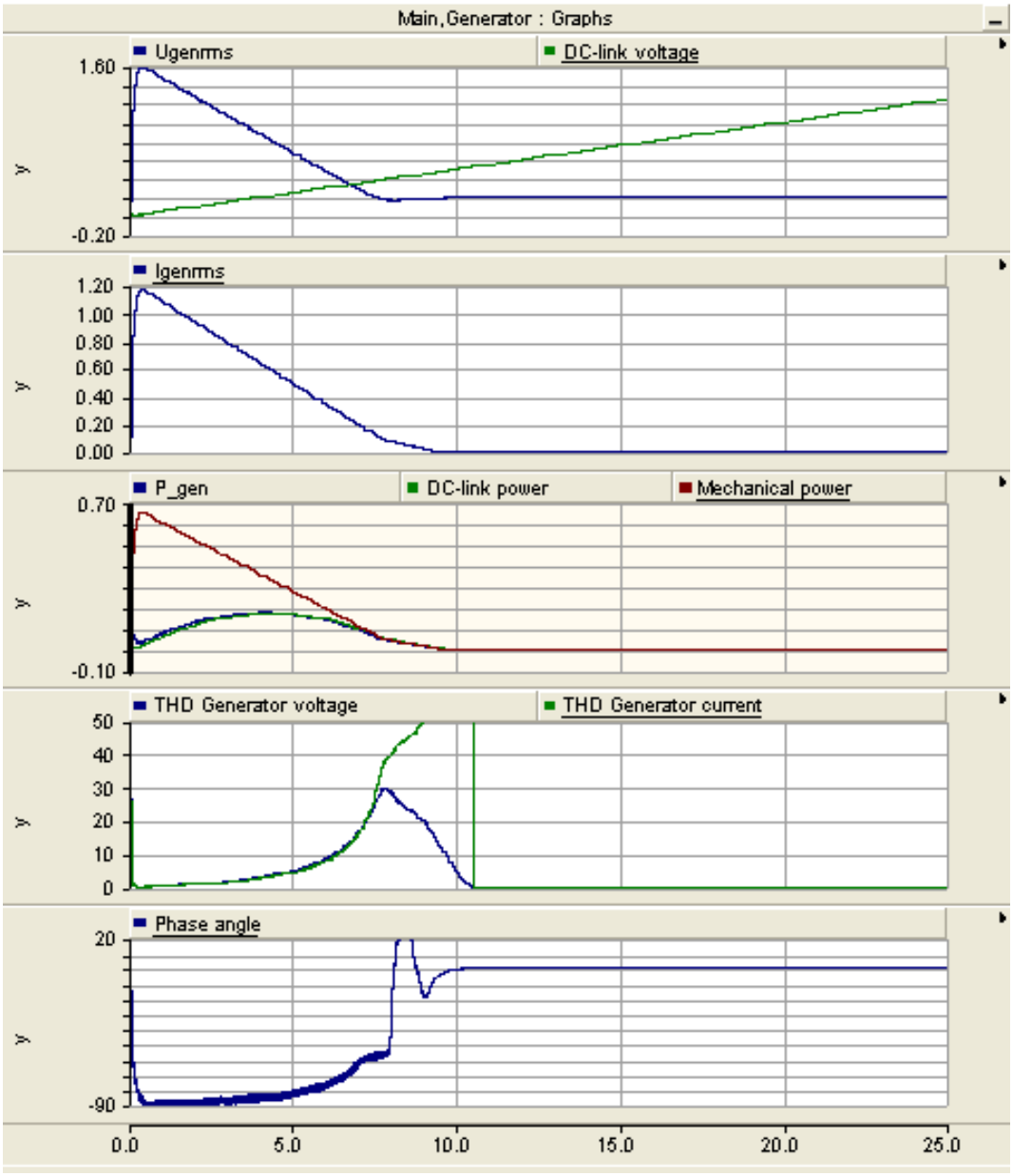

Figure 77: Simulated generator voltage [kV], generator current [kA], generator power [MW], mechanical power [MW], DC-link power [MW], generator voltage THD and generator current THD for increasing DC-link voltage and 50Hz with 100% series reactive compensation

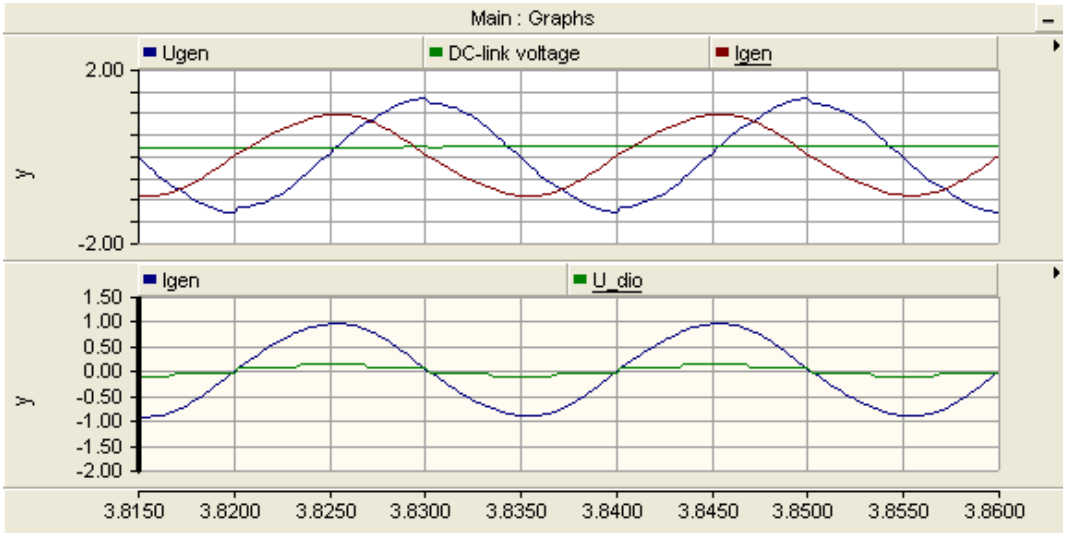

Figure 78: Simulated generator voltage [kV], generator current [kA], diode voltage [kV] and DC-link voltage [kV] for 50Hz with 100% series reactive compensation

8 Simulation of a 2 MW wind turbine with radial PMSG

8.1 Efficiency for parallel compensated PMSG, series compensated PMSG and PMSG with ideal load

In this section, the generator current, generator voltage, DC-link voltage, generator efficiency and diode rectifier efficiency for parallel compensated PMSG, series compensated PMSG and PMSG with ideal load are compared. Simulations for paralleled and series compensated PMSG are carried out in PSCAD/EMTDC while the calculation of the ideal voltage and currents are carried out in MatLab. The purpose of these computations is to compare parallel compensated PMSG with diode rectifier, series compensated PMSG with diode rectifier and PMSG with active rectifier. A 2MW wind turbine is used and the calculations are carried out for wind speeds from $5 - 12m/s$. Simulations have shown that the power losses of the generator are independent of the generator rated voltage when the pu values are given.

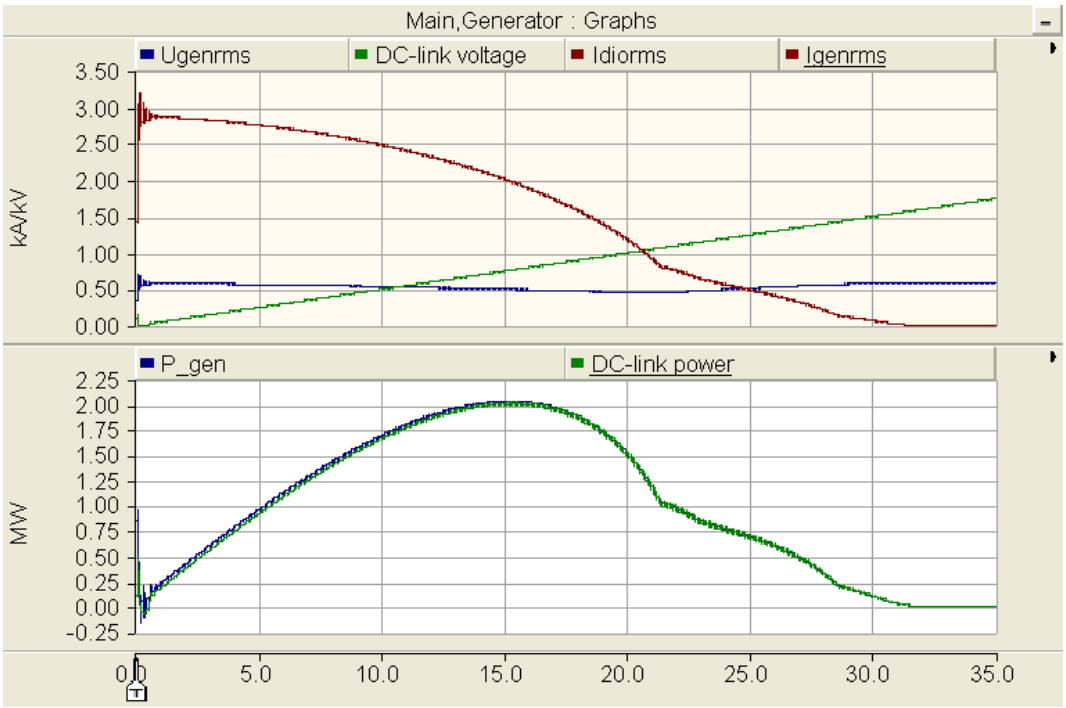

Figure 79: Generator voltage [kV], generator current [kA], DC-link voltage [kV], generator power [MW] and DC-link power [MW] for 2MW series compensated PMSG, nominal rotation speed and increasing DC-link voltage

Both the parallel and series compensated PMSGs are operating at the right side of the power curve shown in Figure 79. This is necessary to achieve low generator losses. When the generator speed is rotating at rated speed and the generator power

needs to be lower than the maximum power, the DC-link voltage is increased. In this way the generator voltage increases and the generator current rms decreases. The DC-link voltage should therefore be higher than 0.75kV when the generator is rotating at nominal speed. This will reduce the generator current and the generator losses. The problem is that the generator current THD becomes very high as the DC-link voltage increases. This value can be reduced by connecting a inductance to the DC-link, as explained in Chapter 9.

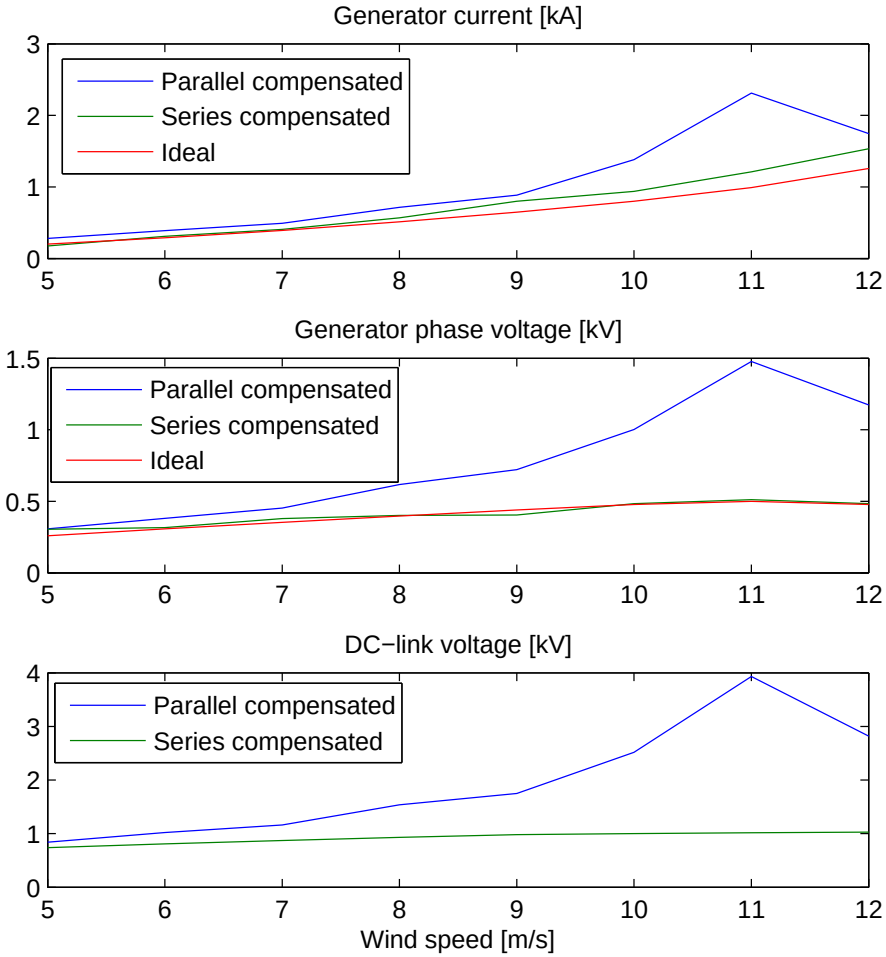

Figure 80: Generator current, generator voltage and DC-link voltage as a function of wind speed for series and parallel compensated PMSG with diode rectifier

Figure 80 shows the generator current rms, generator voltage rms and DC-link voltage for the three different configurations. The generator current increases when the wind speed increases. This relationship is necessary to keep the generator losses low for

low wind speeds. Both the series compensated and parallel compensated generators are operating at the right side of the power curve. This explains the relatively low currents at low wind speeds.

As seen from the figure, the parallel compensated PMSG have the largest current. For the low wind speeds the high generator current THD could be used to explain this. When the wind speed is between 9 and 12m/s, the currents through the synchronous inductance and the capacitors causes the generator voltage to rise. The reactive power produced by the capacitors will therefore be very large and the generator is overcompensated. This also causes large generator currents and large generator losses. The generator current and voltage are reduced when the wind speed reaches the nominal wind speed, 12m/s.

The generator voltage for the series compensated generator is approximately equal to the ideal generator voltage. However, the generator current is some higher due to the generator current THD. The voltage varies little as a function of the wind speed. A lower variation in the step-up ratio of the DC/DC converter is therefore needed

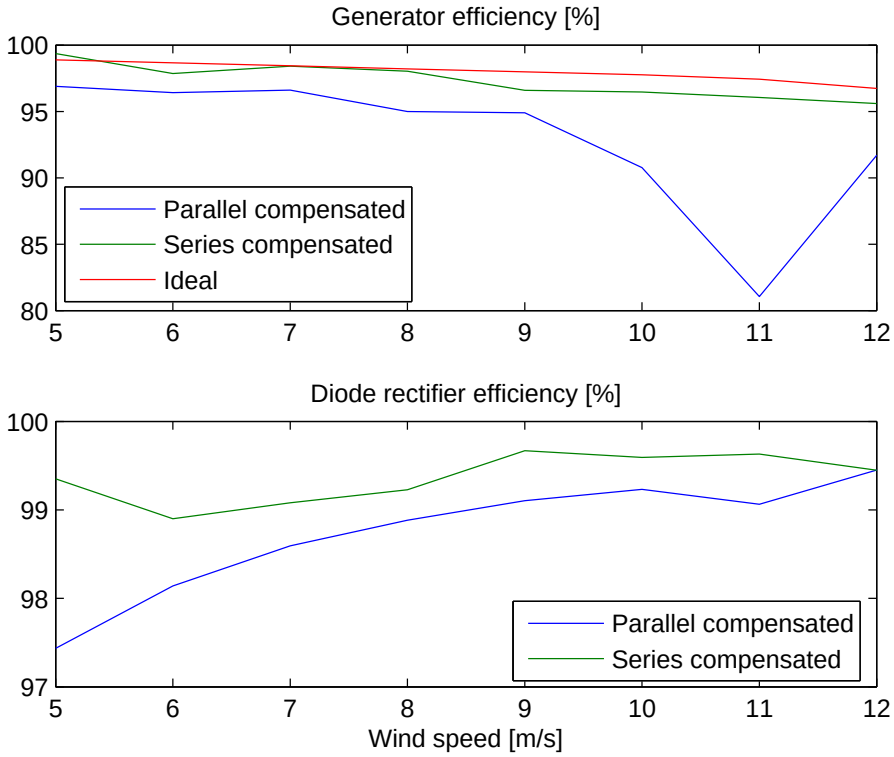

Figure 81: Generator efficiency and diode rectifier efficiency as a function of wind speed for series and parallel compensated PMSG with diode rectifier

Figure 81 shows the generator and diode efficiency for the three different configurations. Both the generator and diode efficiency is related to the generator current. As

seen, the losses are largest for the situation with parallel compensated generator because the generator current is higher in this case. However, the capacitance losses are not considered.

The figure shows that the series compensated PMSG have much smaller losses than the parallel compensated PMSG. The diode rectifier efficiency is between 99.0 and 99.7%. However, the diode losses can be reduced by connecting diodes in parallel. The generator efficiency is 95.5% for rated wind speed which is about 1% lower than the ideal case. However, the losses of the capacitors are not considered. These losses are probably much lower than the generator losses, and are neglected.

The high losses for the parallel compensated PMSG with 11m/s wind speed could be a problem. Losses cause heat in the generator, which has to be transported away. To solve this problem the size of the capacitances has to be adjustable so that the reactive power production is reduced when the wind speed is between 9 and 12 m/s.

8.2 Simulation of WECS with constant DC-link voltage

In this section, the wind turbine system is simulated in PSCAD with constant DC-link voltage. The purpose of these tests is to find how the turbine power is affected by using the Cluster step-up concept. In this case, the DC-link voltage will be more or less the same for all turbines. To get a maximum turbine power, the turbine rotation speed has to have a specific value. The best way of controlling the rotation speed is to control the DC-link voltage. The pitch angle can also be controlled to reduce the rotation speed; however this results in lower turbine efficiency. Also, the pitch controller is supposed to control the swaying of the turbine.

The wind speed varies inside the wind farm and the optimal rotation speed can therefore not be reached for all turbines. Simulations in PSCAD are accomplished to find how much the turbine power decrease when the DC-link voltage is not optimal compared to the ideal DC-link voltage for the specific wind speed. The average wind speed and the local wind speeds at each turbine are assumed to be constant. The simulations are performed with three different average wind speeds, $6m/s$, $9m/s$ and $12m/s$.

8.2.1 Parallel compensated PMSG and $9m/s$ average wind speed

The simulation with $9m/s$ wind speed is shown in Figure 82. The DC-link voltage is $1750V$ for all simulations, which is the ideal DC-link voltage for $9m/s$ wind speed. The maximal rotation speed of the turbine is $2.1rad/s$. Seven simulations are accomplished with wind speeds from $6m/s$ to $12m/s$. In each simulation, the rotation speed is increased from $0rad/s$ to $3rad/s$ within $30sec$. If the wind speed is constant, as assumed, the rotation speed of the turbine will be the value where the electrical torque equals the mechanical torque. This happens after $17.7sec$ in Figure 82. The rotation speed is then $1.77rad/sec$. Until the rotating speed reaches this value, the mechanical torque is larger than the electrical torque. The turbine will therefore accelerate. And visa versa; when the rotating speed is above this value, the electrical torque is larger than the mechanical, and the turbine is slowing down. The turbine rotation speed will therefore be stabilized at this value.

As seen from the figure, the diodes first start to conduct when the rotation speed reaches $1.5rad/sec$. This is when the induced voltage peak is larger than the DC-link voltage. When the rotating speed increase further, booth the generators currents, voltages, power and torque increase.

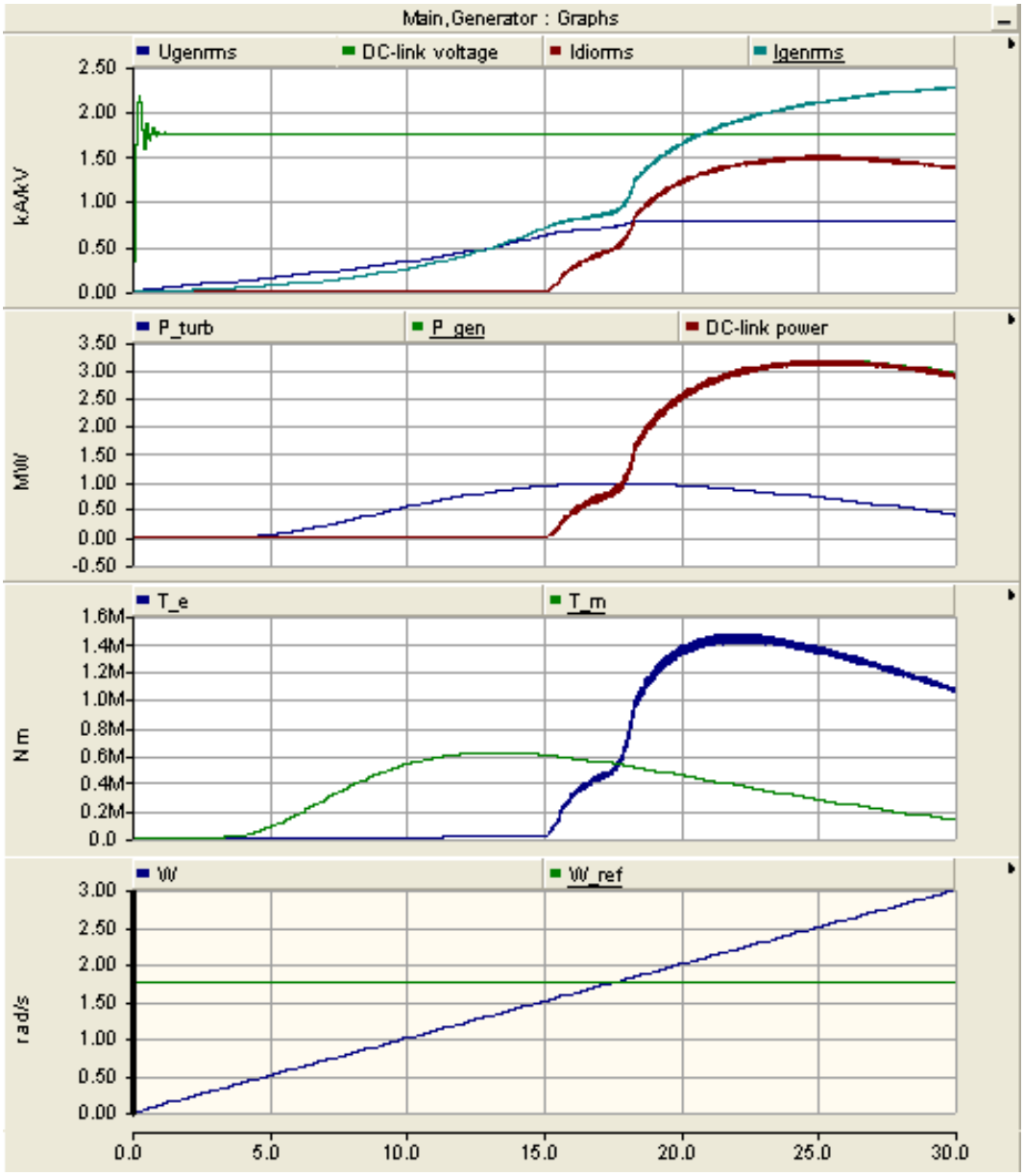

Figure 82: Simulation with $9m/s$ wind speed, constant DC-link voltage and increasing rotation speed

8.2.2 $6m/s$ average wind speed

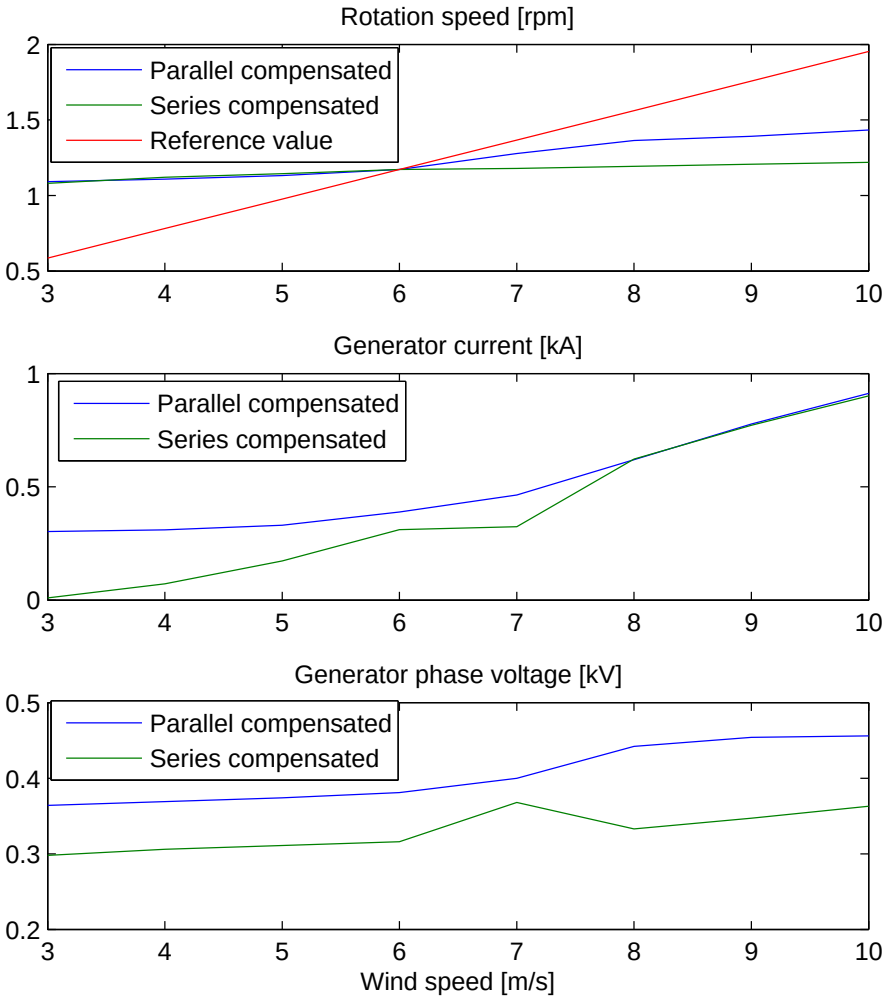

Figure 83: Rotation speed, generator current and generator voltage for increasing local wind speed and $6m/s$ average wind speed

Figures 83 and 84 show the stationary situation of a specific wind turbine when the average wind speed is $6m/s$. The common DC-link voltage is in this case 1.02kV for parallel compensated generators and 0.81kV for series compensated generators. The rotating speed is found for each wind speed as described above. The turbine power, generator power, generator current and generator voltage for this rotation speed is found. The maximal turbine power is also found. This appears when the rotation speed equals the reference rotation speed. The relationship between the turbine power and the

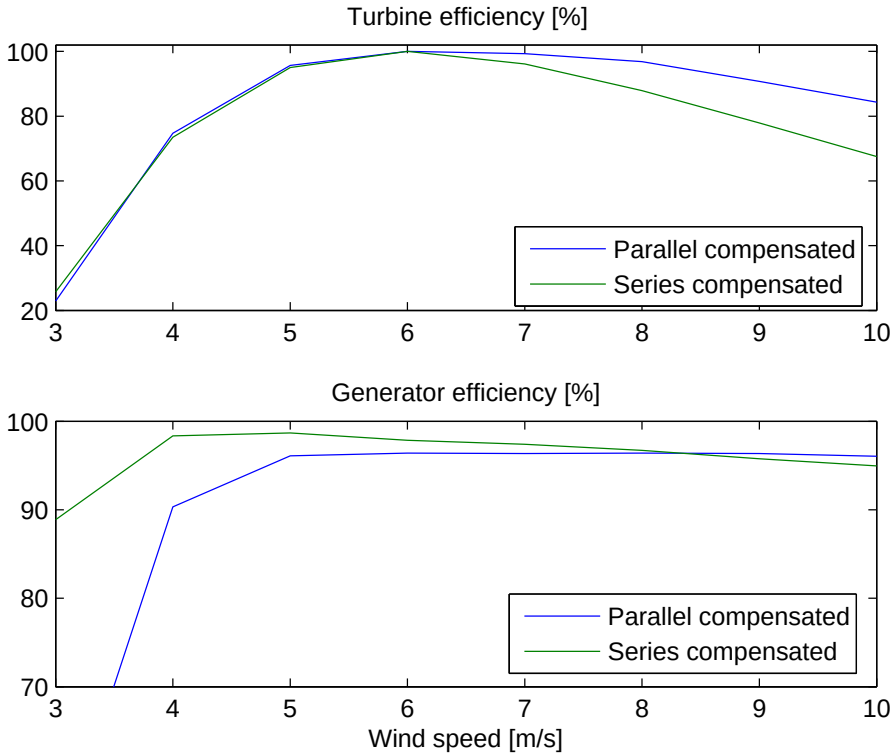

Figure 84: Turbine efficiency and generator efficiency for increasing local wind speed and $6m/s$ average wind speed

maximum turbine power is calculated. This is later referred to as the turbine efficiency.

As seen from Figure 83, the rotating speed is almost constant when the local wind speed changes. However, the generator with parallel compensating is rotating a little faster for high wind speeds. The turbine efficiency of this turbine is therefore higher, as shown in Figure 84. The turbine power is 100% of the maximal turbine power when the wind speed is $6m/s$. If the wind speed is $1m/s$ lower, the turbine power is reduced to 96% of the maximal turbine power. If the wind speed is $2m/s$ lower, the turbine power is reduced to 75% of the maximal turbine power. A larger difference between the local wind speed and the average wind speed in the park will cause the turbine power efficiency to decrease even more. The generator current is lower for the series compensated generator, and the generator efficiency of this generator is therefore highest.

8.2.3 $9m/s$ average wind speed

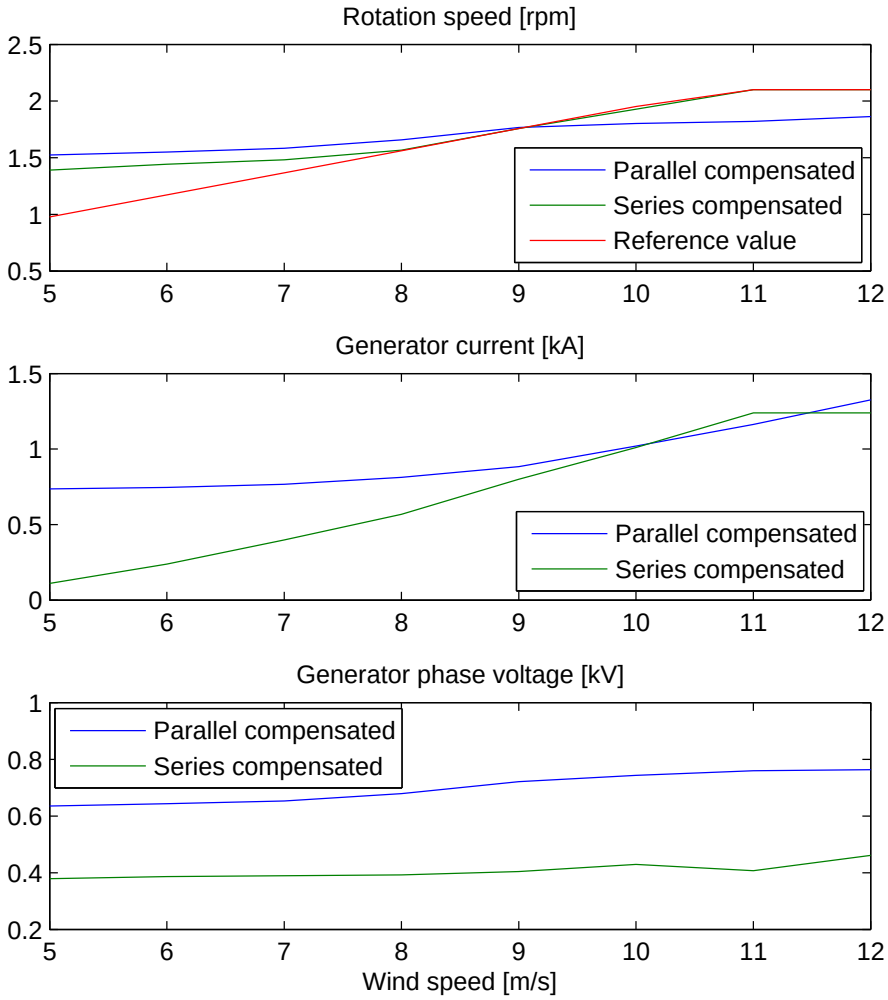

Figure 85: Rotation speed, generator current and generator voltage for increasing local wind speed and $9m/s$ average wind speed

Figures 85 and 86 show the stationary situation as a function of the local wind speed when the average wind speed is $9m/s$. The common DC-link voltage is in this case 1.75kV for parallel compensated generators and 0.98kV for series compensated generators. The rotation speed is decreasing very little when the wind speed is lower than $9m/s$ and the turbine efficiency is therefore decreasing when the local wind speed decreases. However, the rotation speed follows the reference speed when the wind speed is higher and series compensation is used. This means that the turbine efficiency

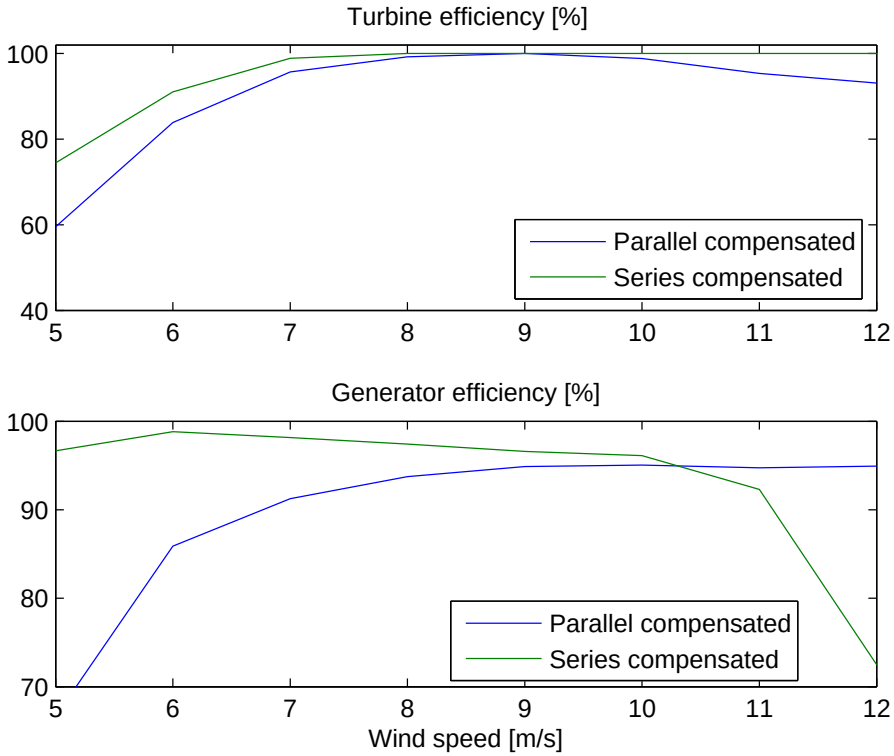

Figure 86: Turbine efficiency and generator efficiency for increasing local wind speed and $9m/s$ average wind speed

is 100% in this case, as seen from Figure 86.

The generator efficiency is low for parallel compensated PMSG for low wind speed because of the large current. The loss of the series compensated PMSG is lower because of the low generator current. However, the generator efficiency is higher for the parallel compensated PMSG for high wind speeds.

8.2.4 $12m/s$ average wind speed

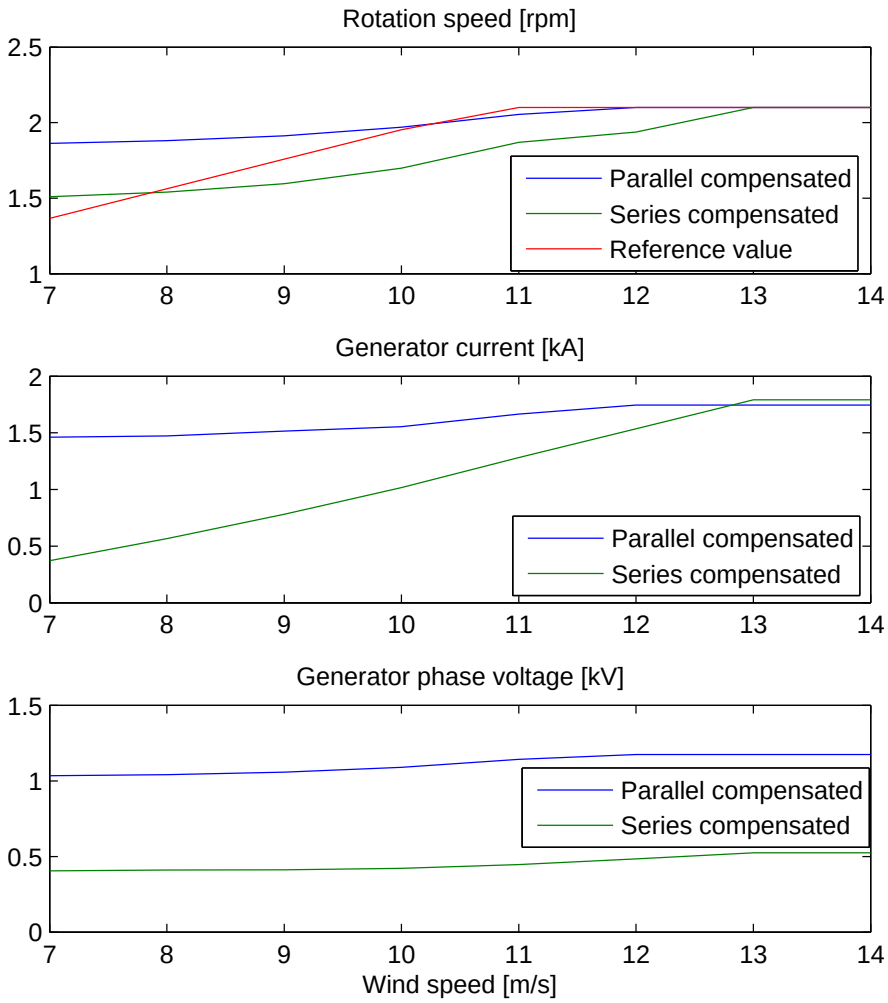

Figure 87: Rotation speed, generator current and generator voltage for increasing local wind speed and $12m/s$ average wind speed

Figures 87 and 88 show the stationary situation as a function of the local wind speed when the average wind speed is $12m/s$. The common DC-link voltage is in this case 2.82kV for parallel compensated generators and 1.03kV for series compensated generators.

In this case the parallel compensated generator has the highest turbine efficiency because the generator speed is closest to the ideal rotating speed. However, the generator current is much higher for the parallel compensated generator, so the

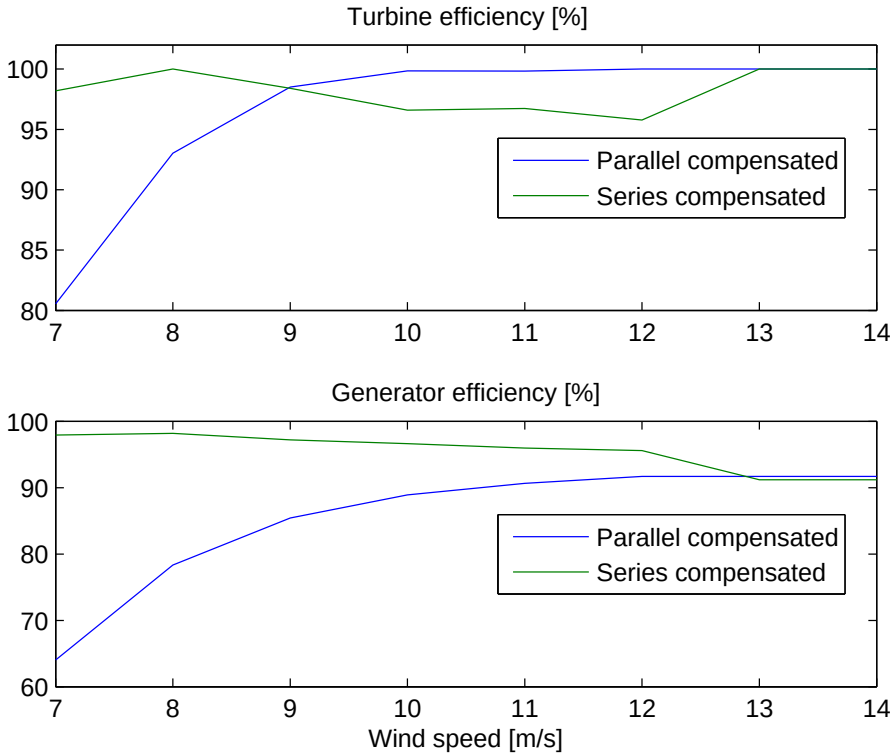

Figure 88: Turbine efficiency and generator efficiency for increasing local wind speed and 12m/s average wind speed

generator efficiency is lower than if a series compensated generator is used.

8.2.5 Power efficiency of WECS with constant DC-link voltage

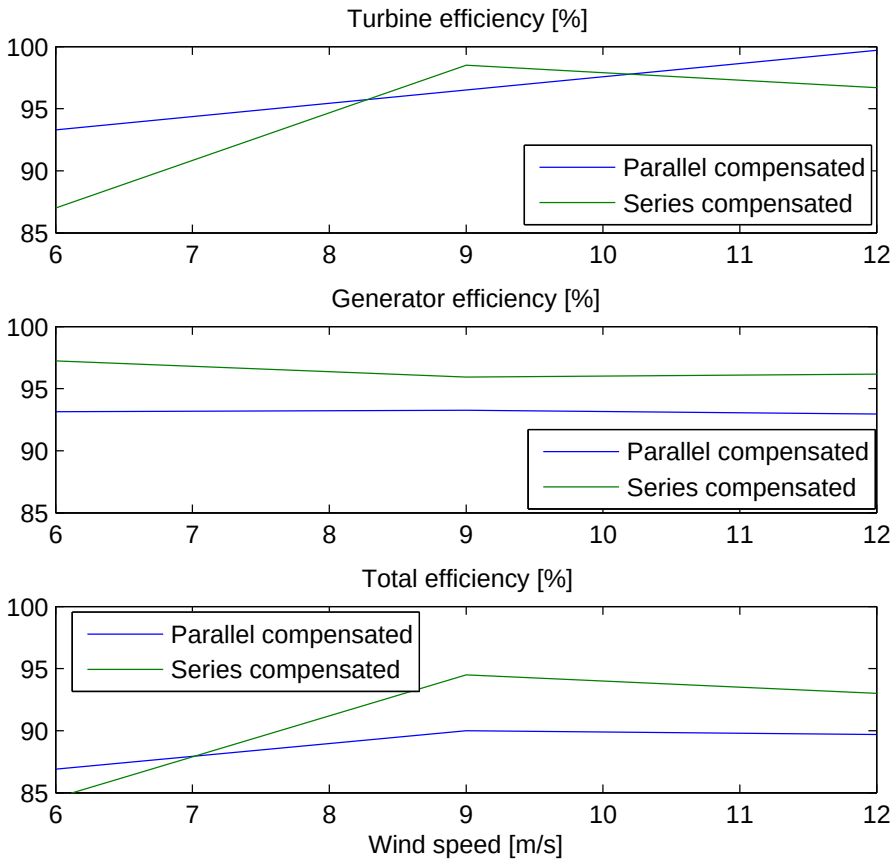

Figure 89: Turbine and generator efficiency for constant DC-voltage control

Figure 89 shows the turbine, generator and total efficiency for 6, 9 and 12m/s average wind speed when the DC-link voltage is constant for a whole wind farm. The results from the sections above are used to find an estimate of the average power efficiency due to the fact that the turbine is not rotating at ideal speed all the time. The average generator efficiency and total efficiency (turbine and generator efficiency) is also found. Wind data from Frøya a January day in 1955 is used to find how much the wind varies. The wind farm size is assumed to be 10km times 10km and it is assumed that the wind uses 30min to pass the area. The average wind speed within 30 min is therefore found. The wind speed distribution within these 30 min are found and compared to the turbine efficiency and generator efficiency. Then the average

efficiencies within the 30 min are found. This is done for 6, 9 and 12m/s average wind speed.

As seen from Figure 89, the turbine efficiency is highest for the parallel compensated PMSG. However, the generator efficiency is less, so the total turbine and generator efficiency is highest for the series compensated PMSG for 9 and 12 m/s. The efficiency at 6 m/s is less important since only a small part of the total power is produced when the wind speed is so low.

To find how much less the power production is when a cluster step-up configuration is used, the total efficiency could be compared to the generator efficiency for varying DC-link voltage, as shown in Figure 81. The generator output power is about 3% lower when cluster step-up configuration and series compensated PMSG are used and the wind speed is 9m/s or higher. The difference is much larger when the average wind speed is lower. The average power loss due to the constant DC-link current is therefore about $3 - 4\%$.

9 Simulation of a 3 MW ironless PMSG

A 3MW ironless axial flux PMSG generator with diode rectifier is simulated in PSCAD. The data is obtained from SmartMotor A/S, which currently is developing an ironless PMSG for wind turbines. The turbines are supposed to have an efficiency at 98% and are going to weight up to 40% less than conventional PMSG generators. [29] The generator data is shown in Table 6. The generator efficiency is in this case 94%. Due to the little use of iron, the synchronous reactance is very small compared to conventional permanent magnet synchronous generators. The value of the synchronous reactance for a radial flux PMSG is from 0.7 to 0.9 pu, while this generator has a synchronous reactance at 0.11pu. As seen in the following, the low synchronous reactance causes problems.

Figure 90 shows the currents, voltages, powers and total harmonic distribution when the DC-link voltage increases. The generator is operating at nominal speed. The parallel connected capacitors are chosen in such way that the reactive power produced by these capacitors equals the reactive power produced by the synchronous reactance at rated speed and power.

Since the synchronous reactance is small, the generator current is very high when the DC-link voltage is low. As the DC-link voltage increases, the generator current decreases. The rated current of the generator is 2933A. The DC-link voltage has to be increased very much until the generator current and generator power are reduced to the rated values. When the generator power is 3MW, the current THD has increased to 64%, which is unacceptably large. This causes additional losses. Also, the generator could be very difficult to control when it is operating at the right side of the power curve and the short circuit current of the generator is also very high. The capacitors do not work as supposed, they just causes fluctuations in the generator current. Since the synchronous reactance is low, the reactive power produced by the synchronous reactance is low and the reactive compensation is not necessary.

Figure 91 shows the shows the same measurements as Figure 90, but without reactive compensation. As seen, there are no principal differences between these two figures. However, the current THD is actually lower in this case; 51.1% when the generator power is 3MW. The current shape is shown in Figure 92. As seen, the generator current is zero for most of the time, which causes a high THD. The peak of the current is also high.

The generator current THD can be lowered by installing a DC-link inductor. After some testing, a suitable value of the inductance is found to be 1mH. The result of the simulation is found in Figures 93 and 94. As seen from Figure 93, the generator current THD is reduced from 54.1% to 18.6% at rated power. The generator current rms is also reduced, from 3571A to 3342A.

The 3MW generator is also tried simulated with series compensation. However, the capacitor needs to be very large, $772mF$, due to the small synchronous reactance. This value is too large to be simulated in PSCAD/EMTDC, and it is also probably also to large to be used in a real turbine.

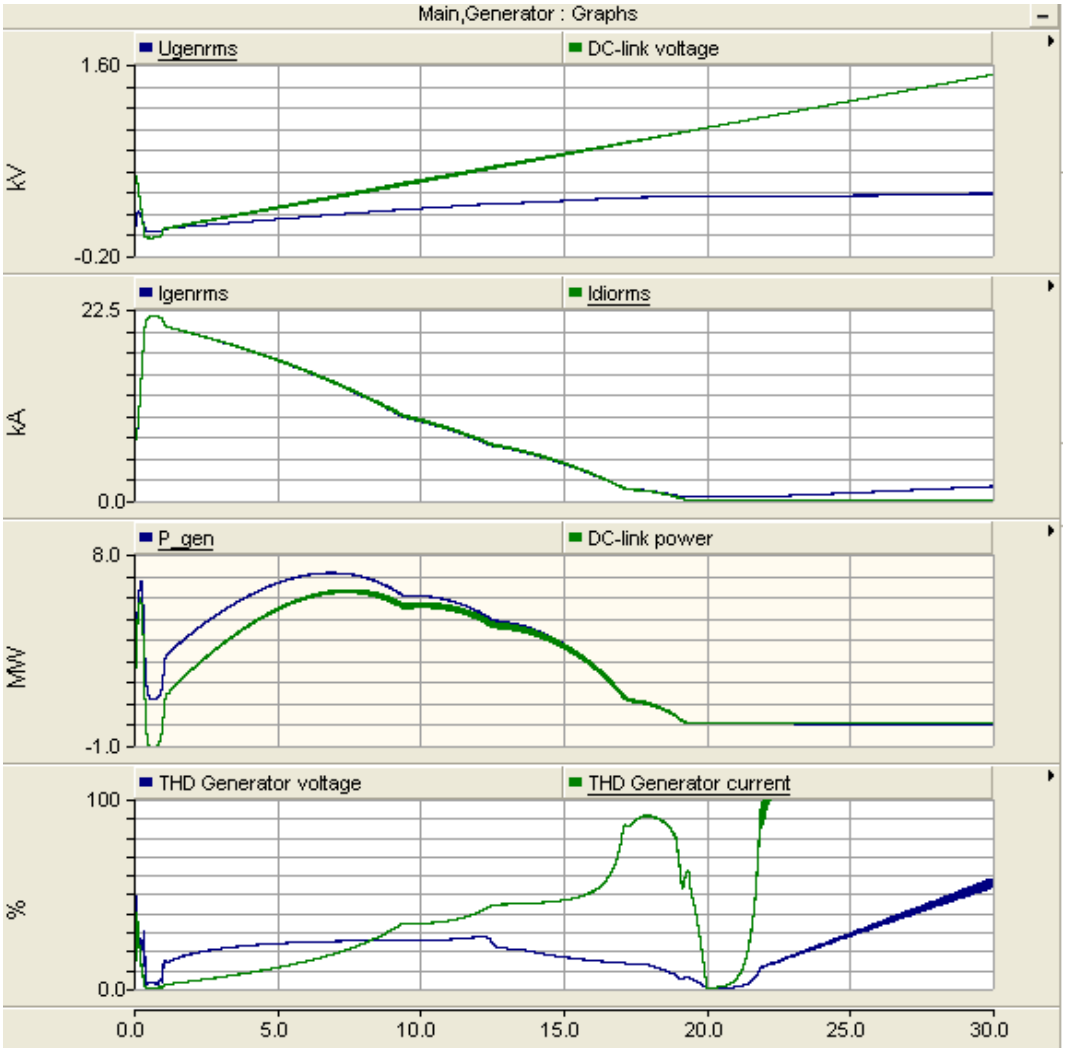

Figure 90: Simulation of 3MW ironless PMSG with constant rotation speed, reactive compensation and increasing DC-link voltage

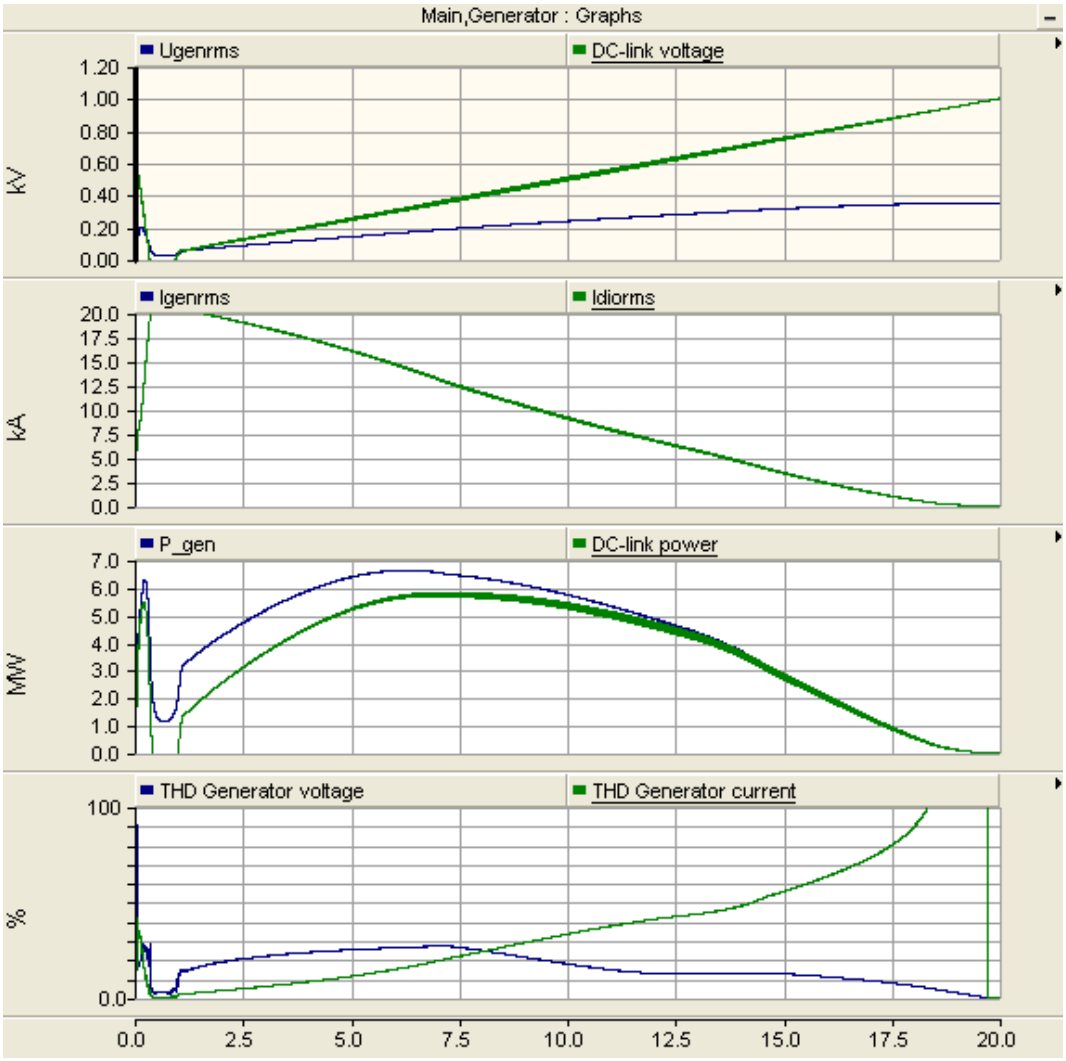

Figure 91: Simulation of 3MW ironless PMSG with constant rotation speed, no reactive compensation and increasing DC-link voltage

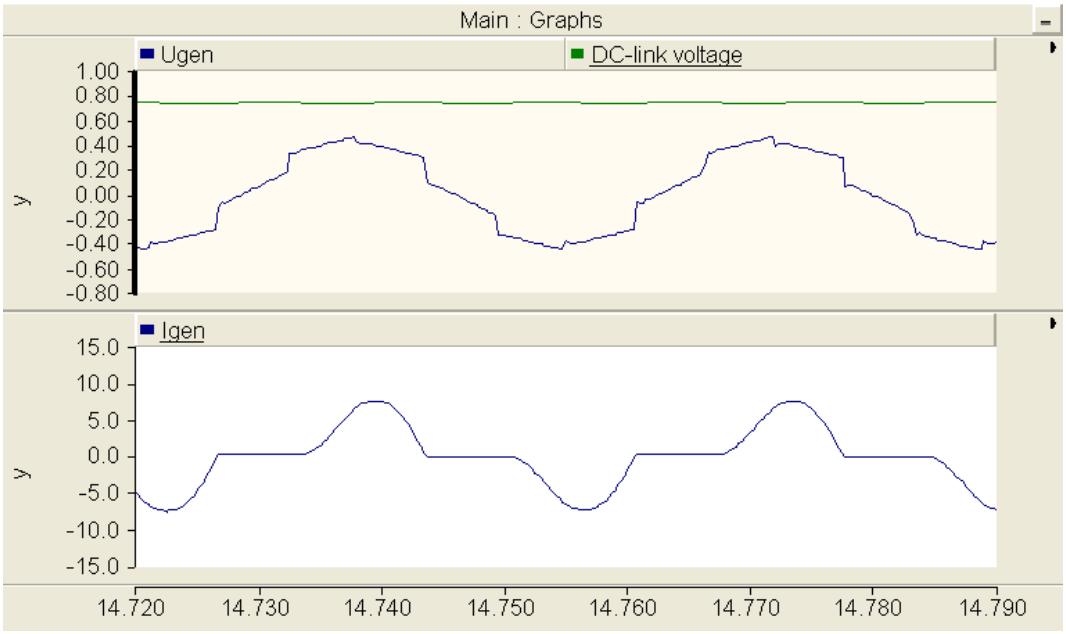

Figure 92: Phase current and phase voltage when the turbine is operating at 3MW and rated speed

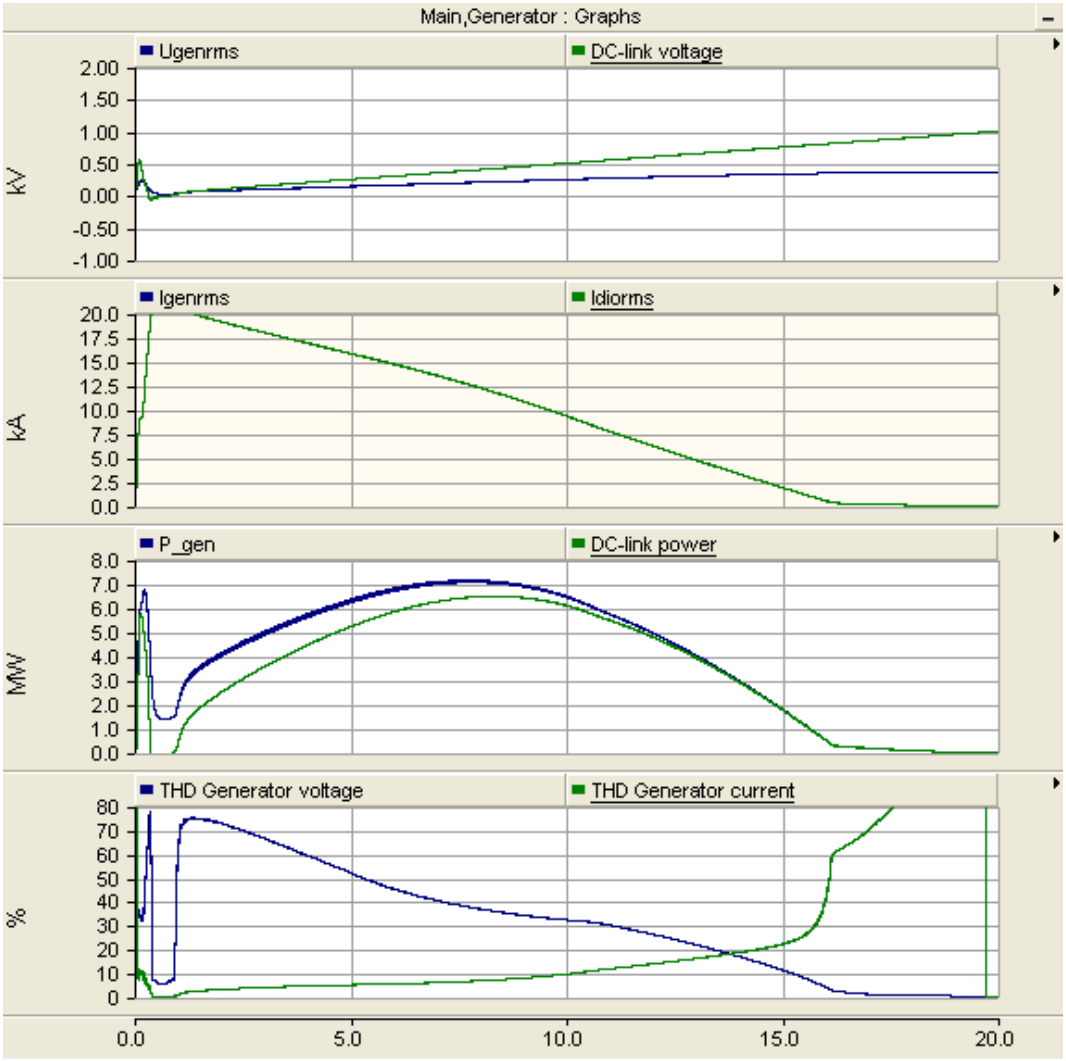

Figure 93: Simulation of 3MW ironless PMSG with constant rotation speed, no reactive compensation, DC-link inductance at 1mH and increasing DC-link voltage

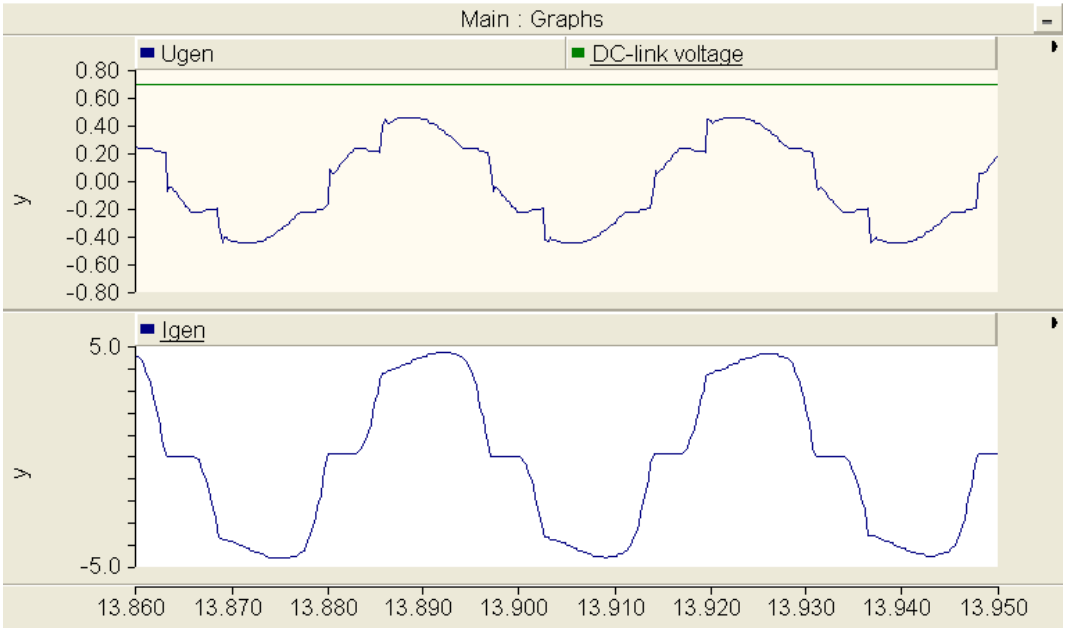

Figure 94: Phase current and phase voltage when the turbine is operating at 3MW and rated speed and a DC-link inductance at 1mH is installed

10 Discussion and conclusion

10.1 AC or DC offshore grid?

If the transmission distance to shore exceeds 50-100km, a DC grid solution will both have the lowest power losses and be the best choice economically. This can be explained with the fact that most of the DC transmission losses are related to the power converters, while most of the AC transmission losses are related to the cables. The AC cable losses increase very fast when the transmission distance increases, due to the reactive power production in the cables. This decision does not depend on the power level of the wind farm.

The transmission losses in the DC cables are small and the total transmission losses will therefore increase slowly when the transmission distance increases. The cables can therefore in many cases profitably be connected to a stronger point of common connection farther away instead of the nearest grid point. This will improve the stability of the grid.

A DC transmission system will probably be the only rational choice for offshore floating wind turbines, due to the size of the offshore wind farms and the transmission distance.

10.2 Series or parallel compensated PMSG?

Weight of the nacelle is an important issue for floating offshore wind turbines. Extra weight in the nacelle causes need for a stronger tower which results in extra costs. The lightest electrical generator solution for large wind turbines seems to be the direct-driven permanent magnet synchronous generator. A lot of research is going on to make the generator even lighter. A solution with asynchronous generator and gear will be much heavier because the weight of the gear is increasing very fast when the turbine size increases.

Due to the large synchronous reactance of the radial PMSG, some kind of reactive compensation is needed to reach the maximum power output of the generator. When an IGBT rectifier is used, the rectifier delivers reactive power to the generator. However, a diode rectifier is not able to do this. The solution is to connect capacitors to the generator, either in parallel or in series. Both methods are considered in this thesis and both simulations in PSCAD/EMTDC and laboratory tests are used to learn how these two methods work.

The results show that both methods have advantages and disadvantages. The generator losses are $2-15\%$ lower for series compensated generators, as shown in Figure 81. This is caused by two main reasons. Firstly, the generator current THD is lower because the synchronous inductance and the series connected capacitance force one of the two diodes connected to a phase to conduct. The generator current will therefore be more sinusoidal and more power is produced per Ampere. The solution with parallel connected capacitors will have a larger generator current THD because the

capacitors cause the generator current to be more squared. The diode rectifier losses are also lower.

Secondly, the generator current rms is lower at a specific wind speed when series connection is used. This is caused by the fact that the THD is lower, but also that both the reactive power consumed by the synchronous reactance and the reactive power produced by the capacitors are proportional to the squared of the generator current. Therefore, the compensation level is independent of the generator current and voltage. However, the power consumed by the synchronous reactance is proportional to the frequency of the generator, while the power produced by the capacitors is proportional to the inverse of the generator frequency. This causes the generator to be overcompensated when the wind speed and the generator frequency decreases, which means that too much reactive power is produced.

The compensation level of the parallel connected capacitors is no ideal either. The capacitors are chosen to fit the rated power. When the wind speed decreases, the DC-link voltage, and therefore the generator voltage, will decrease. The reactive power consumed by the synchronous reactance is proportional to the squared of the generator current, while the reactive power produced by the capacitors is proportional to the squared of the generator voltage. As seen from Figure 80, the generator voltage is decreasing quicker than the generator current when the wind speed decreases. This means that the reactive power produced by the capacitors becomes larger than the reactive power consumed by the synchronous reactance when the wind speed is between 9 and 12 m/s. The generator is therefore overcompensated. The generator losses can be reduced by reducing the size of the capacitors and with that the compensation level. The DC-link voltage can also be reduced, causing generator current, generator losses and rotation speed. However, this will result in lower turbine efficiency.

The series connected capacitors will conduct much more current than the parallel connected capacitors and the power losses in the capacitors will therefore be higher. The series compensated PMSGs will also have a larger short circuit current due to the low total reactance of the synchronous reactance and the capacitors. This also makes the regulation of the turbine difficult. The generator has to operate at the right side of the power curve to obtain a low generator current. If the DC-link voltage increases when the generator operates in this area, the power decreases. Also, if the DC-link voltage decreases too much too fast, this will cause a large current in the generator and large generator power and torque. Hopefully this will cause the generator to retard and the current and power will then decrease. A regulator has to handle this in a proper way.

As seen, the series compensated PMSG seems to be the best alternative, due to the low power losses. However, special attention to the DC-link voltage regulator is needed to avoid large currents in the generator.

10.3 Laboratory tests of a 55kW PMSG

Measurements on a 55kW PMSG with diode rectifier is carried out in "Vindlabben". Simulations are also performed in PSCAD/EMTDC. The generator is operating on the left side of the power curve in this case. The shapes of the generator current and generator voltage are found to be approximately the same for the measurements and the simulation. However, the generator current seems to be more squared in the measurements. The measured and simulated current and voltage THD differ slightly. The measured values are higher than the simulated values. The actual machine and capacitor data can differ from the given values and this could explain the differences in generator current shape and THD. The differences could also be related to the generator design.

Also the generator current is found to be 5 times as high in the simulations as in the measurements. An explanation for this is that the generator parameters could be incorrect. The generator current is very dependent on the synchronous reactance and resistance. A higher value of these parameters will cause the generator current to decrease.

Both the measurements of the generator and simulations in PSCAD show that the maximal power output is much larger when reactive compensation is used. The power output might be about 3-4 times larger. The power output is also lower when the generator is operating at a lower frequency.

10.4 Layouts of DC grid wind farms

Several different DC grid layouts are considered. The difference consists of where the converters are placed, how many voltage steps are used and whether the turbines are parallel connected or series connected.

The series connected wind turbines were proposed by Lundberg in [28]. He claims that this solution will be 10% cheaper than the parallel connected solution because no offshore platform is required and because the cables are cheaper. This solution includes a DC/DC converter in each generator, which makes it possible to control each generator individually. This solution will therefore probably work well together with a PMSG with diode rectifier.

The other solutions include parallel connected turbines. Three alternatives are considered; only one common DC/DC converter (cluster step-up), one DC/DC converter in each turbine (turbine step-up) and both a DC/DC converter in each turbine and a common DC/DC converter (two step-ups). The cable losses are neglected.

According to [27], the two step-ups solution has the highest power losses, about 4.5%. It will also be the most expensive solution because many power converters and an offshore platform are required. Max claims in [14] that the losses can be reduced to 2.2% if a series parallel resonant converter is used and the variation of step-up ratio is performed by the converters in the turbines.

The turbine step-up solution has a power loss of about 3%, according to [27]. When

a PMSG and a diode rectifier are used, the step-up ratio of this converter needs to be adjustable. This will probably increase the losses. An offshore platform is not required, but the voltage level in the turbine is very high and a lot of high voltage cables are required inside the wind park.

The cluster step-up solution requires that the DC-link voltages of all the generators are equal. The electrical generator torque can therefore not be controlled individually since the DC-link voltage has to be controlled for the whole wind farm. The generator speed and the power output will therefore depend on the wind speed and the common DC-link voltage. Simulations show that the turbine efficiency is reduced when the wind speed differs inside the wind farm because the turbines can not be controlled to keep the optimal rotational speed. The generator efficiency is also decreased a little. Calculations based on the wind speed on Frøya a January day in 1955 show that the turbine efficiency is reduced $3-5\%$ because of the constant DC-link voltage. However, the DC/DC converter losses are very small, about 1%.

The two step-up solution seems to have the best total efficiency. However, this also seems to be the most expensive solution. The cluster step-up solution is cheaper because only one converter is needed. This can be placed on a platform where it is accessible for maintenance almost all the time. The turbine will contain very few power components. A simple construction increases the reliability of the turbine. The cost of the turbines is also important. A cluster step-up solution may have a lower total efficiency, but it is also cheaper than the two step-up solution. If the system is much cheaper, the cost per MWh may be reduced.

10.5 Ironless PMSG with diode rectifier

A 3MW ironless PMSG is simulated in PSCAD. The main difference of these generators is that the synchronous reactance is much smaller, just 0.11pu. This causes problems when a diode rectifier is used because the generator current will be very large when the DC-link voltage is low. However, the generator current is reduced to an acceptable level when the DC-link voltage increases. The generator is then operating at the right side of the power curve. The problem is that the current THD is unacceptably high because the diodes only conduct for a small amount of time. The current THD can be reduced by connecting an inductance at for instance 1mH to the DC-link. The generator current THD is than reduced to $15-25\%$, depending on the power level.

Simulations have shown that the use of parallel connected capacitors have no positive affects, they just cause ripples in the generator current. Series compensation could not be used either because a very large capacitor is needed due to the low synchronous reactance.

10.6 Diode or IGBT rectifier?

A simple comparison between the total power losses of a PMSG with IGBT rectifier and a PMSG with diode rectifier is performed in the following. The IGBT rectifier losses are about 2% due to Figure 21. The generator losses will in this case be more or less the same as the ideal case in Figure 81, because the generator flux and the generator current can be controlled. The total losses will therefore be about 0.5% higher than if a diode rectifier is used. The diode rectifier is also much smaller than an IGBT rectifier. This is an advantage because less space is required in the nacelle.

A cluster step-up solution and a PMSG with IGBT rectifier could be a good solution. The generator speed could be regulated to the optimal even if the DC-link voltage is constant and total power loss in the system will be very low. However, the reliability is not as good as for the PMSG with diode rectifier. To use this solution, a high voltage PMSG and active rectifier is needed.

10.7 Further work

Costs are important when technical solutions for an offshore wind farm are to be chosen. The cost of the different system layouts in this thesis could be investigated to find the cheapest solution pr MWh produced power. Especially the cluster solution could be investigated. The power efficiency of this solution is lower; however the solution is so simple that it might be the cheapest.

It is difficult to control the electrical torque when parallel or series compensation is used. The generator operates at the right side of the power curve and an increase of the DC-link power instantly causes a decrease of the generator torque. The system is nonlinear and depends on wind speed, generator rotation speed and DC-link voltage. A proper DC-link voltage regulator has to be developed. Fluctuations in the electrical torque could also be investigated.

Passive filters could be used to reduce the generator current THD. Different filter layouts could be simulated to find suitable parameters and to find the power losses. It is difficult to tune the filters because they have to work for varying generator frequencies. Further work can be performed on calculating power losses. Active filters could also be further investigated.

The use of diode rectifiers causes the generator current to be somewhat higher than if an active rectifier is used. Research on how this affects the generator design and how much this affects the weight of the generator could be performed.

References

[1] A.B.Morton, S.Cowdroy, J.R.A.Hill, M.Halliday, and G.D.Nicholson. Ac or dc? economics of grid connection design for offshore wind farms. *AC and DC Power Transmission*, 2006.

[2] A.E.Fitzgerald, C.Kingsley, and S.D.Umans. *Electric Machinery*. McGraw-Hill, Singapore, 1992.

[3] A.Grauers and A.Lindskog. Pm generator with series compensated diode rectifier. *Nordic Workshop on Power and Industrial Electronics (NORpie'2OOO)*, 2002.

[4] A.Mirecki, X.Roboam, and F.Richardeau. Comparative study of maximum power strategy in wind turbines. *International Symposium on Industrial Electronics, IEEE*, 2004.

[5] Manitoba HVDC Research Centre. http://pscad.com/, 2007.

[6] C.Meyer, M.Höing, A.Peterson, and R.W.De Doncker. Control and design of dc-grids for offshore wind farms. *The 2006 IEEE Industry Applications Conference*, 3, 2006.

[7] E.Koutroulis and K.Kalaitzakis. Design of a maximum power tracking system for wind-energy-conversion applications. *IEE Tranxacions on Industrial Electronics*, 53, 2006.

[8] E.Spooner and A.Williamson. Modular, permanent-magnet wind-turbine generators. *Industry Applications Conference, Thirty-First IAS Annual Meeting, IAS, IEEE*, 1996.

[9] F.Iov, A.D.Hansen, P.Sørensen, and F.Blaabjerg. *Wind Turbine Blocset in Matlab/Simulink - General Overview and Description of the Models*. Institute of Energy Technology, Aalborg University, 2004.

[10] G.Hua and Y.Geng. A novel control strategy of mppt taking dynamics of wind turbine into account. *Power Electronics Specialists Conference, PESC '06. 37th IEEE*, 2006.

[11] J.G.Balchen, T.Andresen, and B.A.Foss. *Reguleringsteknikk*. Institutt for teknisk kybernetikk, NTNU, 2004.

[12] J.Todorovic. *Losses Evaluation of HVAC Connection of Large Offshore Wind Farms*. PhD thesis, Royal Institute of Technology, Stockholm, 2004.

[13] K.Tan and S.Islam. Optimum control stragegies in energy conversion of pmsg wind turbine system without mechanical sensors. *IEEE Transactions on Energy Conversion*, 2004.

[14] L.Max and S.Lundberg. System efficiency of a dc/dc converter based wind turbine grid system. *Nordic Wind Power Conferance*, 2006.

[15] L.Xu and B.R.Andersen. Grid connection of large offshore wind farms using hvdc. Available from: www.interscience.wiley.com, 2006.

[16] M.Henschel, T.Hartkopf, H.Schneider, and E.Troester. A reliable and efficient new generator system for offshore wind farms with dc farm grid. *Power Electronics Specialists Conference, IEEE*, 2002.

[17] M.Ikonen, O.Laakkonen, and M.Kettunen. http://www.elkraft.ntnu.no/smola2005/, 2005.

[18] N.Barberis Negra, J.Todorovic, and T.Ackermann. Loss evaluation of hvac and hvdc transmission solutions for large offshore wind farms. *Available online at www.sciencedirect.com*, 2006.

[19] R Nilsen. *Elekriske motordrifter*. Institutt for elkraftteknikk, NTNU, 2004.

[20] N.M.Kirky, L.Xu, M.J.Luckett, and W.Siepmann. Hvdc transmission for large offshore wind farms. *Power Engineering Journal*, June 2002.

[21] N.M.Kirky, M.J.Luckett, L.Xu, and W.Siepmann. Hvdc transmission for large offshore windfarms. *AC-DC Power Transmission*, 2001.

[22] N.Mohan, T.M.Undeland, and W.P.Robbins. *Power Electronics - Converters, Applications, and Design*. John Wiley & Sons Inc, 2003.

[23] South China University of Technology. http://www.scut.edu.cn/english, 2007.

[24] O.Ojo and O.Omozusi. Modelling and analysis of an interior permanent-magnet dc-dc converter generator system. *Power Electronics Specialists Conference, IEEE*, 1997.

[25] F.S.dos Reis, J.A.V.Alè, F.D.Adegas, R.Tonkosi, S.Slan, and K.Tan. Active shunt filter for harmonic mitigation in wind turbines generators. *37th Power Electronics Specialists Conference, IEEE*, 2006.

[26] F.S.dos Reis, K.Tan, and S.Islam. Using pfc for harmonic mitigation in wind turbine energy conversion systems. *30th Annual Conference of Industrial Electronics Society, IEEE*, 2004.

[27] S.Lundberg. Evaluation of wind farm layouts. Available from: www.elkraft.ntnu.no/norpie [Accessed 23 7May 2006].

[28] S.Lundberg. *Wind Farm Configuration and Energy Efficiency Studies - Series DC versus AC Layouts*. PhD thesis, Charmers University of Technology, 2006.

[29] SmartMotor. www.smartmotor.no, 29.05.2007.

[30] T.M.H.Nicky, K.Tan, and S.Islam. Mitigation of harmonics in wind turbine driven variable speed permanent magnet synchronous generators. *The 7th International Power Engineering Conference, IPEC.*, 2005.

[31] T.Tafticht, K.Agbossou, and A.Cheriti. Dc bus control of variable speed wind turbine using a buck-boost converter. *Power Engineering Society General Meeting, IEEE*, 2006.

[32] Z.Chen and E.Spooner. A modular, permanent-magnet generator for variable speed wind turbines. *Seventh International Conference on Electrical Macines and Drives, IEEE*, 1995.

[33] Ø.Krøvel, R.Nilssen, and A.Nysveen. A study of the research activity in the nordic countries on large permanent magnet synchronous machines. *NORPIE 2004*, 2004.